Synthesis and aggregation dynamics of amylin

by

Karen Pillay (née Muthusamy)

Submitted in fulfilment of the academic requirements for the degree of

Doctor of Philosophy (Biochemistry)

in the

School of Life Sciences
College of Agriculture, Engineering and Science
University of KwaZulu-Natal

December 2012

As the candidate's supervisor I have approved this thesis for submission.

Signed: _____ Name: Dr Patrick Govender Date: _____

DECLARATIONS

Form EX1-5

COLLEGE OF AGRICULTURE, ENGINEERING AND SCIENCE

DECLARATION 1 - PLAGIARISM

I, Mrs Karen Pillay declare that

1. The research reported in this thesis, except where otherwise indicated, and is my original research.

2. This thesis has not been submitted for any degree or examination at any other university.

3. This thesis does not contain other persons' data, pictures, graphs or other information, unless specifically acknowledged as being sourced from other persons.

4. This thesis does not contain other persons' writing, unless specifically acknowledged as being sourced from other researchers. Where other written sources have been quoted, then:

a. Their words have been re-written but the general information attributed to them has been referenced

b. Where their exact words have been used, then their writing has been placed in italics and inside quotation marks, and referenced.

5. This thesis does not contain text, graphics or tables copied and pasted from the Internet, unless specifically acknowledged, and the source being detailed in the thesis and in the References sections.

Signed

……

COLLEGE OF AGRICULTURE, ENGINEERING AND SCIENCE

DECLARATION 2 - PUBLICATIONS

DETAILS OF CONTRIBUTION TO PUBLICATIONS that form part and/or include research presented in this thesis (include publications in preparation, submitted, *in press* and published and give details of the contributions of each author to the experimental work and writing of each publication)

Publication 1

Pillay, K., and Govender, P. Amylin Uncovered: A review on the polypeptide responsible for type II diabetes. Accepted for publication by the *Journal of Biomedicine and Biotechnology* on 21 February 2013.

Pillay, K. was solely responsible for all experimental work and writing of the publication.
Govender, P. was responsible for proof-reading the manuscript.

Publication 2

Muthusamy, K., Albericio, F., Arvidsson, P. I., Govender, P., Kruger, H. G., Maguire, G. E. M., and Govender, T (2010) Microwave Assisted SPPS of Amylin and Its Toxicity of the Pure Product to RIN-5F Cells, *Peptide Science 94*, 323-330.

Muthusamy, K. was solely responsible for all experimental work and writing of the publication.
Albericio, F., Arvidsson, P. I., Govender, P., Kruger, H. G., Maguire, G. E. M., and Govender, T. were responsible for proof-reading the manuscript.

Publication 3

Muthusamy, K., Arvidsson, P. I., Govender, P., Kruger, H. G., Maguire, G. E. M., and Govender, T. (2010) Design and study of peptide-based inhibitors of amylin cytotoxicity, *Bioorganic & Medicinal Chemistry Letters 20*, 1360-1362.

Muthusamy, K. was solely responsible for all experimental work and writing of the publication.
Arvidsson, P. I., Govender, P., Kruger, H. G., Maguire, G. E. M., and Govender, T. were responsible for proof-reading the manuscript.

Publication 4

Pillay, K., and Govender, P. Novel insights into amylin aggregation. Submitted to *Biotechnology and Biotechnological Equipment*. Submitted on 12/12/12. Submission number yet to be generated.

Pillay, K. was solely responsible for all experimental work and writing of the publication.
Govender, P. was responsible for proof-reading the manuscript.

Publication 5

Muthusamy, K., and Govender, P. A direct fluorescent-based technique for cellular localization of amylin. Accepted for publication by *Biotechnology and Applied Biochemistry* on 11 March 2013.

Pillay, K. was solely responsible for all experimental work and writing of the publication.
Govender, P. was responsible for proof-reading the manuscript.

Signed: ……..

SUMMARY

Amylin is a 37 amino acid long peptide that aggregates into toxic oligomers and fibrils. Since amylin is secreted by and also acts on pancreatic *beta* cells, type II diabetes is classified as an amyloidogenic disease. This study focuses on the development of a cost effective chemical synthetic strategy for amylin synthesis as previous studies relied on extremely expensive pseudoproline derivatives. Furthermore, commercially available amylin varies between batches and also contains impurities that could generate anomalies and affect reproducibility of experiments. Secondly, chemically synthesized non-methylated and *N*-methylated derivatives of amylin were shown to inhibit toxicity of full length amylin. A fluorescently-labeled chemically synthesized derivative of amylin was used to track cellular localization of amylin via confocal microscopy. Amylin aggregation kinetics was established using a surface plasmon resonance (SPR) biosensor. In addition, nanoparticle tracking analysis (NTA) was used as a novel technique to determine the size of oligomers over real time. This technology indicated that the size range of the toxic species of amylin is between 200-300 nm. Furthermore, it can be suggested that NTA could potentially be developed into a screening tool for inhibitors of amylin-mediated cytotoxicity.

This thesis is dedicated to Lord Ganesha, Keags, Mum and Dad.

BIOGRAPHICAL SKETCH

Karen Pillay was born in Durban on 29 December 1984. She matriculated in 2002 with six distinctions and her love for Science led her to pursue a Bachelor of Science degree at the then University of Natal. Karen graduated *cum laude* with a major in Biomedical Science and went on to graduate with a Bachelor of Science (Honors) degree *summa cum laude*. Karen's passion was drug development which prompted her to enroll for an MSc research study on peptide synthesis of potential inhibitors of amylin aggregation. During her MSc study, Karen was an *ad hoc* lecturer at the Durban University of Technology, being responsible for level two Biochemistry lectures to Chiropractic and Homeopathy students.

Seeing as her MSc research explored potential inhibitors of type II diabetes and the many gaps in amylin research, Karen decided to embark on a Doctor of Philosophy (PhD) study in the Department of Biochemistry. During the first year of her PhD study, Karen was a successful incumbent of the Leadership and Equity Advancement Program (LEAP) which allowed her to gain invaluable lecturing experience whilst still working on her PhD study. At the end of the three year LEAP, Karen fulfilled all requirements of the program and was appointed as a permanent lecturer in the Department of Biochemistry, School of Life Sciences, University of KwaZulu-Natal. One of the highlights of Karen's research career is being awarded a Women in Science Doctoral Scholarship from the Department of Science and Technology, South Africa in August 2011.

Karen is married and in her spare time enjoys gardening.

PREFACE

This thesis is presented as a compilation of seven chapters.

Chapter 1 **General Introduction and Project Aims**

Chapter 2 **Literature Review**

Chapter 3 **Research Results I**
Microwave assisted SPPS of amylin and toxicity of the pure product to RIN-5F cells

Chapter 4 **Research Results II**
Design and study of peptide-based inhibitors of amylin cytotoxicity

Chapter 5 **Research Results III**
Novel insights into amylin aggregation

Chapter 6 **Research Results IV**
A direct fluorescent-based technique for cellular localization of amylin

Chapter 7 **General Discussion and Conclusion**

CONTENTS

ACKNOWLEDGEMENTS

I wish to express my sincere gratitude and appreciation to the following people and institutions:

- The higher force, God, that gave me the perseverance and strength to complete this study and for clearing my path of any negativity that arose.

- My devoted husband, Keagan, for always reminding me of my potential and for being my pillar of strength during difficult times, and for the many cups of tea that kept me going.

- My proud parents, Siva and Theresa, for nurturing me to be the person that I am today and especially my mum for going out of her way to relieve me of duties, thus ensuring that I have time for my PhD study.

- My supervisor, Dr Patrick Govender, for motivating me to overcome obstacles and to be the best that I can be, without whom this study would not have reached completion.

- Prof. Bala Pillay for his sound advice and encouragement.

- My colleagues in the Lab., Uraisha, Sizwe, Anushka, Lethu, Dr Reddy, Dr Naidu, Ramesh, Nazia, and Raj for their camaraderie, for creating an awesome working environment, and for maintaining the faith that we will all complete our respective degrees.

- Dinesh, for going out of his way to offer assistance.

- University of KwaZulu-Natal for supporting my research study and for providing an environment conducive for me to attain my goals.

- The National Research Foundation (NRF) for funding this study through the Thuthuka program.

- The Leadership and Equity Advancement Program (LEAP) and especially my LEAP coordinator, Dr Paddy Ewer, for providing me with funds to complete part of my research study in the United Kingdom.

- Mrs Shelley McKellar for comradeship at the Centre of Electron Microscopy, UKZN (Pietermaritzburg campus) during my long hours of confocal imaging.

- Dr James Wesley-Smith for going out of his way to assist with transmission electron microscopy and for his sage advice.

- Dr Celia Snyman for her expert advice on use of the confocal electron microscope.

- Mark Ware, Claire Hannell, Agnieszka Siupa and Patrick Hole for the warm welcome and invaluable assistance at NanoSight Ltd., Amesbury.

ABBREVIATIONS

A.u.	Arbitrary units
Aβ	Amyloid β protein
AcOH	Acetic acid
AFM	Atomic force microscopy
ANOVA	One-way analysis of variance
ATCC	American Type Culture Collection
Boc	*t*-butyloxycarbonyl
Carboxy-amy	Carboxyfluorescein-labeled amylin
CCD	Charge-coupled device
CD	Circular dichroism
CGRP	Calcitonin-gene-related-peptide
Cos-1	Simian fibroblast cell line
DCM	Dichloromethane
DIPEA	Di-isopropyl ethylamine
DMEM	Dulbecco's minimal essential medium
DMF	Dimethylformamide
DMSO	Dimethylsulfoxide
EDC	*N*-ethyl-*N*′-[(dimethylamino)propyl]-carbodiimide
Eq.	Equivalents
ESI-QTOF	Electrospray ionization time-of-flight spectroscope
Et_3SiH	Triethylsilane
FCS	Fetal calf serum (heat-inactivated)
Fmoc	9-fluorenylmethoxycarbonyl
FT-IR	Fourier transform infrared
Gdn-HCl	Guanidine hydrochloride
GUVs	Giant unilamellar vesicles
HBTU	O-Benzotriazole-*N*, *N*, *N*, *N*-tetramethyl-uronium-hexafluoro-phosphate
HATU	1-[bis-(dimethyl-amino)methyliumyl]-1H-1,2,3-triazolo[4,5-b]pyridine-3-oxide hexaflurophosphate
HCl	Hydrochloric acid
HEPES	2-[4-(2-hydroxyethyl)-1-piperazinyl] ethanesulfonic acid
HFIP	1,1,1,3,3,3-hexafluoro-2-propanol
HIT-T15	Syrian hamster β-cells
HPLC	High pressure liquid chromatography
HTB-14	Human glioblastoma/astrocytoma cells
IAPP	Islet amyloid polypeptide
INT	2-(4-iodophenyl)-3-(4-nitrophenyl)-5-phenyltetrazolium chloride
INS-1E	Rat insulinoma *beta*
K_2CO_3	Potassium carbonate
LD_{50}	Lethal dose
LDH	Lactate dehydrogenase
MA	Modified amylin

MALDI-TOF MS	Matrix-assisted laser desorption ionization time-of-flight mass spectroscopy
MBHA	4-methylbenzhydrylamine
MCF-7	Human adenocarcinoma cells
MDBK	Madin Darby bovine kidney epithelium
MeOH	Methanol
µL	Micro-liters
µm	Micro-meters
µM	Micro Molar
$MgSO_4$	Magnesium sulphate
mL	Milliliters
MS	Mass spectra
MTT	3-(4,5-dimethylthiazol-2-yl)-2,5-diphenyltetrazolium bromide
NaCl	Sodium chloride
NAD^+	Nicotinamide adenine dinucleotide
$NADH/H^+$	Dihydronicotinamide adenine dinucleotide
NADPH	Dihydronicotinamide adenine dinucleotide phosphate
$NaHCO_3$	Sodium bicarbonate
NHS	*N*-hydroxysuccinimide
nm	Nano-meters
N-Me	*N*-methylated
NMR	Nuclear magnetic resonance
NTA	Nanoparticle tracking analysis
OD	Optical density
Pbf	2,2,4,6,7-pentamethyl-dihydrobenzofuran-5-sulfonyl
PBS	Phosphate buffer saline
PC12	Rat phaeochromocytoma cells
PC2	Prohormone convertase
PDEA	2-(2-Pyridinyldithio)-ethaneamine hydrochloride
ppm	Parts per million
PrP	prion protein
RIN	Rat insulinoma cells
SD	Standard deviation
SDS	Sodium dodecyl sulfate
SDS-PAGE	Sodium dodecyl sulfate polyacrylamide gel electrophoresis
SEM	Scanning electron microscopy
SPPS	Solid phase peptide synthesis
SPR	Surface plasmon resonance
STEM	Scanning transmission electron microscopy
t-Bu	*tert*-butyl
TEM	Transmission electron microscopy
TFA	Trifluoroacetic acid
ThT	Thioflavin T
TLC	Thin layer chromatography
Trt	Trityl
WHO	World Health Organization.

LIST OF FIGURES

DIC image. Different colored arrows are used to indicate the cellular localization of amylin over time. Scale bars represent 200 μm.

Figure 6.7 NTA size distribution profile of disaggregated carboxy-amy (30 μM) in 10 mM sodium phosphate buffer, pH 7.4 containing 50 mM NaCl after incubation at 37°C for 10 minutes (A) and 180 minutes (B). (C) NTA size distribution profile of the carboxy-amy sample that was recovered from the completed confocal microscopy experiments. Video recordings (duration of 60 seconds) of each sample were taken for NTA using the single shutter and gain mode.

LIST OF TABLES

Chapter 1

INTRODUCTION AND PROJECT AIMS

1. INTODUCTION AND PROJECT AIMS

1.1 INTRODUCTION

Type II diabetes is a debilitating disease that is associated with numerous secondary medical complications. It is remarkable that more than a century ago a link was established between the deposition of fibrillar material in the pancreas and manifestation of this disease.[1] The fibrillar material was found to be composed of amylin, a 37 amino acid polypeptide, and thus type II diabetes was classified as an amyloid disease.[2, 3]

Amylin is released together with insulin from pancreatic *beta* cells and it has been suggested that a high carbohydrate/fat diet results in increased insulin secretion, which is coupled to a concomitant increase in amylin secretion.[4, 5] This monomeric form of amylin can then aggregate into oligomeric and fibrillar *β*-sheet structures, the former of which has been observed to impose toxicity to pancreatic *beta* cells.[6-9]

In view of the above, a range of molecules were evaluated as potential inhibitors of amylin-mediated aggregation and which could be subsequently employed to prevent aggregated amylin-induced cytotoxicity. Polycyclic compounds were shown to be efficient inhibitors of amylin aggregation and were also found to reduce cytotoxicity. These compounds include Congo red, resveratrol and tetracycline and it has been suggested that heteroaromatic interactions between these molecules and amylin result in geometric constraints that prevent fibrillogenesis.[10-14] Peptide-based inhibitors which are homologous to distinct regions of the amino acid sequence of amylin were also evaluated as potential inhibitors. Peptidomimetics incorporating *N*-methylated amino acids were also assessed as likely inhibitor candidates as they would facilitate disruption of the hydrogen bonding capacity of amylin and thereby prevent formation of *β*-sheet structures. An amylin derivative of full length amylin with *N*-methylated amino acids at residues 24 and 26, amylin$_{22\text{-}27}$ with *N*-methylated amino acids at residues 23 and 25, amylin$_{13\text{-}18}$ and amylin$_{20\text{-}25}$ were found to significantly decrease amylin cytotoxicity.[15-18] However, despite patents being granted on some of the above mentioned derivatives, none of them have been used in clinical trials.[19, 20] Moreover, short peptides spanning the length of amylin are yet to be evaluated for their inhibitory effect on amylin-mediated cytotoxicity. In view of the above, the development of peptide- and peptidomimetic therapeutics against amylin aggregation is an attractive research niche.

Some of the techniques used to monitor amylin aggregation are circular dichroism, Fourier transform infrared (FT-IR) spectroscopy, transmission electron microscopy (TEM), atomic force microscopy (AFM), the thioflavin T (ThT) assay and the sedimentation assay.[6, 7, 21-25] However, with the exception of AFM, none of the techniques are able to identify the oligomeric species of amylin and thus cannot be used as a screening method for potential inhibitors of amylin-mediated cytotoxicity. In addition, AFM is labor-intensive and samples must be adsorbed to a mica surface in order to monitor fibril growth over time which is a cause for concern since it has been reported that the type of amylin fibrils that form in the presence of a mica surface is significantly different in morphology from that formed free in solution.[26, 27] Currently, the mammalian cell line-based cytotoxicity assay is the preferred strategy when screening for potential therapeutic agents against amylin aggregation-induced type II diabetes.[11, 15-17, 28-37] Although this assay yields quantitative data with regard to the protective potential of compounds, it is very expensive and time-consuming as it is dependent on the growth rate of a particular mammalian cell line. Consequently, there exists a need for the development of a cell-free strategy that would allow efficient screening of potential inhibitors of amylin-mediated cytotoxicity.

In addition, the cytotoxicity assay is dependent on the use of full length human amylin. However, the isolation and purification of human amylin from biological resources is extremely expensive. Moreover, the hydrophobic nature of the peptide makes it a challenging entity to chemically synthesize, and currently available synthetic procedures for full length human amylin make use of very expensive pseudoproline derivatives.[38-43] Of note, it was reported that commercially available amyloidogenic peptides from manufacturers have differing fibrillogenic properties.[44] Thus, to enable extensive amylin-based research, a cost-effective synthetic strategy for full length human amylin should be developed.

Moreover, for effective design of potential therapeutic agents of type II diabetes that would act by preventing amylin-cell interactions, an in-depth insight into the cellular localization of amylin would be highly beneficial. Although previous studies have been performed that sheds some light on amylin localization, all studies to date have made use of an indirect fluorescent labeling approach.[45-47] Amongst other dyes, Congo red has been used to identify amylin aggregates. However, Congo red was demonstrated to bind non-specifically to cellular membranes [47] and it was also found to decrease both the rate of amylin fibrillogenesis and its cytotoxic effect.[11, 13] It can thus be suggested that use of an indirect labeling approach would affect amylin-amylin and amylin-cell interactions thereby complicating data interpretation. A direct fluorescent labeling approach is therefore necessary to cellular localize amylin via fluorescent microscopy.

1.2 SCOPE OF THESIS AND AIMS OF STUDY

The main aim of this study was to synthesize and evaluate the aggregation dynamics of amylin. This thesis is divided into seven chapters, including this introduction (**Chapter 1**).

In **Chapter 2**, a comprehensive literature review encompassing the molecular dynamics of amylin aggregation, proposed mechanisms of amylin-mediated cytotoxicity, techniques used to monitor amylin aggregation and toxicity, inhibitors of amylin-mediated cytotoxicity and synthetic strategies for amylin are presented. This chapter has been accepted for publication in *Journal of Biomedicine and Biotechnology*.

In **Chapter 3**, different coupling conditions and oxidation methods were evaluated in an attempt to develop a cost effective, microwave-assisted solid-phase peptide synthetic strategy for production of amylin. The fibrillogenic and cytotoxic properties of chemically synthesized amylin was also ascertained to establish its suitability as a substitute for naturally occurring amylin. This aspect of the study was reported in the journal *Peptide Science*.[44]

With a cost effective chemical synthetic strategy for amylin production in place, attention switched to synthesis and evaluation of amylin derivatives as potential inhibitors of amylin aggregation and its resultant cytotoxicity which are described in **Chapter 4**. Five peptide derivatives spanning the length of amylin and their *N*-methylated counterparts were synthesized using a microwave-assisted solid-phase strategy. These amylin derivatives were co-incubated with chemically synthesized full length human amylin (Chapter 1), and transmission electron microscopy (TEM) analysis was performed to assess the effect of each of the amylin derivatives on amylin fibrillogenesis. The potential of each amylin derivative as an inhibitor of amylin-mediated toxicity was also evaluated using a mammalian cell line-based cytotoxicity assay. This aspect of the research study was published in *Bioorganic and Medicinal Chemistry Letters*.[48]

Chapter 5 describes the suitability of surface plasmon resonance (SPR), dynamic light scattering (DLS), and nanoparticle tracking analysis (NTA) as cell-free systems for monitoring amylin aggregation and for screening potential inhibitors of amylin-mediated cytotoxicity. Each technique was used to monitor amylin aggregation dynamics, and only SPR and NTA were observed to generate useful data. The SPR technique yielded quantitative association and dissociation kinetics of amylin whilst NTA shed light on the size of amylin

aggregates that developed over real time. The latter two techniques were then employed to monitor changes in amylin aggregation dynamics that arose as a consequence of co-incubating amylin with each of its derivatives that were synthesized in Chapter. 4. The potential of SPR and NTA as screening tools for amylin-mediated cytotoxicity was evaluated by comparison of this data set to earlier cytotoxicity results (Chapter 4)

In **Chapter 6**, the cellular localization of amylin was studied using imaging of *in vitro* cell cultures. Full length human amylin bearing a carboxyfluorescein group on the *N*-terminus was chemically synthesized and used in confocal microscopy investigations to establish the cellular localization of the fluorescently-labeled amylin. The novelty aspect of this study is that a direct labeling approach was utilized, thus negating any impact that external dyes may have on amylin aggregation kinetics or amylin-cell interactions. This aspect of the research study has been accepted for publication in *Biotechnology and Applied Biochemistry*.

Finally, **Chapter 7** presents a general conclusion and ideas on future research concepts.

1.3 REFERENCES

1. Opie, E., *The relation of diabetes mellitus to lesions of the pancreas. Hyaline degeneration of the islands of Langerhans.* The Journal of Experimental Medicine, 1901. **5**: p. 528-540.
2. Cooper, G.J.S., Willis, A.C., Clark, A., Turner, R.C., Sim, R.B. and Reid, K.B.M., *Purification and characterization of a peptide from amyloid-rich pancreases of type 2 diabetic patients.* Proceedings of the National Academy of Science, 1987. **84**: p. 8628-8632.
3. Cooper, G.J.S., Leighton, B., Dimitriadis, G. D., Parry-Billings, M., Kowalchuk, J. M., Howland K., Rothbard, J. B., Willis, A. C., and Reid, K. B. M, *Amylin found in amyloid deposits in human type 2 diabetes mellitus may be a hormone that regulates glycogen metabolism in skeletal muscle.* Proceedings of the National Academy of Science, 1988. **85**: p. 7763-7766.
4. Hull, R.L., Andrikopoulos, S., Verchere, C. B., Vidal, J., Wang, F., Cnop, M., Prigeon, R. L., and Kahn, S. E., *Increased dietary fat promotes islet amyloid formation and beta-cell secretory dysfunction in a transgenic mouse model of islet amyloid.* Diabetes, 2003. **52**(2): p. 372-379.
5. Hoppener, J.W.M., Jacobs, H. M., Wierup, N., Sotthewes, G., Sprong, M., de Vos, P., Berger, R., Sundler, F., and Ahren, B., *Human islet amyloid polypeptide transgenic mice: in vivo and ex vivo models for the role of hIAPP in type 2 diabetes mellitus.* Experimental Diabetes Research, 2008.
6. Janson, J., Ashley, R.H., Harrison, D., McIntyre, S. and Butler, P.C., *The mechanism of islet amyloid polypeptide toxicity is membrane disruption by intermediate-sized toxic amyloid particles.* Diabetes, 1999. **48**: p. 491–498.
7. Konarkowska, B., Aitken, J. F., Kistler, J., Zhang, S. P., and Cooper, G. J. S., *The aggregation potential of human amylin determines its cytotoxicity towards islet beta-cells.* Febs Journal, 2006. **273**(15): p. 3614-3624.
8. Meier, J.J., Kayed, R., Lin, C., Gurlo, T., Haataja, L., Jayasinghe, S., Langen, R., Glabe, C.G., and Butler, P.C., *Inhibition of human IAPP fibril formation does not prevent beta-cell death: evidence for distinct actions of oligomers and fibrils of human IAPP.* American Journal of Physiology, Endocrinology and Metabolism, 2006. **291**: p. E1317–E1324.
9. Ritzel, R.A., Meier, J. J., Lin, C., Veldhuis, J. D., and Butler, P. C., *Human islet amyloid polypeptide oligomers disrupt cell coupling, induce apoptosis, and impair insulin secretion in isolated human islets.* Diabetes, 2007. **56**: p. 65-71.
10. Forloni, G., Colombo, L., Girola, L., Tagliavini, F., and Salmona, M., *Anti-amyloidogenic activity of tetracyclines: studies in vitro.* FEBS Letters, 2001. **487**(3): p. 404-407.
11. Aitken, J.F., Loomes, K.M., Konarkowska, B. and Cooper, G.J.S, *Suppression by polycyclic compounds of the conversion of human amylin into insoluble amyloid.* Biochemical Journal, 2003. **374**: p. 779–784.

12. Mishra, R., Sellin, D., Radovan, D., Gohlke, A., and Winter, R., *Inhibiting islet amyloid polypeptide fibril formation by the red wine compound resveratrol.* Chembiochem, 2009. **10**(3): p. 445-449.
13. Zraika, S., Hull, R. L., Udayasankar, J., Aston-Mourney, K., Subramanian, S. L., Kisilevsky, R., Szarek, W. A., and Kahn, S. E., *Oxidative stress is induced by islet amyloid formation and time-dependently mediates amyloid-induced beta cell apoptosis.* Diabetologia, 2009. **52**(4): p. 626-635.
14. Jiang, P., Li, W., Shea, J. E., and Mu, Y., *Resveratrol inhibits the formation of multiple-layered beta-sheet oligomers of the human islet amyloid polypeptide segment 22-27.* Biophysical Journal, 2011. **100**(8): p. 2076-2076.
15. Scrocchi, L.A., Chen, Y., Waschuk, S., Wang, F., Cheung, S., Darabie, A.A., McLaurin, J. and Fraser, P.E., *Design of peptide-based inhibitors of human islet amyloid polypeptide fibrillogenesis.* Journal of Molecular Biology, 2002. **318**: p. 697–706.
16. Tatarek-Nossol, M., Yan, L., Schmauder, A., Tenidis, K., Westermark, G., and Kapurniotu, A., *Inhibition of hIAPP amyloid-fibril formation and apoptotic cell death by a designed hIAPP amyloid-core-containing hexapeptide.* Chemistry & Biology, 2005. **12**: p. 797–809.
17. Yan, L., Tatarek-Nossol, M., Velkova, A., Kazantzis, A. and Kapurniotu, A., *Design of a mimic of nonamyloidogenic and bioactive human islet amyloid polypeptide (IAPP) as nanomolar affinity inhibitor of IAPP cytotoxic fibrillogenesis.* Proceedings of the National Academy of Science, 2006. **103**(7): p. 2046–2051.
18. Potter, K.J., Scrocchi, L. A., Warnock, G. L., Ao, Z., Younker, M. A., Rosenberg, L., Lipsett, M., Verchere, C. B., and Fraser, P. E., *Amyloid inhibitors enhance survival of cultured human islets.* Biochimica Et Biophysica Acta-General Subjects, 2009. **1790**(6): p. 566-574.
19. Albrecht, E., Jones, H., Gaeta, L.S.L., Prickett, K.S., and Beaumont, K. *Amylin antagonist peptides and uses thereof.* (1996). Patent no. 5580953.
20. Fezoui, Y., and Soto-Jara, C. *Amylin aggregation inhibitors and uses thereof.* (2007). Patent no. US2007/0155955 A1.
21. Anguiano, M., Nowak, R.J. and Lansbury, P.T., *Protofibrillar islet amyloid polypeptide permeabilizes synthetic vesicles by a pore-like mechanism that may be relevant to type II diabetes.* Biochemistry, 2002. **41**: p. 11338-11343.
22. Kayed, R., Sokolov, Y., Edmonds, B., McIntire, T.M., Milton, S.C., Hall, J.E. and Glabe, G.C., *Permeabilization of lipid bilayers is a common conformation-dependent activity of soluble amyloid oligomers in protein misfolding diseases.* The Journal of Biological Chemistry, 2004. **279**(45): p. 46363–46366.
23. Meier, J.J., Kayed, R., Lin, C. Y., Gurlo, T., Haataja, L., Jayasinghe, S., Langen, R., Glabe, C. G., and Butler, P. C., *Inhibition of human IAPP fibril formation does not prevent beta-cell death: evidence for distinct actions of oligomers and fibrils of human IAPP.* American Journal of Physiology-Endocrinology and Metabolism, 2006. **291**(6): p. E1317-E1324.
24. Ritzel, R.A., J.J. Meier, C.Y. Lin, J.D. Veldhuis, and P.C. Butler, *Human islet amyloid polypeptide oligomers disrupt cell coupling, induce apoptosis, and impair insulin secretion in isolated human islets.* Diabetes, 2007. **56**(1): p. 65-71.
25. Aitken, J.F., Loomes, K. M., Scott, D. W., Reddy, S., Phillips, A. R. J., Prijic, G., Fernando, C., Zhang, S. P., Broadhurst, R., L'Huillier, P., and Cooper, G. J. S., *Tetracycline treatment retards the onset and slows the progression of diabetes in human amylin/islet amyloid polypeptide transgenic mice.* Diabetes, 2010. **59**(1): p. 161-171.
26. Goldsbury, C., Kistler, J., Aebi, U., Arvinte, T. and Cooper, G.J.S., *Watching amyloid fibrils grow by time-lapse atomic force microscopy.* Journal of Molecular Biology, 1999. **285**: p. 33-39.
27. Green, J.D., Goldsbury, C., Kistler, J., Cooper, G.J.S and Aebi, U., *Human amylin oligomer growth and fibril elongation define two distinct phases in amyloid formation.* The Journal of Biological Chemistry, 2004. **279**(13): p. 12206–12212.
28. Kapurniotu, A., Schmauder, A. and Tenidis, K., *Structure-based design and study of non-amyloidogenic, double n-methylated IAPP amyloid core sequences as inhibitors of IAPP amyloid formation and cytotoxicity.* Journal of Molecular Biology, 2002. **315**: p. 339-350.
29. Saafi, E.L., Konarkowska, B., Zhang, S., Kistler, J. and Cooper, G.J.S., *Ultrastructural evidence that apoptosis is the mechaism by which human amylin evokes death in RINm5F pancreatic islet cells.* Cell Biology International, 2001. **25**(4): p. 339–350.
30. Tenidis, K., Waldner, M., Bernhagen, J., Fischle, W., Bergmann, M., Weber, M., Merkle, M., Voelter, W., Brunner, H. and Kapurniotu, A., *Identification of a Penta- and Hexapeptide of Islet Amyloid Polypeptide (IAPP) with Amyloidogenic and Cytotoxic Properties.* Journal of Molecular Biology, 2000. **295**: p. 1055-1071.
31. Krampert, M., Bernhagen, J., Schmucker, J., Horn, A., Schmauder, A., Brunner, H., Voelter, W. and Kapurniotu, A., *Amyloidogenicity of recombinant human pro-islet amyloid polypeptide (ProIAPP).* Chemistry & Biology, 2000. **7**: p. 855-871.

32. Zhang, S., Liu, J., Saafi, E.L. and Cooper, G.J.S, *Induction of apoptosis by human amylin in RINm5F islet L-cells is associated with enhanced expression of p53 and p21$^{(WAF1=CIP1)}$.* FEBS Letters, 1999. **455**: p. 315-320.
33. Bai, J., Saafi, E.L., Zhang, S. and Cooper, G.J.S., *Role of Ca2+ in apoptosis evoked by human amylin in pancreatic islet b-cells.* Biochemical Journal, 1999. **343**: p. 53-61.
34. Tomiyama, T., Kaneko, H., Kataoka, K., Asano, S. and Endo, N., *Rifampicin inhibits the toxicity of pre-aggregated amyloid peptides by binding to peptide fibrils and preventing amyloid-cell interaction.* Biochemical Journal, 1997. **322**: p. 859-865.
35. Kapurniotu, A., Bernhagen, J., Greenfield, N., Al-Abed, Y., Teichberg, S., Frank, R.W., Voelter, W. and Bucala, R., *Contribution of advanced glycosylation to the amyloidogenicity of islet amyloid polypeptide.* European Journal of Biochemistry, 1998. **251**: p. 208-216.
36. Scrocchi, L.A., Ha, K., Chen, Y., Wu, L., Wang, F., and Fraser, P.E., *Identification of minimal peptide sequences in the (8–20) domain of human islet amyloid polypeptide involved in fibrillogenesis.* Journal of Structural Biology, 2003. **141**: p. 218–227.
37. Porat, Y., Mazor, Y., Efrat, S., and Gazit, E., *Inhibition of islet amyloid polypeptide fibril formation: a potential role for heteroaromatic interactions.* Biochemistry, 2004. **43**(45): p. 14454-14462.
38. Raleigh, D.P., and Abedini, A., *Incorporation of pseudoproline derivatives allows the facile synthesis of human IAPP, a highly amyloidogenic and aggregation-prone polypeptide.* Orgnic Letters, 2005. **7**(4): p. 693-696.
39. Raleigh, D.P., Abedini, A., and Singh, G., *Recovery and purification of highly aggregation-prone disulfide-containing peptides: application to islet amyloid polypeptide.* Analytical Biochemistry 351 (2006) 181–186, 2006. **351**: p. 181-186.
40. Park, J.H., Page, K., Hood, C.A., Patel, H., Fuentes, G., Menakuru, M., *Fast Fmoc synthesis of hAmylin1–37 with pseudoproline assisted on-resin disulfide formation.* Journal of Peptide Science, 2007. **13**: p. 833-838.
41. Kelly, J.W., Yonemoto, I. T., Kroon, G. J. A., Dyson, H. J., and Balch, W. E., *Amylin proprotein processing generates progressively more amyloidogenic peptides that initially sample the helical state.* Biochemistry, 2008. **47**: p. 9900–9910.
42. Park, J.H., Hood, C.A., Fuentes, G., Patel, H., Page, K., Menakuru, M., *Fast conventional Fmoc solid-phase peptide synthesis with HCTU.* Journal of Peptide Science 2008. **14**: p. 97-101.
43. Marek, P., Woys, A. M., Sutton, K., Zanni, M. T., and Raleigh, D. P., *Efficient microwave-assisted synthesis of human islet amyloid polypeptide designed to facilitate the specific incorporation of labeled amino acids.* Organic Letters, 2010. **12**(21): p. 4848-4851.
44. Muthusamy, K., Albericio, F., Arvidsson, P. I., Govender, P., Kruger, H. G., Maguire, G. E. M., and Govender, T., *Microwave assisted SPPS of amylin and its toxicity of the pure product to RIN-5F cells.* Biopolymers, 2010. **94**(3): p. 323-330.
45. Hiddinga, H.J., and Eberhardt, N.L., *Intracellular amyloidogenesis by human islet amyloid polypeptide induces apoptosis in COS-1 cells.* American Journal of Pathology, 1999. **154**(4): p. 1077-1088.
46. Sparr, E., Engel, M. F. M., Sakharov, D. V., Sprong, M., Jacobs, J., de Kruijff, B., Hoppener, J. W. M., and Killian, J. A., *Islet amyloid polypeptide-induced membrane leakage involves uptake of lipids by forming amyloid fibers.* Febs Letters, 2004. **577**(1-2): p. 117-120.
47. Radovan, D., Opitz, N., and Winter, R., *Fluorescence microscopy studies on islet amyloid polypeptide fibrillation at heterogeneous and cellular membrane interfaces and its inhibition by resveratrol.* Febs Letters, 2009. **583**(9): p. 1439-1445.
48. Muthusamy, K., Arvidsson, P. I., Govender, P., Kruger, H. G., Maguire, G. E. M., and Govender, T., *Design and study of peptide-based inhibitors of amylin cytotoxicity.* Bioorganic & Medicinal Chemistry Letters, 2010. **20**(4): p. 1360-1362.

CHAPTER 2

LITERATURE REVIEW

This chapter has been accepted as a review article for publication by
Journal of Biomedicine and Biotechnology
on 21 February 2013.

2 LITERATURE REVIEW

2.1 Introduction

As mused by Reynaud (2010), "*as our life expectancy increases, the chances of getting a degenerative disease also increases…caused by something conceptually quite simple…incorrect protein folding*."[1] There are currently more than a dozen protein misfolding diseases which have been classified as amyloid diseases, with an equivalent number of amyloidogenic proteins responsible for each of them.[2] The amyloid diseases include Alzheimer's disease [3-9], Parkinson's disease [10, 11], Huntington's disease [11], Prion disease [12], primary and secondary systemic amyloidosis [2], and type II diabetes [13-18] for which the responsible misfolded protein is amyloid *beta* (A*β*), huntingtin, *α*-synuclein, prion protein (PrP), immunoglobulin (Ig) light chain, serum amyloid A, and amylin respectively. Other than Alzheimer's disease, type II diabetes is the most prevalent in modern society with currently 346 million diabetic people world-wide and the World Health Organization (WHO) predicts that the number of deaths that result from this disease will double between 2005 and 2030.[19] Type II diabetes is responsible for a number of secondary complications such as heart attack, stroke, blindness and renal failure [20] and thus research on amylin is of paramount importance in the fight against this debilitating disease.

Amylin, also referred to as islet amyloid polypeptide (IAPP), is composed of 37 amino acid residues and as seen in Figure 2.1 contains a disulfide bridge between residues two and seven.

Figure 2.1 Amino acid sequence of amylin. Redrawn from Cooper *et al*. (1987).[21]

Amylin is produced after an 89-amino acid long precursor protein referred to as preProIAPP is cleaved at the *N*-terminal yielding ProIAPP and which is subsequently post-translationally processed by the prohormone convertase (PC2).[22] These processes occur in pancreatic *beta* cells and hence amylin is secreted together with insulin in a 20 to 1 molar ratio of insulin to amylin.[23] Insulin is released following a diet rich in carbohydrates, as it is the hormone responsible for lowering blood glucose levels. Insulin functions by the following strategies; stimulation of mainly the muscle cells and adipocytes to increase their uptake of glucose,

activation of enzymes responsible for glucose metabolism, increasing conversion of glucose to glycogen, and inhibiting protein and lipid breakdown and stimulating their synthesis.[20] Initially, it was reported that amylin works antagonistically to insulin by inhibiting glycogenesis and promoting glycolysis.[24-27] However, other studies have suggested that amylin plays a critical role in glucose homeostasis by suppressing the release of glucagon from pancreatic *alpha* cells, and hence prevents release of glucose from the liver, decreases gastric emptying and stimulates the satiety center in the brain.[23, 28-31] The latter two events are important features that prevent an individual from feeling hungry thereby averting the condition of having even more stored glucose being released into the blood. Since amylin is co-released with insulin, consuming an excess amount of carbohydrates and fat may lead to an elevated amount of amylin being secreted that could eventually initiate amylin aggregation, since it was found that a high carbohydrate or high fat diet promoted amyloid formation in transgenic mice.[32, 33]

Amylin aggregation has been suggested to occur in a step-wise manner, with soluble monomeric amylin forming oligomeric structures, protofibrils and eventually amyloid fibrils, some of which are toxic to the pancreatic *beta* cells.[34] Destruction of the pancreatic *beta* cells results in decreased insulin production, and manifests as type II diabetes, a condition that is characterized by excess extracellular glucose with an intracellular deficit. The most commonly used treatment for diabetes is metformin and insulin. Although these two therapeutic agents help to manage the disease, they do not stop progression nor do they cure this debilitating disease.

An extensive review on amylin was conducted more than a decade ago by Kapurniotu (2001) which focused primarily on the morphological and structural features of amylin aggregates, mechanism of aggregation, and the effects of amylin on cell viability with a brief over-view on the potential of *N*-methylated peptides as inhibitors of amylin-mediated cytotoxicity.[13] More recently, two extensive reports on amylin have been published. One of the review articles focuses on the structural characteristics of amylin, mechanisms of its aggregation, factors affecting aggregation, and touched briefly on mechanisms of toxicity and inhibitors of aggregation [17], whilst the other gave a very insightful overview of the physiological and pathophysiological role of amylin, the toxic species of amylin and briefly highlighted a potential mechanism of amylin pathogenesis.[18]

This literature review aims to provide an in-depth and up-to-date over-view of the molecular mechanism of amylin aggregation, all possible mechanisms of amylin-mediated toxicity, commonly used techniques for evaluating inhibitors of fibril formation and toxicity, compounds that have been tested as potential inhibitors of amylin-mediated cytotoxicity, as well as a brief overview of the chemical strategies that are used to synthesize amylin.

2.2 Molecular mechanism of amylin aggregation

As amylin aggregation is central to this peptide acquiring cytotoxic properties, numerous researchers have over the last two decades either observed or proposed the molecular mechanism and region responsible for amylin aggregation (Table 2.1), with a common feature among all studies being that the aggregates are in a β-sheet conformation. The first study on the amyloidogenic region of amylin was performed by Westermark *et al.* (1990) and based on the non-amyloidogenic nature of amylin from different species and experimental data using synthetic peptides, proposed that the 25-29 region is the shortest amyloidogenic region of amylin.[35] With the exception of the 1-7 region of amylin, the entire length of this peptide has at some stage been shown to have amyloidogenic properties (Table 2.1). Of note, it was found that the 22-27 region coiled around each other into typical amyloid fibrils [36] and also increased fibril formation.[37] In addition, the 11-20 region was found to bind to amylin with the highest affinity when compared to peptides that were homologous to other regions of amylin and the 14-18 region was suggested to be the core recognition site for amylin binding.[38]

One of the earliest models for β-sheet formation was proposed by Jaikaran *et al*. (2001) (Figure 2.2A).[39] According to this model, β-turns are predicted at residue 31 thereby allowing the 24-29 and 32-37 regions to form an anti-parallel β-sheet, and at residue 20 which would allow the 18-23 region to extend the β-sheet.[39] This model also proposes that hydrophobic interactions are responsible for initiating the aggregation process and that hydrogen bonds stabilizes the β-sheet structure.[39] A later study proposed that the 12-17, 22-27 and 31-37 regions form anti-parallel β-sheets with the 18-21 and 28-30 regions forming the β-turns (Figure 2.2B).[40] In addition, it was also suggested that the hydrophobic side chains in the 15-17 and 32 region interacts with that of the 23-27 region whilst there is inter-strand hydrophilic association between the 28-31 regions of amylin (Figure 2.2C).[41] It is noteworthy that there is considerable overlap between the β-sheet forming regions proposed by all three model-predicting studies. In addition, the predicted β-sheet forming regions

contains the proposed nucleation sites for aggregation [42] as well as aromatic amino acids which have been reported to play a significant role in amyloid formation due to interactions between the planar aromatic structures which are also referred to as π-π interactions.[43] Taking all models into consideration, a proposed model of the β-sheet and β-turn regions of amylin is illustrated in Figure 2.2D. This model proposes that the 12-17, 23-27, and 32-37 regions make up the β-sheet structure with regions 20-21 being constituents of the β-turn region. Residues 18, 19, 22, and 28-31 could participate in forming either the β-sheet or β-turn.

Table 2.1 Observed and predicted amyloid forming regions of amylin

Year	Amyloidogenic region	Predicted or Observed
1990[35]	20-29	Observed
1999[44]	17-34, 24-37, 30-37	Observed
2000[45]	20-29	Observed
2000[36]	23-27 and 22-27	Observed
2001[46]	22-29	Observed
2001[39]	8-20	Observed
2002[38]	14-18, 14-22, 14-20, 15-20, 15-19	Observed
2002[37]	22-27	Observed
2003[47]	12-17, 15-20	Observed
2005[40]	12-17, 22-27, 31-37	Observed
2006[48]	13-18	Predicted
2007[41]	8-17, 28-37	Predicted
2007[49]	12-18, 15-20, 22-28	Predicted
2009[42]	8, 13, 17, 25, 27, 32*	Predicted

* Nucleation sites

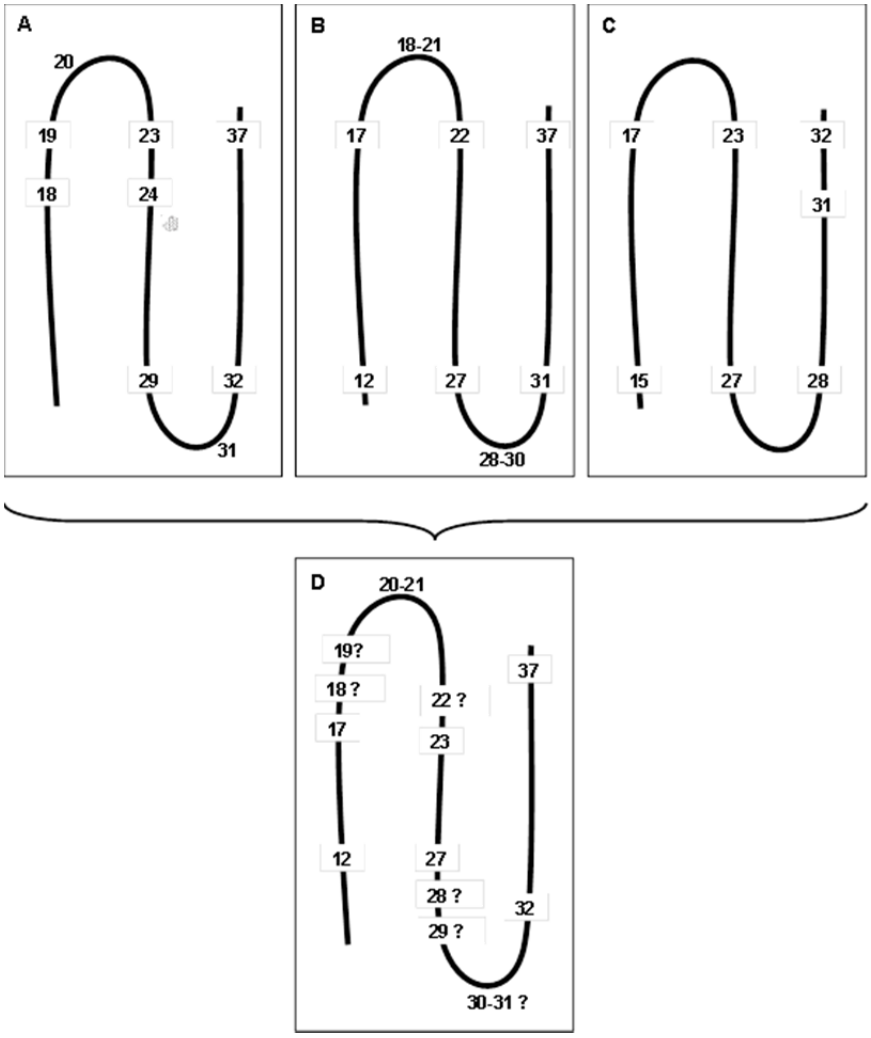

Figure 2.2 Schematic representation of the *β*-sheet and *β*-turn regions of amylin as predicted by (A) Jaikaran *et al.* (2001), (B) Kajava *et al.* (2005), and (C) Luca *et al.* (2007).[39-41] Data integration for a comprehensive understanding of previous predictions (A, B and C) is illustrated in D.

Thus, soluble monomeric amylin can associate into soluble *β*-sheet oligomeric states [50] which further progresses to protofibrils and insoluble amyloid fibrils.[51] According to Kodali *et al.* (2007), the oligomer which is formed prior to the protofibril is defined as being a "*...metastable multimer in an amyloid formation reaction*."[34] These soluble intermediates were reported to have diameters between 2.7-4 nm whilst protofibrils have a width of 5 nm and are "*...non-spherical filamentous structures lacking a periodic substructure that are often found at intermediate times during the formation of mature fibrils*," and amyloid fibrils, are "*...relatively straight, unbranched protein fibrils, with diameters in the 10 nm range, and often (but not always) consist of multiple protofilaments twisted around the fibril axis*" (Figure 2.3).[34, 52]

Analysis of amyloid fibrils has revealed that individual *β*-strands are orientated perpendicular to the long fiber axis and thus form *β*-sheets.[53-56] Research studies by Goldsbury *et al.* (1999), revealed that amylin fibrils grow bidirectionally at a rate of approximately 1.1 nm per minute and that the width of fibrils ranged between 6-8 nm.[52] Thus, there is still no conclusively accepted size of each of the different types of amylin aggregates.

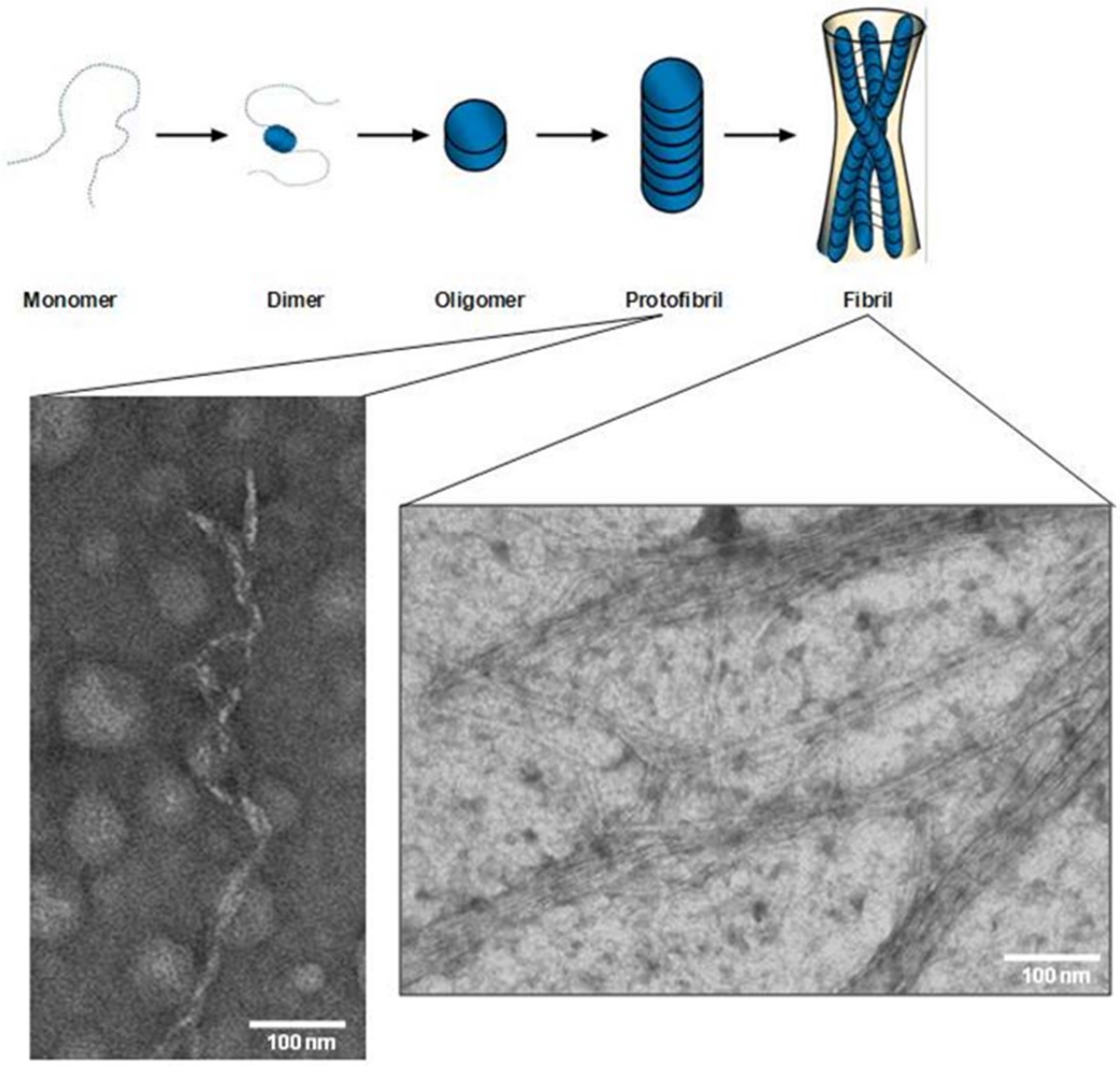

Figure 2.3 Schematic process of amylin forming nanoparticulate fibrils. Adapted from Dobson (2003).[57]

2.3 Mechanism of Amylin Toxicity

Previously there was general acceptance that the fibrillar form of amylin is the toxic species [58-66], however the more recent consensus is that the soluble oligomeric structures exert the toxic effect.[67-73] Two noteworthy experiments for the latter hypothesis were conducted in 2006 and 2010.[73, 74] Meier *et al.* (2006) evaluated rifampicin as a potential inhibitor of type II diabetes and found that although it did prevent fibril formation, toxicity of amylin was still present, thus concluding that the soluble oligomers are the toxic species.[74] The second study showed that the fibrillar species of amylin was positively correlated with longevity of transgenic mice, once again suggesting that the prefibrillar or oligomeric form is toxic.[73] Although there is currently a general acceptance that the oligomeric form of amylin is the toxic species, there are numerous theories regarding its mechanism of cytotoxicity.

The first mechanism of toxicity postulated is membrane disruption and subsequent disturbance of intracelluar homeostasis. It was initially reported by Westermark *et al.* (1990) that amylin disrupts cell membranes thereby causing cell death.[35] Thereafter Lorenzo *et al.* (1994) exposed islet cells sandwiched between coverslips as well as unprotected cells to human amylin aggregates and found using Nomarsky microscopy that amylin interaction with the cell membrane was crucial for toxicity.[75] Subsequent studies supported this theory by demonstrating that amylin aggregates formed pores or channels in lipid bilayers.[59, 68, 69, 76] Planar phospholipid bilayer membranes were used to demonstrate that non-selective ion voltage-dependent channels were formed in the presence of amylin.[59] This will promote the influx of Ca^{2+} and Na^{+}, and K^{+} efflux, thereby disrupting ionic homeostasis.[59] Kayed *et al.* (2004) also employed lipid bilayers and showed that there was increased conductance in the presence of amylin oligomers and fibrils.[69] In addition, intracellular calcium levels were found to be elevated after exposure to amylin and it is noteworthy that destabilization of intracellular Ca^{2+} homeostasis was a mechanism used by other amyloidogenic peptides to induce toxicity.[58, 77]

Subsequent studies also demonstrated that fibril formation was increased in the presence of anionic lipid membranes.[55, 78] and it was suggested that electrostatic interactions between amylin and the negatively charged lipids on membranes are responsible for amylin association with the cell membrane.[79] In addition, amylin was found to insert into plasma membranes and incorporated membrane lipids into the growing amyloid fibril, thereby causing membrane disruption.[79-82] Using human islets and amylin oligomers, Ritzel *et al.* (2007)

demonstrated that amylin oligomers could promote the loss of rat pancreatic *β*-cells (RINm5F) by disrupting the cell membrane as well as the islet achitecture such as cell-to-cell adherence, both of which are crucial for cell survival.[72] Reviews by Engel and coworkers (2008 and 2009) extensively describe amylin-mediated membrane disruption [16, 83] and it thus appear that membrane disruption could be a leading cause of amylin-mediated toxicity.

The second proposed mechanism of amylin-mediated toxicity is generation of reactive oxygen species (ROS) such as hydrogen peroxide (H_2O_2), which results in cell death.[58] ROS are able to damage DNA, and oxidizes the constituent amino acids of proteins as well as polyunsaturated fatty acids that are present in lipids, all of which can lead to apoptosis. ROS damages DNA by causing strand breakage, base modification, oxidation of deoxyribose, and DNA-protein cross-links.[84] Since cell membranes are made up of a large amount of polyunsaturated fatty acids, oxidation by ROS causes harmful changes in membrane fluidity, permeability and metabolic functions. Oxidative damage to proteins results in either protein degradation or alteration of its properties such as causing a soluble protein to aggregate, both of which are detrimental to cell survival.[84] It was also shown that generation of ROS was a mechanism used by other amyloidogenic peptides for toxicity.[58] At the same time, Schubert *et al.* (1995) detected peroxides using 2',7'-dichlorofluorescin diacetate and also demonstrated that amylin increased the accumulation of H_2O_2 in B12 cells.[85]

The third hypothesis of amylin-mediated toxicity is apoptosis. Apoptosis is defined as programmed cell death and is characterised by cell shrinkage, membrane blebbing (detachment of the cell membrane from the cytoskeleton), disruption of nuclear architecture and DNA laddering (breaking of chromosomal DNA into fragments containing 180 base pairs).[86]

In early experiments, Lorenzo *et al.* (1994) showed that aurintricarboxylic acid, an endonuclease inhibitor that stops apoptosis, is able to reduce amylin-mediated toxicity of islet cells.[75] They had also stained islet cells with propidium iodide and with the aid of epifluorescence microscopy showed that there was chromatin condensation.[75] In addition, agarose gel electrophoresis revealed that DNA fragmentation had also occurred.[75]

Thereafter the TUNEL assay and gel electrophoresis was employed to reveal that amylin triggered DNA fragmentation and apoptosis in RINm5F cells.[87] This research team also used quantitative Northern blot analysis to demonstrate that amylin increased expression of the p21 and p53 tumor suppressor genes, both of which encode for proteins that arrest cell proliferation, leading to apoptosis (Figure 2.4).[87] This finding was later supported by transmission electron microscopy (TEM) and scanning electron microscopy (STEM) analysis of RINm5F cells that were exposed to amylin which clearly illustrated ultra-structural evidence of apoptotic damage.[88] The theory that apoptosis is the mechanism by which amylin causes cell death was further supported by the finding that amylin increases the expression of c-Jun, a gene that is involved in the apoptotic pathway (Figure 2.4), in RINm5F and the human insulinoma cell line (CM).[89] Moreover, it was reported that amylin could elevate the levels of Fas ligand (FasL) and Fas-associated death domain (FADD) [90], both of which are involved in apoptosis (Figure 2.4), and Huang *et al.* (2007) demonstrated that amylin could trigger endoplasmic reticulum stress-induced apoptosis.[91] More recently, it was concluded that amylin oligomers could increase cytosolic levels of Ca^{2+} in the rat insulinoma cell line INS 832/13 which resulted in hyper activation of the protease calpein-2, leading to apoptosis.[92]

The above mentioned mechanisms could possibly work together to eventually result in cell death. For example, membrane damage caused by the toxic species of amylin or ROS damage could potentially result in activation of the apoptotic pathway and previous studies have also shown that there is significant overlap of the different mechanisms responsible for amylin-mediated cytotoxicity.[67, 93, 94] One such study used rat cortical neurons and demonstrated that amylin aggregates induced the apoptotic genes c-Jun, junB, c-fos and fosB as well as the oxidative stress genes cox-2 and lκB-α.[93] In addition, oligomers were found to contribute to membrane instability of voltage-clamped planar bilayer membranes by increasing conductance and electrical noise in the membrane as well as inducing the formation of abnormal vesicle-like membrane structures which resulted in apoptosis.[67] Gurlo *et al.* (2010) performed *in vivo* experiments with an oligomer-specific antibody and cryo-immunogold labeling and showed that the toxic oligomer is present in the secretory pathway and is able to disrupt membranes therein as well as mitochondrial membranes.[94] These events results in cellular dysfunction and apoptosis.[94] Lim *et al.* (2010) further supported the hypothesis that the mechanism of amylin toxicity is membrane disruption by showing that mitochondrial proteins were deregulated when SH-SY5Y neuroblastoma cells were exposed to amylin.[95] However, this group also showed that production of ROS increased when cells were exposed to amylin.[95]

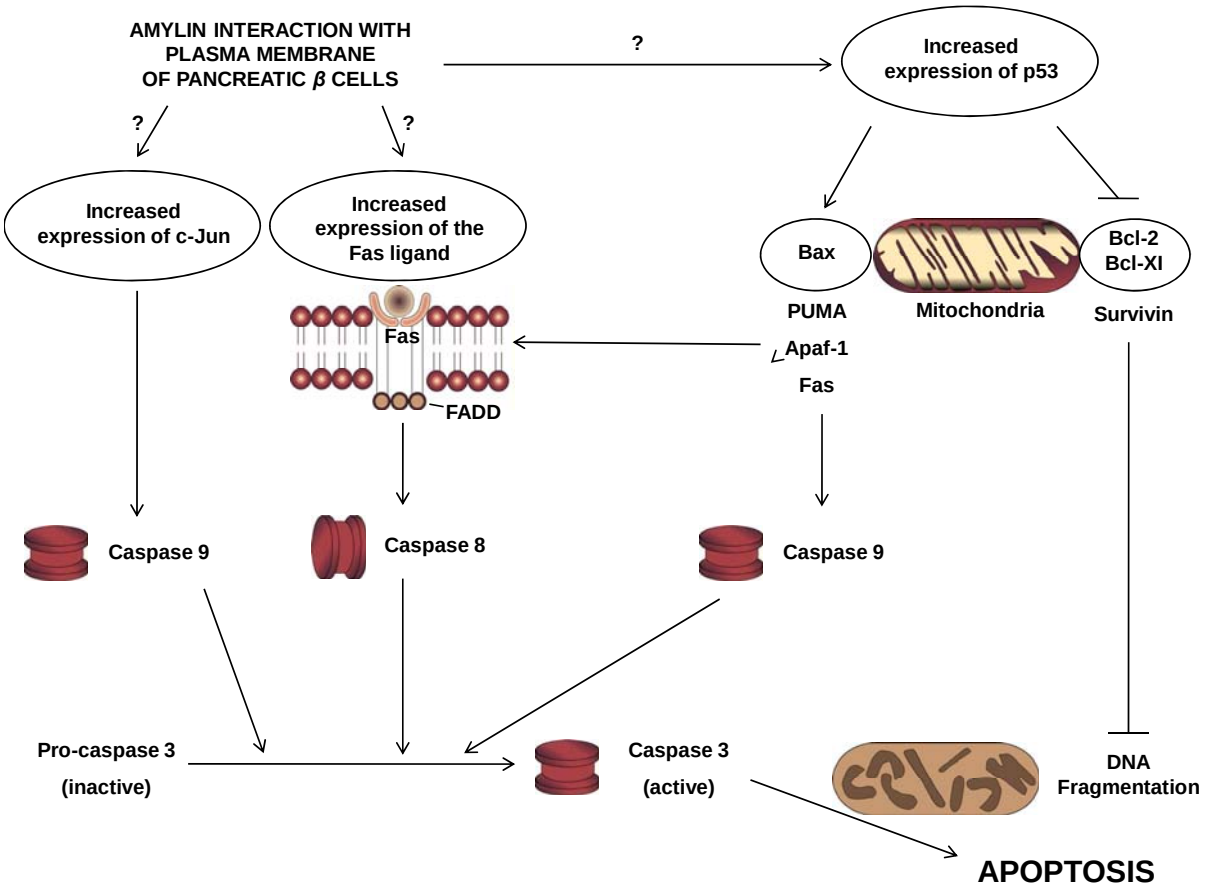

Figure 2.4 The proposed roles of the c-Jun, Fas and p53 proteins in apoptosis induced by human amylin in pancreatic *beta* cells.

Taking into account all of the proposed and observed mechanisms of amylin-induced cytotoxicity, it thus appears that membrane disruption, generation of ROS and apoptosis are inter-related. Membrane disruption appears to have a direct effect on apoptosis and thus these two mechanisms could actually be working together to induce amylin-mediated cytotoxicity.

2.4 Techniques used to monitor amylin aggregation and toxicity

There are numerous techniques that are employed to monitor amylin aggregation and toxicity, and inhibition thereof. Two commonly used dyes for identification of the fibrillar form of amylin is Congo red and thioflavin T (ThT) (Figure 2.5). It was found that when bound to amyloid fibrils, Congo red produced a characteristic yellow-green birefringence under polarized light, and it was assumed that this dye interacted with the *β*-sheet structure that is present in all amyloid deposits.[96, 97] Thus, Congo red staining was initially used for classification purposes to ascertain if an aggregate is amyloidogenic in nature.[21, 96, 97]

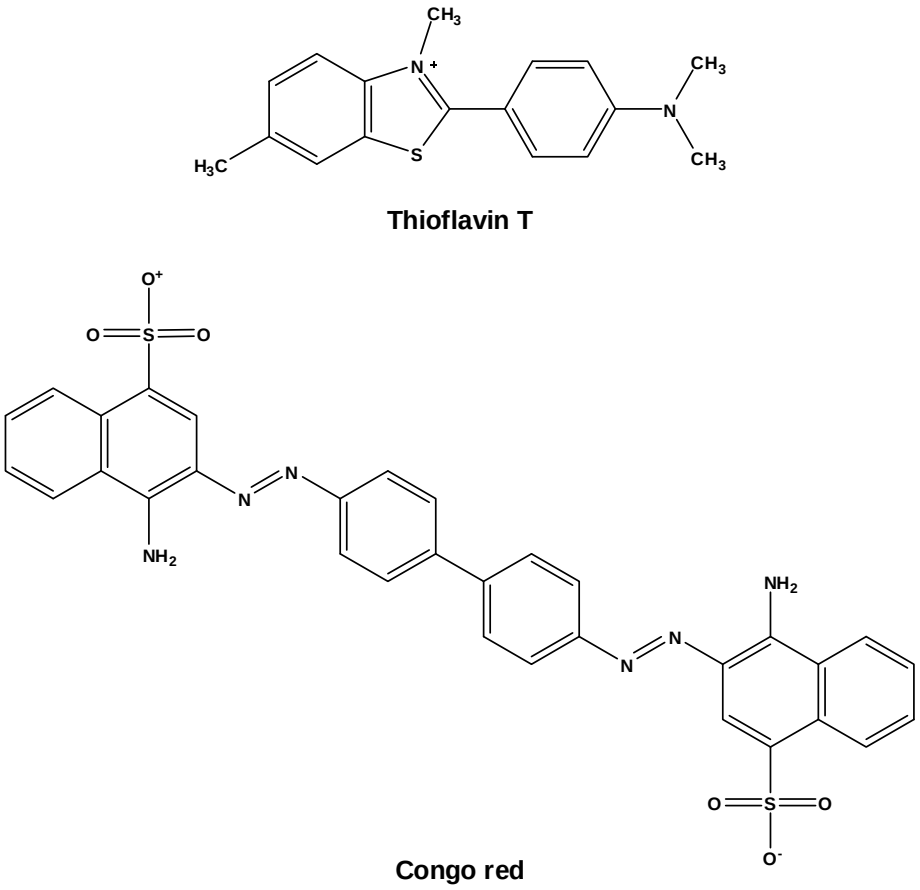

Figure 2.5 Structures of Thioflavin T and Congo red. Adapted from Aitken *et al.* (2003).[98]

Since Congo red staining is relatively easy to perform, it has been used to identify amyloid fibrils in pancreatic islets as well as in cell-based assays.[80, 96, 99] In addition, Congo red staining was used to identify the shortest fragment of amylin that retained amyloidogenic properties [36], to assess if modifications of the amylin structure could alter its amyloidogenic potential [61, 100], and to evaluate potential inhibitors of amylin fibril formation.[64] However, Congo red staining is neither very sensitive nor specific as it has been shown to stain amorphous aggregates [99] as well as having the ability to bind to cellular membranes.[101] Moreover, since Congo red is thought to bind β-sheet structures, it is quite possible that non-specific interactions could occur in a cell-based system, components of which may have β-sheet structures. It is also noteworthy that Congo red was found to reduce amyloid formation and affected the amyloidogenic properties of amylin [98, 102], thus precluding it as a suitable label for monitoring fibrillogenesis.

The other molecule used to detect amyloid fibrils is thioflavin T (ThT).[103] ThT is a thiazine dye that has a maximal excitation at 385 nm and emission at 445 nm. When attached to amyloid fibrils however, the maximum excitation is 450 nm and the emission is enhanced at 485 nm.[103] The ThT assay is thus one of the most widespread assays used to detect the fibrillar species of amylin [69, 104] and also to screen molecules as potential inhibitors of amylin fibril formation.[60, 65, 74, 90, 98, 105, 106] However, to date, the exact mechanism of ThT binding to amyloid fibrils is yet to be determined. One hypothesis draws on the fact that ThT has both polar (the benzothiazole group containing nitrogen and sulphur) and hydrophobic (the dimethylamino group attached to a phenyl group) regions thereby allowing micelle formation in an aqueous environment.[107] The positively charged nitrogen pointing outside could then hydrogen bond to hydroxyl groups on amyloid fibrils, causing a change in excitation leading to enhanced fluorescence emission.[107] Although the ThT assay is very simple to perform, it does not yield quantitative data and could produce false positive results in the presence of amorphous aggregates.[99] Although Congo red and ThT can detect amylin aggregates, it does not indicate if these aggregates are the oligomeric or fibrillar species.

To this end, microscopy techniques increased in popularity and transmission electron microscopy (TEM) became the technique of choice for visualizing amylin fibrils. Similar to the previous two techniques, TEM was used to identify the shortest fragment of amylin that formed typical amyloid fibrils [36, 47], to assess if modifications of the amylin sequence could alter its amyloidogenic potential [22, 61, 100], to follow amylin aggregation [68, 69, 104], and hence to assess the potential of molecules as inhibitors of amylin fibril formation.[37, 60, 64, 65, 98, 106, 108] Although it is relatively easy to prepare the sample grids for TEM, image analysis requires a certain degree of skill and can be quite time-consuming with each grid taking hours to be visually assessed. Since a very small volume of sample is used on each grid, fibrils can be missed leading to false negative results. However, scanning transmission electron microscopy (STEM) made a significant contribution to understanding the conformational changes during amylin agrgegation as it was the first technique used to determine the size of amylin aggregates that form.[45, 109] Some of the ground-breaking data garnered from STEM are that the amylin protofibril is 5 nm in width, higher order fibrils are formed by coiling of two protofibrils with a 25 nm axial cross-over repeat and are 8 nm in width, and that each 1 nm of protofibril length contains 2.6 human amylin molecules.[109] In addition, STEM-generated data were used in part to predict previously described models for β-sheet formation.[40, 41]

The other technique that allows visualization of amylin fibrils is atomic force microscopy (AFM). This technique was used to visualize fibril formation from full length amylin as well as a fragment of amylin that is homologous to the 20-29 region, and to size the aggregates that formed.[52, 110] One of the significant findings of AFM-based studies on amylin is that fibrils grow at a rate of 1.1 nm/minute and that the growth of the fibril is bidirectional.[52] The drawback to this technique is that it is not quantitative, it is labor-intensive, and samples must be adsorbed to a mica surface in order to monitor fibril growth over time. The latter drawback is a cause for concern since it has been reported that the type of amylin fibrils that form in the presence of a mica surface is significantly different in morphology from that formed free in solution.[52, 110]

Since amylin aggregates adopt a β-sheet structure, techniques such as circular dichroism (CD) and Fourier transform infrared spectroscopy (FT-IR) that are able to give insight into the secondary structure of the peptide were extensively used. Circular dichroism (CD) is based on the concept that random coil structures have a maximum absorbance at 220 nm and minimum at 200 nm, the α-helix state absorbs maximally between 190-195 nm with a minimum absorbance between 208-222 nm, whilst β-sheets have a maximum absorbance between 195-200 nm and a minimum between 215-220 nm.[37, 61] FT-IR spectroscopy is similar to CD in that it also uses differences in absorbance to identify the secondary structure of amylin.[13, 35, 63, 98] A maximum absorbance at 1625-1630 cm^{-1} indicates the presence of β-sheets, whereas a maximum absorbance at 1660-1670 cm^{-1} reveals that a random coil structure is present.[13] These peaks are due to the stretching vibration of *C=O* and *C-N* groups and the shift to lower values is an indication of decreased hydrogen bonding interactions between these groups.

Both CD and FT-IR spectroscopy techniques have been employed to determine the amyloidogenic region of amylin, the minimal sequence of amylin that retained fibrillogenic properties [36, 38, 39, 44, 47], and to monitor amylin aggregation and hence to elucidate the effect of potential inhibitors on the secondary structure of amylin.[13, 22, 37, 61, 64, 65, 68, 100, 104, 105, 108, 111] Interestingly, CD was one of the earliest techniques used to determine that the oligomeric form of amylin is in a β-sheet conformation.[111] Although CD and FT-IR spectroscopy are easy to perform and can accurately determine the secondary structure of amylin, these techniques suffer a major drawback when used as a screening technique for potential inhibitors of amylin-induced cytotoxicity. This is due to the

observation that both the oligomeric and fibrillar forms of amylin are in a β-sheet conformation and thus these techniques cannot differentiate between these two species of amylin.[51, 111] Since it is widely accepted that the oligomeric form of amylin is cytotoxic whilst the fibrillar form is non-toxic [67-73], neither CD nor FT-IR spectroscopy can be exclusively used to screen inhibitors of amylin-mediated cytotoxicity.

The sedimentation/precipitation assay is another technique that has been employed to determine the effect of peptides and other compounds on amylin fibril formation.[37, 98, 105] Initially this technique made use of the intrinsic fluorescence of tyrosine.[37] At specific time points, peptide samples are centrifuged and emission spectra of the supernatant are documented to determine the amount of amylin that has not precipitated and thus the amount of amylin that has aggregated can be ascertained.[37] An improved version of this assay made use of trace amounts of radio-labeled amylin, which are added to native amylin in the presence or absence of potential inhibitors.[98] After centrifugation, the amount of radio-labeled amylin remaining in the supernatant is ascertained, hence allowing the amount of amylin that has been used for fibril formation to be calculated. Although this assay cannot differentiate between fibrils and oligomers, it has been used in conjunction with other assays to evaluate the potential of compounds as inhibitors of amylin-induced cytotoxicity. [37, 98, 105]

Thus, except for AFM, all previously mentioned techniques cannot solely identify amylin oligomers and since the oligomer is the toxic species [67-73], these techniques cannot be used to evaluate compounds as potential inhibitors of amylin-mediated cytotoxicity.

The technique that clearly identifies the suitability of a compound as a potential therapeutic agent for type II diabetes is the cytotoxicity assay. This assay is conducted by exposing mammalian cells to amylin alone or mixtures of amylin and potential inhibitors, and evaluating cell viability after a set period of time. The following cell lines have been used for assessing inhibition of amylin-mediated cytotoxicity, PC12 (rat phaeochromocytoma cells), HIT-T5 (Syrian Hamster *beta* cells), HTB-14 (human glioblastoma/astrocytoma cells) and RIN-5F (rat pancreatic *beta* cells).[22, 36, 37, 60-62, 64, 65, 87, 88, 98, 105, 108, 112] To date, the RIN-5F cell line is the most commonly utilized for testing inhibitors of amylin-mediated toxicity possibly due to the fact that it is a pancreatic *beta* cell line and hence the target of amylin-mediated cytotoxicity as would occur in an *in vivo* system.

The terminal deoxynucleotidyl transferase-mediated dUTP nick-end labeling (TUNEL) [71, 72, 91, 113], alamar blue [37, 112, 113], caspase [90], and (3-[4,5-dimethylthiazol-2-yl]-2,5-diphenyl tetrazolium bromide (MTT) [22, 36, 62, 64, 71, 105, 108] assays have been used to assess cytotoxicity, with the TUNEL and caspase assays detecting apoptosis specifically.

The MTT assay is however, the most favored and relies on the fact that mitochondrial dehydrogenase that is present in actively metabolizing cells is able to cleave the tetrazolium salt 3-(4, 5-dimethylthiazol-2-yl)-2, 5-diphenyltetrazolium bromide (MTT) to yield purple formazan crystals. These crystals are thereafter solubilized and spectrophotometrically analyzed to yield quantitative data with respect to cell viability as the amount of purple crystals formed is directly proportional to the amount of viable cells present.[114] An improvement on the MTT assay is the MTS assay which involves a single-step protocol with the formazan product readily dissolving in cell culture medium thus reducing the assay time.[115] Although the MTT and MTS assay gives quantitative data with regard to the protective function of compounds, it is very expensive and time-consuming as it is dependent on the growth rate of a particular cell line.

To the best of our knowledge, the only other cell-based technique for monitoring inhibition of amylin-mediated cytotoxicity makes use of fluorescence microscopy. This technique involves use of fluorescent-labeled amylin (Bodipy-amylin) and a fluorescent cellular membrane marker (Texas Red-DHPE), and cell imaging using a confocal microscope.[101] Once cells are exposed to amylin and the test compound, this technique allows detection of any changes in cell morphology that would indicate cell death. One of the most defining features of amylin-mediated cytotoxicity is the loss of cellular membrane integrity and this can be easily visualized using fluorescent-labeled amylin and a fluorescent cell membrane marker. Although this type of investigation gives excellent qualitative data, it has a few drawbacks. As with the cytotoxicity assay discussed earlier, this technique requires growth of mammalian cell lines which is both expensive and time-consuming. It is also critical to ensure that the fluorescent label does not interfere with the aggregation kinetics and toxic properties of amylin. It is therefore not feasible to use fluorescence microscopy as a screening technique for inhibitors of amylin-mediated toxicity.

Seeing as cell-based systems can be quite time-consuming and labor intensive, and that no cell-free technique can be used exclusively to detect the oligomeric form of amylin, it is quite evident that a breakthrough is needed in development of a technique that would allow efficient screening of potential inhibitors of amylin-mediated cytotoxicity.

2.5 Inhibitors of amylin-mediated cytotoxicity

The intitial strategy to design inhibitors of amylin-mediated cytotoxicity was based on the hypothesis that generation of ROS is the mechanism of toxicity. To circumvent the toxic effect of amylin-generated ROS, a number of quinone derivatives that were known to scavenge free radicals were evaluated.[60] However, it was found that only rifampicin and its analogs *p*-benzoquinone and hydroquinone inhibited the toxic effect of amylin whereas other anti-oxidants with scavenging ability did not exhibit any inhibitory effect on amylin toxicity.[60] This study was the first to observe that an inhibitor (rifampicin) could bind to amylin aggregates and prevent its attachment to the cell surface.[60] It was thus suggested that rifampicin and its analogs could have a dual mechanism to exert their protective function, preventing amylin-cell interaction and also scavenging ROS.[60] The thiol anti-oxidants *N*-acetyl-L-cysteine, dithiothreitol, and the reduced form of glutathione were also found to significantly decrease amylin-mediated apoptosis whereas the free radical scavengers catalase and *n*-propyl gallate did not.[116] These results suggested that a protective function can be achieved by inhibiting the signalling pathways that are regulated by the redox state of thiol-containing molecules as these could be responsible for amylin-induced cytotoxicity.[116]

Thus, although amylin-mediated toxicity involves generation of ROS, as stated previously the toxic oligomeric species of amylin facilitates membrane disruption and could trigger a number of events that lead to apoptosis and cell death.[67, 94] To this end a significant amount of research focused on the core problem, inhibiting formation of the toxic species of amylin.

Based on the finding that heteroaromatic interactions between amylin and polycyclic compounds resulted in geometric constraints that reduced fibrillogenesis, Aitken *et al.* (2003) highlighted the potential of polycyclic compounds as inhibitors of amylin-mediated cytotoxicity by reporting that Congo red, acridine orange and tetracycline could reduce amylin fibrillogenesis (Figure 2.6).[98] However, cytotoxicity testing was only performed with Congo red as it had no intrinsic toxicity and two separate studies found that Congo red reduced amyloid formation and ROS production, subsequently decreasing *beta* cell apoptosis.[98, 102] Another polycyclic compound, phenol red (Figure 2.6), was also found to reduce amylin-mediated cytotoxicity on *beta* cells, once again highlighting the role that heteroaromatic interactions have in inhibiting formation of amylin fibrils.[108]

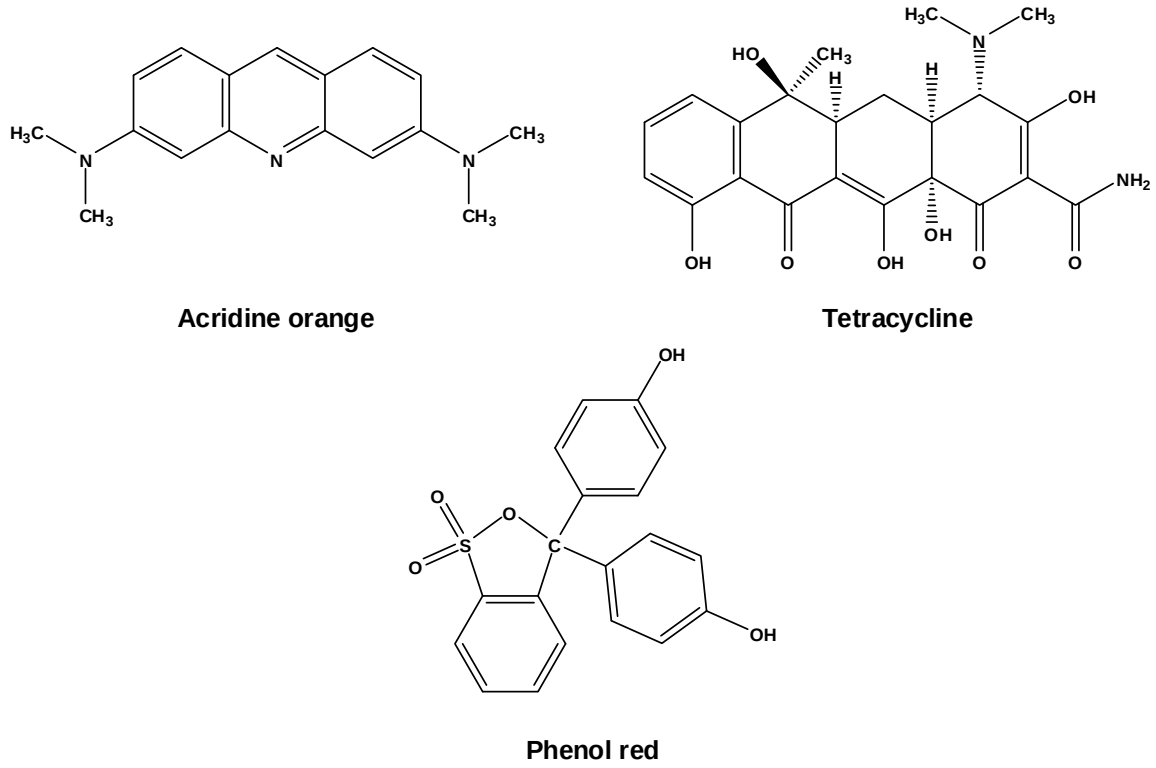

Figure 2.6 Structures of acridine orange, tetracycline and phenol red. Adapted from Aitken *et al.* (2003) and Gazit (2005).[98, 117]

The polyphenolic compound resveratrol that is found in grapes and red wine was also shown to significantly inhibit amylin fibril formation and the associated cytotoxicity [118]. Based on replica-exchange molecular-dynamics simulations, it was proposed that resveratrol reduces fibrillogenesis by preventing lateral growth of the amylin β-sheet.[119] A recent review indicated that even though resveratrol could have an impact on diabetes by a multitude of mechanisms as observed from *in vitro* testing, few clinical human trials have been conducted possibly due to its poor bioavailability.[120] To date, there is only one peer-reviewed human clinical trial that monitored the effect of resveratrol on insulin sensitivity in type II diabetes.[121] Although it was found that resveratrol does improve insulin sensitivity and reduces ROS [121], its effect on amyloid formation or inhibition of amylin-mediated cytotoxicity is yet to be monitored in an *in vivo* system.

Interestingly, the only study that has performed *in vivo* testing to evaluate the effect of a known anti-amyloidogenic agent on diabetes was performed by Aitken *et al.* (2010).[73, 122] This study made use of transgenic mice and demonstrated that tetracycline (Figure 2.6) could delay onset and progression of diabetes.[73] However, to truly probe whether tetracycline acts by inhibiting amyloid formation, histopathological analysis would have been necessary and it is unfortunate that this type of examination was not performed.

Extending the search for molecules that could prevent amylin agggregation and its subsequent cytotoxicity, attention turned to peptides since it has low toxicity, high specificity and thus could be a viable option as a therapeutic agent. Since analysis of the rat amylin sequence implied that the unique presence of proline residues could be responsible for the lack of amyloid formation in rodents, the design of an inhibitor containing a proline substitution was encouraged. With this in mind, Abedini *et al.* (2007) synthesized full length amylin but substituted the serine at position 26 with proline and found that this modified peptide could bind to amylin and prevent fibril formation.**[**123**]** A possible explanation for this observation is that proline is known to induce *β*-turns in peptides, and since fibril growth requires a *β*-sheet conformation of incoming amylin chains, a modified bent peptide will therefore disrupt the free stacking of *β*-sheet amylin molecules.[124]. Although this modified form of amylin inhibited amylin-mediated cytotoxicity, another amylin derivative that contains three substitutions with proline at residues 25, 28 and 29 was already undergoing clinical trials.[125-138] This amylin derivative was found to reduce blood glucose levels by decreasing glucagon secretion. This derivative was initially named symlin and thereafter marketed as pramlintide, and is currently used as an adjunct to insulin in the management of type II diabetes.[125-138] However, it should be noted that this peptide has not been evaluated as an inhibitor of amylin aggregation or amylin-mediated cytotoxicity.

However, two other therapeutic agents of diabetes, Metformin and Rosiglitazone, were evaluated in an *in vivo* system to determine their effect on amyloid formation.[139] One of the therapeutic functions of Metformin and Rosiglitazone is to increase insulin sensitivity and hence reduce secretion of insulin from pancreatic *beta* cells.[139] In this study, transgenic mice that express amylin were treated with either Metformin or Rosiglitazone for twelve months and subsequent histopathological analysis revealed that these therapeutic agents significantly reduced the amount of amyloid deposits that formed in the pancreata of the treated animals.[139] As previously mentioned, amylin is secreted together with insulin from pancreatic *beta* cells and thus it was suggested that both Metformin and Rosiglitazone could possibly reduce amyloid formation by decreasing the amount of amylin secreted.[23, 139] This study thus highlights the need for developing molecules that could either prevent amylin secretion or reduce amyloid formation from amylin.

Since full length amylin is difficult to chemically synthesize, attention shifted to shorter peptide sequences as potential inhibitors of amylin aggregation and subsequent amylin-mediated cytotoxicity. A breakthrough was made whem Rijkers and coworkers (2002) found that the introduction of *N*-alkylated amino acids or ester functionalities into peptide sequences allowed the peptides to behave as *β*-sheet inhibitors that prevented the formation of toxic amylin *β*-sheets.[140]

As depicted in Figure 2.7A, single amylin strands form *β*-sheets by hydrogen bonding between *N*-*H* and *C*=*O* dipoles that point outward from the amylin backbone. However, peptides containing *N*-alkylated amino acids and which exhibit a *β*-sheet conformation are able to bind to native amylin and prevent attachment of any further peptide strands by disrupting the hydrogen-bonding capacity of the peptide and by causing steric hindrance (Figure 2.7B).

The presence of *N*-methylated (*N*-Me) amino acids improves the biostability of the peptide by being resistant to proteolysis and it also increases the membrane permeablity of the peptide.[141] Employing this approach, numerous amylin derivatives that incorporated *N*-methylated amino acids were synthesized as potential inhibitors of fibril formation. The first of these inhibitors having the sequence SNNF(*N*-Me)GA(*N*-Me)ILSS was reported by Kapurniotu *et al*. in 2002.[64] This amylin derivative was shown to inhibit aggregation of the 20-29 region of amylin, and prevented its cytotoxicity.[64] It was also found that the presence of *N*-methylations allowed the peptide to exist in an ordered *β*-sheet structure which is of importance since a stable conformation is crucial if the peptide is to be used as an inhibitor.[64] However, it should be noted that the effects of this amylin derivative was not assessed using full length amylin. The amylin derivatives that were evaluated as potential inhibitors of cytotoxicity caused by full-length human amylin are presented in Table 2.2.

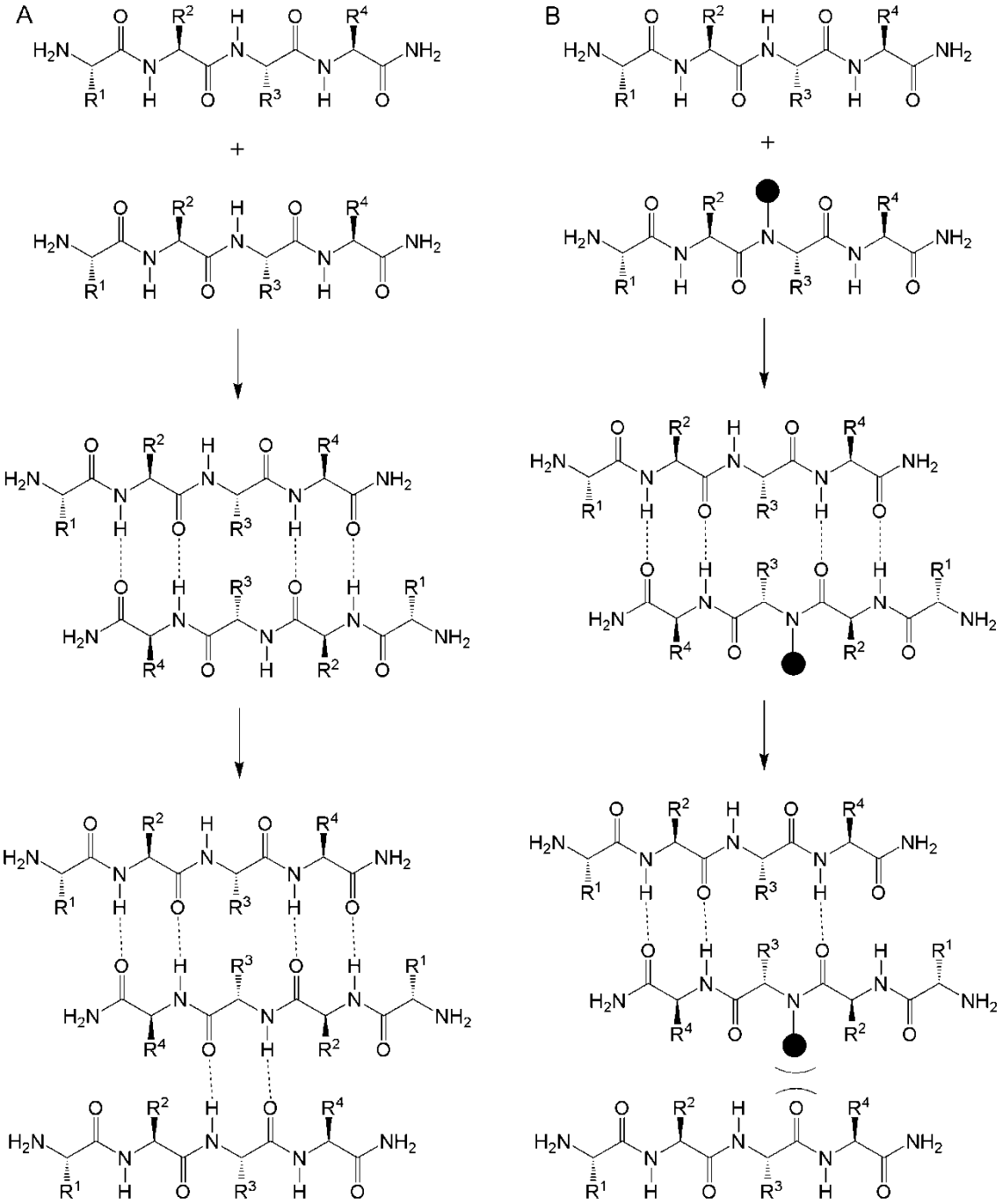

Figure 2.7 Illustration of how (A) unmodified amino acids can form *β*-sheet structures via hydrogen bonding (represented as ---) and how (B) *N*-methylations (expressed as dark circles) replaces hydrogen in a polypeptide and thus prevent *β*-sheet stacking. R^1 – R^4 represent the side groups of the amino acids. Adapted from Rijkers *et al.* (2002).[140]

Table 2.2 Amylin derivatives as potential inhibitors of cytotoxicity caused by full-length human amylin

Amylin derivative	Position of *N*-methylated residue	Decrease in Cytotoxicity	Cell line used	Reference
$Amylin_{20-25}$		25%	RIN-1056A	[37]
$Amylin_{24-29}$		0%	RIN-1056A	[37]
$Amylin_{12-17}$		0%	RIN-1056A	[112]
$Amylin_{15-20}$		0%	RIN-1056A	[112]
$Amylin_{22-27}$	23 and 25	20%	RIN 5fm	[65]
$Amylin_{1-37}$	24 and 26	50%	RIN 5fm	[105]
$Amylin_{13-18}$		50%	RIN-1056A	[111]
$Amylin_{20-25}$		50%	RIN-1056A	[111]
$Amylin_{3-6}$		45%	RIN 5fm	[142]
$Amylin_{3-6}$	3-5	0%	RIN 5fm	[142]
$Amylin_{9-13}$		40%	RIN 5fm	[142]
$Amylin_{9-13}$	9, 12 and 13	0%	RIN 5fm	[142]
$Amylin_{15-20}$		20%	RIN 5fm	[142]
$Amylin_{15-20}$	15-17 and 19	0%	RIN 5fm	[142]
$Amylin_{22-27}$		40%	RIN 5fm	[142]
$Amylin_{22-27}$	23-27	0%	RIN 5fm	[142]
$Amylin_{29-34}$		50%	RIN 5fm	[142]
$Amylin_{29-34}$	30, 32-34	50%	RIN 5fm	[142]

To the best of our knowledge, no *in vivo* testing was performed using any of the peptide inhibitors mentioned above. It is however noteworthy that two patents have been granted for peptide derivatives of amylin that can prevent amylin aggregation and amylin-mediated cytotoxicity, and which have been suggested as potential therapeutic agents of type II diabetes.[143, 144] However, the first patent was granted in 1996 whilst the second was granted in 2007 and to date, none of the derivatives mentioned have been used in clinical trials.[143, 144] Thus, there still exists the need for more potent peptide-based inhibitors of amylin-mediated cytotoxicity.

In addition to peptide derivatives of amylin, a diverse range of other molecules were more recently assessed as potential inhibitors of amylin aggregation and cytotoxicity. The membrane binding protein annexin A5 was shown to decrease the toxic effect of amylin on rat pancreatic *β*-cells by 90%.[106] Cabaleiro-Lago *et al.* (2009) showed that *N*-isopropylacrylamide:*N*-tert-butylacrylamide (NiPAM:BAM) co-polymeric nanoparticles were able to decrease amylin aggregation.[145] They suggested that amylin could possibly be adsorbed onto the nanoparticle surface thereby decreasing the available amount in solution and thus increasing the lag time of fibrillation.[145] It was also found that the sulfonated triphenyl methane derivative, acid fuchsin, decreased amylin-mediated toxicity by approximately 80%.[146] Rigacci *et al.* (2010) showed that oleuropein aglycon, the main phenolic component of extra virgin olive oil, reduced the toxicity of amylin by approximately 20%.[147] However, these molecules need to be scrutinized further to ascertain its biostability and more importantly whether it is biodegradable. It is noteworthy that the toxicity of nanoparticles have been reviewed twice with the conclusion being drawn that nanoparticles are not easily cleared from an *in vivo* system and thus could lead to toxicity.[148, 149]

2.6 Amylin synthesis

At an early stage, it was found that amyloidogenic peptides from different suppliers have diverse properties [150], which was substantiated by a more recent study, that demonstrated the presence of impurities in commercially available amylin[151] It was also reported that the presence of impurities can affect the aggregation kinetics of amyloidogenic peptides [100, 152, 153], thus highlighting the need for synthetic strategies that yielded pure protein. To this end, Raleigh *et al.* (2005) published the first synthetic strategy for amylin.[154] They made use of pseudoproline derivatives and to date there have been numerous improvements to their method.[104, 155-158] It is therefore deemed critical that a more cost effective and efficient synthetic strategy is required to generate amylin of a quality that would afford reproducible results.

2.7 Conclusion

It is thus quite evident that there exists a gap in respect to novel techniques that could enable fast and cheap screening of potential therapeutic agents for type II diabetes. That being said, although much progress has been made in respect to the type of inhibitor that could be used, peptide derivatives that could inhibit amylin-induced cytotoxicity could be developed further in a bid to find a potential therapeutic agent for type II diabetes. Most importantly, to gain more insight into amylin aggregation dynamics and also to screen potential inhibitors of amylin-mediated cytotoxicity, a cost effective strategy to acquire sufficiently pure amylin is deemed critical.

2.8 References

1. Reynaud, E., *Protein misfolding and degenerative diseases.* Nature Education, 2010. **3**(9): p. 28.
2. Sacchettini, J.C., and Kelly, J. W., *Therapeutic strategies for human amyloid diseases.* Nature Reviews Drug Discovery, 2002. **1**(4): p. 267-275.
3. Ghiso, J., and Frangione, B., *Amyloidosis and Alzheimer's disease.* Advanced Drug Delivery Reviews, 2002. **54**(12): p. 1539-1551.
4. Rahimi, F., Shanmugam, A., and Bitan, G., *Structure-function relationships of pre-fibrillar protein assemblies in Alzheimer's disease and related disorders.* Current Alzheimer Research, 2008. **5**(3): p. 319-341.
5. Broersen, K., Rousseau, F., and Schymkowitz, J., *The culprit behind amyloid beta peptide related neurotoxicity in Alzheimer's disease: oligomer size or conformation?* Alzheimers Research and Therapy, 2010. **2**(4): p. 1-14.
6. Miller, Y., Ma, B., and Nussinov, R., *Polymorphism in Alzheimer A-beta amyloid organization reflects conformational selection in a rugged energy landscape.* Chemical Reviews, 2010. **110**(8): p. 4820-4838.
7. Nakamura, T., and Lipton, S. A., *Redox regulation of mitochondrial fission, protein misfolding, synaptic damage, and neuronal cell death: potential implications for Alzheimer's and Parkinson's diseases.* Apoptosis, 2010. **15**(11): p. 1354-1363
8. Humpel, C., *Identifying and validating biomarkers for Alzheimer's disease.* Trends in Biotechnology, 2011. **29**(1): p. 26-32.
9. Marchesi, V.T., *Alzheimer's dementia begins as a disease of small blood vessels, damaged by oxidative-induced inflammation and dysregulated amyloid metabolism: implications for early detection and therapy.* FASEB Journal, 2011. **25**(1): p. 5-13.
10. Dillin, A., and Cohen, E., *Ageing and protein aggregation-mediated disorders: from invertebrates to mammals.* Philosophical Transactions of the Royal Society B-Biological Sciences, 2011. **366**(1561): p. 94-98.
11. Lee, S., Lim, H., Masliah, E., and Lee, H., *Protein aggregate spreading in neurodegenerative diseases: Problems and perspectives.* Neuroscience Research, 2011. **70**(4): p. 339-348.
12. Brown, K., and Mastrianni, J. A., *The Prion diseases.* Journal of Geriatric Psychiatry and Neurology, 2010. **23**(4): p. 277-298.
13. Kapurniotu, A., *Amyloidogenicity and cytotoxicity of islet amyloid polypeptide.* Biopolymers, 2001. **60**(6): p. 438-459.
14. Qiu, W.Q., and Folstein, M. F., *Insulin, insulin-degrading enzyme and amyloid-beta peptide in Alzheimer's disease: review and hypothesis.* Neurobiology of Aging, 2006. **27**(2): p. 190-198.
15. Haataja, L., Gurlo, T., Huang, C. J., and Butler, P. C., *Islet amyloid in type 2 diabetes, and the toxic oligomer hypothesis.* Endocrine Reviews, 2008. **29**(3): p. 303-316.
16. Khemtemourian, L., Killian, J. A., Hoppener, J. W. M., and Engel, M. F. M., *Recent insights in islet amyloid polypeptide-induced membrane disruption and its role in beta-cell death in type 2 diabetes mellitus.* Experimental Diabetes Research, 2008. **2008**: p. 421287.
17. Ahmad, E., Ahmad, A., Singh, S., Arshad, M., Khan, A. H., and Khan, R. H., *A mechanistic approach for islet amyloid polypeptide aggregation to develop anti-amyloidogenic agents for type-2 diabetes.* Biochimie, 2011. **93**(5): p. 793-805.
18. Westermark, P., *Amyloid in the islets of Langerhans: thoughts and some historical aspects.* Upsala Journal of Medical Sciences, 2011. **116**(2): p. 81-9.
19. WHO. *Diabetes Fact sheet*. Accessed: 8 May 2012. Available from: http://www.who.int/mediacentre/factsheets/fs312/en/index.html.
20. Ganong, W.F., *Review of Medical Physiology*. Toronto: Lange Medical Books/McGraw Hill, ed 21 (2003).
21. Cooper, G.J.S., Willis, A.C., Clark, A., Turner, R.C., Sim, R.B. and Reid, K.B.M., *Purification and characterization of a peptide from amyloid-rich pancreases of type 2 diabetic patients.* Proceedings of the National Academy of Science, 1987. **84**: p. 8628-8632.
22. Krampert, M., Bernhagen, J., Schmucker, J., Horn, A., Schmauder, A., Brunner, H., Voelter, W. and Kapurniotu, A., *Amyloidogenicity of recombinant human pro-islet amyloid polypeptide (ProIAPP).* Chemistry & Biology, 2000. **7**: p. 855-871.
23. Martin, C., *The physiology of amylin and insulin: maintaining the balance between glucose secretion and glucose uptake.* The Diabetes Educator, 2006. **32**: p. 101-104.
24. Kogire, M., Ishizuka, J., Thompson, J. C., and Greeley, G. H., *Inhibitory-action of islet amyloid polypeptide and calcitonin gene-related peptide on release of insulin from the isolated perfused rat pancreas.* Pancreas, 1991. **6**(4): p. 459-463.
25. Degano, P., Silvestre, R. A., Salas, M., Peiro, E., and Marco, J., *Amylin inhibits glucose-induced insulin-secretion in a dose-dependent manner - study in the perfused rat pancreas.* Regulatory Peptides, 1993. **43**(1-2): p. 91-96.

26. Rink, T.J., Beaumont, K., Koda, J., and Young, A., *Structure and biology of amylin.* Trends in Pharmacological Sciences, 1993. **14**(4): p. 113-118.
27. Zhu, T., Wang, Y., He, B., Zang, J., He, Q., and Zhang, W., *Islet amyloid polypeptide acts on glucose-stimulated beta cells to reduce voltage-gated calcium channel activation, intracellular Ca2+ concentration, and insulin secretion.* Diabetes-Metabolism Research and Reviews, 2011. **27**(1): p. 28-34.
28. Cooper, G.J.S., *Amylin compared with calcitonin-gene-related peptide - structure, biology, and relevance to metabolic disease.* Endocrine Reviews, 1994. **15**(2): p. 163-201.
29. Kruger, D.F., Gatcomb, P. M., and Owen, S. K., *Clinical implications of amylin and amylin deficiency.* Diabetes Educator, 1999. **25**(3): p. 389-397.
30. Silvestre, R.A., Rodriguez-Gallardo, J., Jodka, C., Parkes, D. G., Pittner, R. A., Young, A. A., and Marco, J., *Selective amylin inhibition of the glucagon response to arginine is extrinsic to the pancreas.* American Journal of Physiology-Endocrinology and Metabolism, 2001. **280**(3): p. E443-E449.
31. Akesson, B., Panagiotidis, G., Westermark, P., and Lundquist, I., *Islet amyloid polypeptide inhibits glucagon release and exerts a dual action on insulin release from isolated islets.* Regulatory Peptides, 2003. **111**(1-3): p. 55-60.
32. Hull, R.L., Andrikopoulos, S., Verchere, C. B., Vidal, J., Wang, F., Cnop, M., Prigeon, R. L., and Kahn, S. E., *Increased dietary fat promotes islet amyloid formation and beta-cell secretory dysfunction in a transgenic mouse model of islet amyloid.* Diabetes, 2003. **52**(2): p. 372-379.
33. Hoppener, J.W.M., Jacobs, H. M., Wierup, N., Sotthewes, G., Sprong, M., de Vos, P., Berger, R., Sundler, F., and Ahren, B., *Human islet amyloid polypeptide transgenic mice: in vivo and ex vivo models for the role of hIAPP in type 2 diabetes mellitus.* Experimental Diabetes Research, 2008.
34. Kodali, R., and Wetzel, R., *Polymorphism in the intermediates and products of amyloid assembly.* Current Opinion in Structural Biology, 2007. **17**: p. 48–57.
35. Westermark, P., Engstrom, U., Johnson, K. H., Westermark, G.T. and Betsholtz, C., *Islet amyloid polypeptide: pinpointing amino acid residues linked to amyloid fibril formation.* Proceedings of the National Academy of Science, 1990. **87**: p. 5036-5040.
36. Tenidis, K., Waldner, M., Bernhagen, J., Fischle, W., Bergmann, M., Weber, M., Merkle, M., Voelter, W., Brunner, H. and Kapurniotu, A., *Identification of a Penta- and Hexapeptide of Islet Amyloid Polypeptide (IAPP) with Amyloidogenic and Cytotoxic Properties.* Journal of Molecular Biology, 2000. **295**: p. 1055-1071.
37. Scrocchi, L.A., Chen, Y., Waschuk, S., Wang, F., Cheung, S., Darabie, A.A., McLaurin, J. and Fraser, P.E., *Design of peptide-based inhibitors of human islet amyloid polypeptide fibrillogenesis.* Journal of Molecular Biology, 2002. **318**: p. 697–706.
38. Mazor, Y., Gilead, S., Benhar, I., and Gazit, E., *Identification and characterization of a novel molecular-recognition and self-assembly domain within the islet amyloid polypeptide.* Journal of Molecular Biology, 2002. **322**(5): p. 1013-1024.
39. Jaikaran, E.T.A.S., Higham, C.E., Serpell, L.C., Zurdo, J., Gross, M., Clark, A. and Fraser, P.E., *Identification of a novel human islet amyloid polypeptide b-sheet domain and factors influencing fibrillogenesis.* Journal of Molecular Biology, 2001. **308**: p. 515-525.
40. Kajava, A.V., Aebi, U., and Steven, A. C., *The parallel superpleated beta-structure as a model for amyloid fibrils of human amylin.* Journal of Molecular Biology, 2005. **348**(2): p. 247-252.
41. Luca, S., Yau, W., Leapman, R., and Tycko, R., *Peptide conformation and supramolecular organization in amylin fibrils: constraints from solid-state NMR.* Biochemistry, 2007. **46**(47): p. 13505-13522.
42. Shim, S.H., Gupta, R., Ling, Y. L., Strasfeld, D. B., Raleigh, D. P., and Zanni, M. T., *Two-dimensional IR spectroscopy and isotope labeling defines the pathway of amyloid formation with residue-specific resolution.* Proceedings of the National Academy of Sciences of the United States of America, 2009. **106**(16): p. 6614-6619.
43. Gazit, E., *A possible role for pi-stacking in the self-assembly of amyloid fibrils.* Faseb Journal, 2002. **16**(1): p. 77-83.
44. Nilsson, M.R., and Raleigh, D.P., *Analysis of amylin cleavage products provides new insights into the amyloidogenic region of human amylin.* Journal of Molecular Biology, 1999. **294**: p. 1375-1385.
45. Goldsbury, C., Goldie, K., Pellaud, J., Seelig, J., Frey, P., Muller, S. A., Kistler, J., Cooper, G. J. S., and and U. Aebi, *Amyloid fibril formation from full-length and fragments of amylin.* Journal of Structural Biology, 2000. **130**(2-3): p. 352-362.
46. Azriel, R., and Gazit, E., *Analysis of the structural and functional elements of the minimal active fragment of islet amyloid polypeptide (IAPP) - An experimental support for the key role of the phenylalanine residue in amyloid formation.* Journal of Biological Chemistry, 2001. **276**(36): p. 34156-34161.
47. Scrocchi, L.A., Ha, K., Chen, Y., Wu, L., Wang, F., and Fraser, P. E., *Identification of minimal peptide sequences in the (8-20) domain of human islet amyloid polypeptide involved in fibrillogenesis.* Journal of Structural Biology, 2003. **141**(3): p. 218-227.

48. Galzitskaya, O.V., Garbuzynskiy, S. O., and Lobanov, M. Y., *Is it possible to predict amyloidogenic regions from sequence alone?* Journal of Bioinformatics and Computational Biology, 2006. **4**(2): p. 373-388.
49. Zhang, Z., Chen, H., and Lai, L., *Identification of amyloid fibril-forming segments based on structure and residue-based statistical potential.* Bioinformatics, 2007. **23**(17): p. 2218-2225.
50. Lansbury, P.T., *The chemistry of scrapie infection - implications of the ice-9 metaphor.* Chemistry & Biology, 1995. **2**(1): p. 1-5.
51. Kayed, R., Bernhagen, J., Greenfield, N., Sweimeh, K., Brunner, H., Voelter, W. and Kapurniotu, A., *Conformational transitions of islet amyloid polypeptide (IAPP) in amyloid formation in vitro.* Journal of Molecular Biology, 1999. **287**: p. 781-796.
52. Goldsbury, C., Kistler, J., Aebi, U., Arvinte, T. and Cooper, G.J.S., *Watching amyloid fibrils grow by time-lapse atomic force microscopy.* Journal of Molecular Biology, 1999. **285**: p. 33-39.
53. Benzinger, T.L.S., Gregory, D.M., Burkoth, T.S., Miller-Auer, H., Lynn, D.G., Botto, R.E. and Meredith, S.C., *Two-dimensional atructure of â-amyloid(10-35) fibrils.* Biochemistry, 2000. **39**: p. 3491-3499.
54. Tycko, R., *Progress towards a molecular-level structural understanding of amyloid fibrils.* Current Opinion in Structural Biology, 2004. **14**: p. 96-103.
55. Jayasinghe, S.A., and Langen, R., *Lipid membranes modulate the structure of islet amyloid polypeptide.* Biochemistry, 2005. **44**: p. 12113-12119.
56. Nelson, R., Sawaya, M.R., Balbirnie, M., Madsen, A., Riekel, C., Grothe R. and Eisenberg, D., *Structure of the cross-b spine of amyloid-like fibrils.* Nature, 2005. **435**: p. 773-778.
57. Dobson, C.M., *Protein folding and misfolding.* Nature, 2003. **426**(6968): p. 884-890.
58. Mattson, M.P., and Goodman, Y., *Different amyloidogenic peptides share a similar mechanism of neurotoxicity involving reactive oxygen species and calcium.* Brain Research, 1995. **676**: p. 219-224.
59. Mirzabekov, T.A., Lin, M. and Kagan, B.L., *Pore formation by the cytotoxic islet amyloid peptide amylin.* The Journal of Biological Chemistry, 1996. **271**: p. 1988–1992.
60. Tomiyama, T., Kaneko, H., Kataoka, K., Asano, S. and Endo, N., *Rifampicin inhibits the toxicity of pre-aggregated amyloid peptides by binding to peptide fibrils and preventing amyloid-cell interaction.* Biochemical Journal, 1997. **322**: p. 859-865.
61. Kapurniotu, A., Bernhagen, J., Greenfield, N., Al-Abed, Y., Teichberg, S., Frank, R.W., Voelter, W. and Bucala, R., *Contribution of advanced glycosylation to the amyloidogenicity of islet amyloid polypeptide.* European Journal of Biochemistry, 1998. **251**: p. 208-216.
62. Bai, J., Saafi, E.L., Zhang, S. and Cooper, G.J.S., *Role of Ca2+ in apoptosis evoked by human amylin in pancreatic islet b-cells.* Biochemical Journal, 1999. **343**: p. 53-61.
63. Hiddinga, H.J., and Eberhardt, N.L., *Intracellular amyloidogenesis by human islet amyloid polypeptide induces apoptosis in COS-1 cells.* American Journal of Pathology, 1999. **154**(4): p. 1077-1088.
64. Kapurniotu, A., Schmauder, A. and Tenidis, K., *Structure-based design and study of non-amyloidogenic, double n-methylated IAPP amyloid core sequences as inhibitors of IAPP amyloid formation and cytotoxicity.* Journal of Molecular Biology, 2002. **315**: p. 339-350.
65. Tatarek-Nossol, M., Yan, L., Schmauder, A., Tenidis, K., Westermark, G., and Kapurniotu, A., *Inhibition of hIAPP amyloid-fibril formation and apoptotic cell death by a designed hiapp amyloid-core-containing hexapeptide.* Chemistry & Biology, 2005. **12**: p. 797–809.
66. Yan, L., Velkova, A., Tatarek-Nossol, M., Andreetto, E., and Kapurniotu, A., *IAPP mimic blocks Ab cytotoxic self-assembly: cross-suppression of amyloid toxicity of Ab and IAPP suggests a molecular link between Alzheimers disease and type II diabetes.* Angewandte Chemie International Edition, 2007. **46**: p. 1246 –1252.
67. Janson, J., Ashley, R.H., Harrison, D., McIntyre, S. and Butler, P.C., *The mechanism of islet amyloid polypeptide toxicity is membrane disruption by intermediate-sized toxic amyloid particles.* Diabetes, 1999. **48**: p. 491–498.
68. Anguiano, M., Nowak, R.J. and Lansbury, P.T., *Protofibrillar islet amyloid polypeptide permeabilizes synthetic vesicles by a pore-like mechanism that may be relevant to type II diabetes.* Biochemistry, 2002. **41**: p. 11338-11343.
69. Kayed, R., Sokolov, Y., Edmonds, B., McIntire, T.M., Milton, S.C., Hall, J.E. and Glabe, G.C., *Permeabilization of lipid bilayers is a common conformation-dependent activity of soluble amyloid oligomers in protein misfolding diseases.* The Journal of Biological Chemistry, 2004. **279**(45): p. 46363–46366.
70. Konarkowska, B., Aitken, J. F., Kistler, J., Zhang, S. P., and Cooper, G. J. S., *The aggregation potential of human amylin determines its cytotoxicity towards islet beta-cells.* Febs Journal, 2006. **273**(15): p. 3614-3624.
71. Meier, J.J., Kayed, R., Lin, C. Y., Gurlo, T., Haataja, L., Jayasinghe, S., Langen, R., Glabe, C. G., and Butler, P. C., *Inhibition of human IAPP fibril formation does not prevent beta-cell death: evidence for distinct actions of oligomers and fibrils of human IAPP.* American Journal of Physiology-Endocrinology and Metabolism, 2006. **291**(6): p. E1317-E1324.

72. Ritzel, R.A., J.J. Meier, C.Y. Lin, J.D. Veldhuis, and P.C. Butler, *Human islet amyloid polypeptide oligomers disrupt cell coupling, induce apoptosis, and impair insulin secretion in isolated human islets.* Diabetes, 2007. **56**(1): p. 65-71.
73. Aitken, J.F., Loomes, K. M., Scott, D. W., Reddy, S., Phillips, A. R. J., Prijic, G., Fernando, C., Zhang, S. P., Broadhurst, R., L'Huillier, P., and Cooper, G. J. S., *Tetracycline treatment retards the onset and slows the progression of diabetes in human amylin/islet amyloid polypeptide transgenic mice.* Diabetes, 2010. **59**(1): p. 161-171.
74. Meier, J.J., Kayed, R., Lin, C., Gurlo, T., Haataja, L., Jayasinghe, S., Langen, R., Glabe, C.G., and Butler, P.C., *Inhibition of human IAPP fibril formation does not prevent beta-cell death: evidence for distinct actions of oligomers and fibrils of human IAPP.* American Journal of Physiology, Endocrinology and Metabolism, 2006. **291**: p. E1317–E1324.
75. Lorenzo, A., Razzaboni, B., Weir, G. C., and Yankner, B. A., *Pancreatic-islet cell toxicity of amylin associated with type-2 diabetes-mellitus.* Nature, 1994. **368**(6473): p. 756-760.
76. Sciacca, M.F.M., Pappalardo, M., Attanasio, F., Milardi, D., La Rosa, C., and Grasso, D. M., *Are fibril growth and membrane damage linked processes? An experimental and computational study of IAPP(12-18) and IAPP(21-27) peptides.* New Journal of Chemistry, 2010. **34**(2): p. 200-207.
77. Demuro, A., Mina, E., Kayed, R., Milton, S. C., Parker, I., and Glabe, C. G., *Calcium dysregulation and membrane disruption as a ubiquitous neurotoxic mechanism of soluble amyloid oligomers.* Journal of Biological Chemistry, 2005. **280**(17): p. 17294-17300.
78. Knight, J.D., and Miranker, A. D., *Phospholipid catalysis of diabetic amyloid assembly.* Journal of Molecular Biology, 2004. **341**(5): p. 1175-1187.
79. Lopes, D.H.J., Meister, A., Gohlke, A., Hauser, A., Blume, A., and Winter, R., *Mechanism of islet amyloid polypeptide fibrillation at lipid interfaces studied by infrared reflection absorption spectroscopy.* Biophysical Journal, 2007. **93**(9): p. 3132-3141.
80. Sparr, E., Engel, M. F. M., Sakharov, D. V., Sprong, M., Jacobs, J., de Kruijff, B., Hoppener, J. W. M., and Killian, J. A., *Islet amyloid polypeptide-induced membrane leakage involves uptake of lipids by forming amyloid fibers.* Febs Letters, 2004. **577**(1-2): p. 117-120.
81. Engel, M.F.M., Yigittop, H., Elgersma, R. C., Rijkers, D. T. S., Liskamp, R. M. J., de Kruijff, B., Hoppener, J. W. M., and Killian, J. A., *Islet amyloid polypeptide inserts into phospholipid monolayers as monomer.* Journal of Molecular Biology, 2006. **356**(3): p. 783-789.
82. Engel, M.F.M., Khemtemourian, L., Kleijer, C. C., Meeldijk, H. J. D., Jacobs, J., Verkleij, A. J., de Kruijff, B., and J.A. Killian, Hoeppener, J. W. M., *Membrane damage by human islet amyloid polypeptide through fibril growth at the membrane.* Proceedings of the National Academy of Sciences of the United States of America, 2008. **105**(16): p. 6033-6038.
83. Engel, M.F.M., *Membrane permeabilization by islet amyloid polypeptide.* Chemistry and Physics of Lipids, 2009. **160**(1): p. 1-10.
84. Bandyopadhyay, U., Das, D., and Banerjee, R. K., *Reactive oxygen species: oxidative damage and pathogenesis.* Current Science, 1999. **77**(5): p. 658-666.
85. Schubert, D., Behl, C., Lesley, R., Brack, A., Dargusch, R., Sagara, Y., and Kimura, H., *Amyloid peptides are toxic via a common oxidative mechanism.* Proceedings of the National Academy of Sciences of the United States of America, 1995. **92**(6): p. 1989-1993.
86. Dash, P. *Cell death*. Accessed: July 2009. Available from: http://www.sgul.ac.uk/depts/immunology/~dash/apoptosis/index.htm.
87. Zhang, S., Liu, J., Saafi, E.L. and Cooper, G.J.S, *Induction of apoptosis by human amylin in RINm5F islet L-cells is associated with enhanced expression of p53 and p21$^{(WAF1=CIP1)}$.* FEBS Letters, 1999. **455**: p. 315-320.
88. Saafi, E.L., Konarkowska, B., Zhang, S., Kistler, J. and Cooper, G.J.S., *Ultrastructural evidence that apoptosis is the mechaism by which human amylin evokes death in RINm5F pancreatic islet cells.* Cell Biology International, 2001. **25**(4): p. 339–350.
89. Zhang, S., Liu, J., MacGibbon, G., Dragunow, M. and Cooper, G.J.S., *Increased expression and activation of c-jun contributes to human amylin-induced apoptosis in pancreatic islet beta-cells.* Journal of Molecular Biology, 2002. **324**: p. 271–285.
90. Zhang, S.P., Liu, H., Yu, H., and Cooper, G. J. S., *Fas-associated death receptor signaling evoked by human amylin in islet beta-cells.* Diabetes, 2008. **57**(2): p. 348-356.
91. Huang, C.J., Haataja, L., Gurlo, T., Butler, A. E., Wu, X. J., Soeller, W. C., and Butler, P. C., *Induction of endoplasmic reticulum stress-induced beta-cell apoptosis and accumulation of polyubiquitinated proteins by human islet amyloid polypeptide.* American Journal of Physiology-Endocrinology and Metabolism, 2007. **293**(6): p. E1656-E1662.
92. Huang, C., Gurlo, T., Haataja, L., Costes, S., Daval, M., Ryazantsev, S., Wu, X., Butler, A. E., and Butler, P. C., *Calcium-activated calpain-2 is a mediator of beta cell dysfunction and apoptosis in type 2 diabetes.* Journal of Biological Chemistry, 2010. **285**(1): p. 339-348.

93. Tucker, H.M., Rydel, R. E., Wright, S., and Estus, S., *Human amylin induces "apoptotic" pattern of gene expression concomitant with cortical neuronal apoptosis.* Journal of Neurochemistry, 1998. **71**(2): p. 506-516.
94. Gurlo, T., Ryazantsev, S., Huang, C. J., Yeh, M. W., Reber, H. A., Hines, O. J., O'Brien, T. D., Glabe, C. G., Butler, P. C., *Evidence for proteotoxicity in beta cells in type 2 diabetes toxic islet amyloid polypeptide oligomers form intracellularly in the secretory pathway.* American Journal of Pathology, 2010. **176**(2): p. 861-869.
95. Lim, Y.A., Rhein, V., Baysang, G., Meier, F., Poljak, A., Raftery, M. J., Guilhaus, M., Ittner, L. M., Eckert, A., and Gotz, J., *A beta and human amylin share a common toxicity pathway via mitochondrial dysfunction.* Proteomics, 2010. **10**(8): p. 1621-1633.
96. Cooper, J.H., *Selective amyloid staining as a function of amyloid composition and structure - histochemical analysis of alkaline congo red, standardized toluidine blue, and iodine methods.* Laboratory Investigation, 1974. **31**(3): p. 232-238.
97. Lansbury, P.T., *In pursuit of the molecular-structure of amyloid plaque - new technology provides unexpected and critical information.* Biochemistry, 1992. **31**(30): p. 6865-6870.
98. Aitken, J.F., Loomes, K.M., Konarkowska, B. and Cooper, G.J.S, *Suppression by polycyclic compounds of the conversion of human amylin into insoluble amyloid.* Biochemical Journal, 2003. **374**: p. 779–784.
99. Nilsson, M.R., *Techniques to study amyloid fibril formation in vitro.* Methods, 2004. **34**(1): p. 151-160.
100. Nilsson, M.R., Driscoll, M., and Raleigh, D. P., *Low levels of asparagine deamidation can have a dramatic effect on aggregation of amyloidogenic peptides: Implications for the study of amyloid formation.* Protein Science, 2002. **11**(2): p. 342-349.
101. Radovan, D., Opitz, N., and Winter, R., *Fluorescence microscopy studies on islet amyloid polypeptide fibrillation at heterogeneous and cellular membrane interfaces and its inhibition by resveratrol.* Febs Letters, 2009. **583**(9): p. 1439-1445.
102. Zraika, S., Hull, R. L., Udayasankar, J., Aston-Mourney, K., Subramanian, S. L., Kisilevsky, R., Szarek, W. A., and Kahn, S. E., *Oxidative stress is induced by islet amyloid formation and time-dependently mediates amyloid-induced beta cell apoptosis.* Diabetologia, 2009. **52**(4): p. 626-635.
103. Levine, H., *Thioflavine T interaction with synthetic Alzheimer's disease beta-amyloid peptides: detection of amyloid aggregation in solution.* Protein Science, 1993. **2**: p. 404-410.
104. Kelly, J.W., Yonemoto, I. T., Kroon, G. J. A., Dyson, H. J., and Balch, W. E., *Amylin proprotein processing generates progressively more amyloidogenic peptides that initially sample the helical state.* Biochemistry, 2008. **47**: p. 9900–9910.
105. Yan, L., Tatarek-Nossol, M., Velkova, A., Kazantzis, A., and Kapurniotu, A., *Design of a mimic of nonamyloidogenic and bioactive human islet amyloid polypeptide (IAPP) as nanomolar affinity inhibitor of IAPP cytotoxic fibrillogenesis.* Proceedings of the National Academy of Science, 2006. **103**(7): p. 2046–2051.
106. Bedrood, S., Jayasinghe, S., Sieburth, D., Chen, M., Erbel, S., Butler, P. C., Langen, R., and Ritzel, R. A., *Annexin A5 directly interacts with amyloidogenic proteins and reduces their toxicity.* Biochemistry, 2009. **48**(44): p. 10568-10576.
107. Khurana, R., Coleman, C., Ionescu-Zanetti, C., Carter, S.A., Krishna, V., Grover, R.K., Roy, R., and Singh, S., *Mechanism of thioflavin T binding to amyloid fibrils.* Journal of Structural Biology, 2005. **151**: p. 229-238.
108. Porat, Y., Mazor, Y., Efrat, S., and Gazit, E., *Inhibition of islet amyloid polypeptide fibril formation: a potential role for heteroaromatic interactions.* Biochemistry, 2004. **43**(45): p. 14454-14462.
109. Goldsbury, C.S., Cooper, G. J. S., Goldie, K. N., Muller, S. A., Saafi, E. L., Gruijters, W. T. M., and Misur, M. P., *Polymorphic fibrillar assembly of human amylin.* Journal of Structural Biology, 1997. **119**(1): p. 17-27.
110. Green, J.D., Goldsbury, C., Kistler, J., Cooper, G.J.S and Aebi, U., *Human amylin oligomer growth and fibril elongation define two distinct phases in amyloid formation.* The Journal of Biological Chemistry, 2004. **279**(13): p. 12206–12212.
111. Cort, J., Liu, Z. H., Lee, G., Harris, S. M., Prickett, K. S., Gaeta, L. S. L., and Andersen, N. H., *Beta-structure in human amylin and 2 designer beta-peptides - CD and NMR spectroscopic comparisons suggest soluble beta-oligomers and the absence of significant populations of beta-strand dimers.* Biochemical Biophysical Research Communications, 1994. **204**(3): p. 1088-1095.
112. Scrocchi, L.A., Ha, K., Chen, Y., Wu, L., Wang, F., and Fraser, P.E., *Identification of minimal peptide sequences in the (8–20) domain of human islet amyloid polypeptide involved in fibrillogenesis.* Journal of Structural Biology, 2003. **141**: p. 218–227.
113. Potter, K.J., Scrocchi, L.A., Warnock, G.L., Ao, Z., Younker, M.A., Rosenberg, L., Lipsett, M., Verchere, C.B., and Fraser, P.E., *Amyloid inhibitors enhance survival of cultured human islets.* Biochimica et Biophysica Acta, 2009: p. 1-9.

114. Rode, H., Eisel, D., and Frost, I., *Apoptosis, cell death, and cell proliferation manual*, in *Apoptosis, Cell Death, and Cell Proliferation Manual*2007, Roche Applied Science.
115. Zarei, A., and Markovic, B. *Refinement in the use and data analysis of the Promega CellTiter 96® aqueous non-radioactive cell proliferation assay*. Promega Corporation, Accessed: October 2012, http://www.promega.com/resources/articles/pubhub/enotes/data-analysis-of-the-celltiter-96-aqueous-nonradioactive-cell-proliferation-assay/.
116. Konarkowska, B., Aitken, J. F., Kistler, J., Zhang, S. P., and Cooper, G. J. S., *Thiol reducing compounds prevent human amylin-evoked cytotoxicity.* Febs Journal, 2005. **272**(19): p. 4949-4959.
117. Gazit, E., *Mechanisms of amyloid fibril self-assembly and inhibition.* Febs Journal, 2005. **272**(23): p. 5971-5978.
118. Mishra, R., Sellin, D., Radovan, D., Gohlke, A., and Winter, R., *Inhibiting islet amyloid polypeptide fibril formation by the red wine compound resveratrol.* Chembiochem, 2009. **10**(3): p. 445-449.
119. Jiang, P., Li, W., Shea, J. E., and Mu, Y., *Resveratrol inhibits the formation of multiple-layered beta-sheet oligomers of the human islet amyloid polypeptide segment 22-27.* Biophysical Journal, 2011. **100**(8): p. 2076-2076.
120. Smoliga, J.M., Baur, J. A., and Hausenblas, H. A., *Resveratrol and health - a comprehensive review of human clinical trials.* Molecular Nutrition & Food Research, 2011. **55**(8): p. 1129-1141.
121. Brasnyo, P., Molnar, G. A., Mohas, M., Marko, L., Laczy, B., Cseh, J., Mikolas, E., Szijarto, I. A., Merei, A., Halmai, R., Meszaros, L. G., Suemegi, B., and Wittmann, I., *Resveratrol improves insulin sensitivity, reduces oxidative stress and activates the Akt pathway in type 2 diabetic patients.* British Journal of Nutrition, 2011. **106**(3): p. 383-389.
122. Forloni, G., Colombo, L., Girola, L., Tagliavini, F., and Salmona, M., *Anti-amyloidogenic activity of tetracyclines: studies in vitro.* FEBS Letters, 2001. **487**(3): p. 404-407.
123. Abedini, A., Meng, F. and Raleigh, D.P., *A single-point mutation converts the highly amyloidogenic human islet amyloid polypeptide into a potent fibrillization inhibitor.* Journal of the American Chemical Society, 2007. **129**: p. 11300-11301.
124. Hayashi, T., Asai, T., and Ogoshi, H., *Conformational analysis of beta-turn structure in tetrapeptides containing proline or proline analogs.* Tetrahedron Letters, 1997. **38**(17): p. 3039-3042.
125. Kong, M.F., King, P., Macdonald, I. A., Stubbs, T. A., Perkins, A. C., Blackshaw, P. E., Moyses, C., and Tattersall, R. B., *Infusion of pramlintide, a human amylin analogue, delays gastric emptying in men with IDDM.* Diabetologia, 1997. **40**(1): p. 82-88.
126. Kong, M.F., Stubbs, T., King, P., Lambourne, J., MacDonald, I., Blackshaw, E., and Perkins, A., *The effect of single doses of pramlintide on gastric emptying of two meals in IDDM.* Diabetes, 1997. **46**: p. 594-594.
127. Thompson, R., Pearson, L., Schoenfeld, S., and Kolterman, O., *Pramlintide improves glycemic control in patients with type II diabetes requiring insulin.* Diabetologia, 1997. **40**: p. 1397-1397.
128. Thompson, R., Pearson, L., Schoenfeld, S., and Kolterman, O., *Pramlintide, an analog of human amylin improves glycemic control in patients with type II diabetes requiring insulin.* Diabetes, 1997. **46**: p. 116-116.
129. Thompson, R.G., Gottlieb, A., Organ, K., Koda, J., Kisicki, J., and Kolterman, O. G., *Pramlintide: A human amylin analogue reduced postprandial plasma glucose, insulin, and C-peptide concentrations in patients with type 2 diabetes.* Diabetic Medicine, 1997. **14**(7): p. 547-555.
130. Thompson, R.G., Pearson, L., and Kolterman, O. G., *Effects of 4 weeks' administration of pramlintide, a human amylin analogue, on glycaemia control in patients with IDDM: effects on plasma glucose profiles and serum fructosamine concentrations.* Diabetologia, 1997. **40**(11): p. 1278-1285.
131. Kong, M.F., Stubbs, T. A., King, P., Macdonald, I. A., Lambourne, J. E., Blackshaw, P. E., Perkins, A. C., and Tattersall, R. B., *The effect of single doses of pramlintide on gastric emptying of two meals in men with IDDM.* Diabetologia, 1998. **41**(5): p. 577-583.
132. Thompson, R.G., Pearson, L., Schoenfeld, S. L., and Kolterman, O. G., *Pramlintide, a synthetic analog of human amylin, improves the metabolic profile of patients with type 2 diabetes using insulin.* Diabetes Care, 1998. **21**(6): p. 987-993.
133. Hollander, P., Ratner, R., Fineman, M., Strobel, S., Shen, L., Maggs, D., Kolterman, O., and Weyer, C., *Addition of pramlintide to insulin therapy lowers HbA(1c) in conjunction with weight loss in patients with type 2 diabetes approaching glycaemic targets.* Diabetes Obesity & Metabolism, 2003. **5**(6): p. 408-414.
134. Weyer, C., Maggs, D., Ruggles, J., Fineman, M., Burrell, T., and Kolterman, O., *The human amylin analog, pramlintide, reduces body weight in insulin-treated patients with type 2 diabetes.* Diabetologia, 2003. **46**: p. A295-A295.
135. Maggs, D.G., Fineman, M., Kornstein, J., Burrell, T., Schwartz, S., Wang, Y., Ruggles, J. A., Kolterman, O. G., and Weyer, C., *Pramlintide reduces postprandial glucose excursions when added to insulin lispro in subjects with type 2 diabetes: a dose-timing study.* Diabetes-Metabolism Research and Reviews, 2004. **20**(1): p. 55-60.

136. Ratner, R.E., Dickey, R., Fineman, M., Maggs, D. G., Shen, L., Strobel, S. A., Weyer, C., and Kolterman, O. G., *Amylin replacement with pramlintide as an adjunct to insulin therapy improves long-term glycaemic and weight control in type 1 diabetes mellitus: a 1-year, randomized controlled trial.* Diabetic Medicine, 2004. **21**(11): p. 1204-1212.
137. Ryan, G.J., Jobe, L. J., and Martin, R., *Pramlintide in the treatment of type 1 and type 2 diabetes mellitus.* Clinical Therapeutics, 2005. **27**(10): p. 1500-1512.
138. Ryan, G., Briscoe, T. A., and Jobe, L., *Review of pramlintide as adjunctive therapy in treatment of type 1 and type 2 diabetes.* Drug design, development and therapy, 2009. **2**: p. 203-14.
139. Hull, R.L., Shen, Z. P., Watts, M. R., Kodama, K., Carr, D. B., Utzschneider, K. M., Zraika, S., Wang, F., and Kahn, S. E., *Long-term treatment with rosiglitazone and metformin reduces the extent of, but does not prevent, islet antyloid deposition in mice expressing the gene for human islet antyloid polypeptide.* Diabetes, 2005. **54**(7): p. 2235-2244.
140. Rijkers, D.T.S., Hoppener, J.W.M., Posthuma, G., Lips, C.J.M. and Liskamp, R.M.J, *Inhibition of amyloid fibril formation of human amylin by N-alkylated amino acid and α-hydroxy acid residue containing peptides.* Chemistry: A European Journal, 2002. **8**(18): p. 4285-4291.
141. Ostresh, J.M., Husar, G. M., Blondelle, S. E., Dorner, B., Weber, P. A., and Houghten, R. A., *Libraries from libraries - chemical transformation of combinatorial libraries to extend the range and repertoire of chemical diversity.* Proceedings of the National Academy of Sciences of the United States of America, 1994. **91**(23): p. 11138-11142.
142. Muthusamy, K., Arvidsson, P. I., Govender, P., Kruger, H. G., Maguire, G. E. M., and Govender, T., *Design and study of peptide-based inhibitors of amylin cytotoxicity.* Bioorganic & Medicinal Chemistry Letters, 2010. **20**(4): p. 1360-1362.
143. Albrecht, E., Jones, H., Gaeta, L.S.L., Prickett, K.S., and Beaumont, K. *Amylin antagonist peptides and uses thereof.* (1996). Patent no. 5580953.
144. Fezoui, Y., and Soto-Jara, C. *Amylin aggregation inhibitors and uses thereof.* (2007). Patent no. US2007/0155955 A1.
145. Cabaleiro-Lago, C., Lynch, I., Dawson, K. A., and Linse, S., *Inhibition of IAPP and IAPP((20-29)) fibrillation by polymeric nanoparticles.* Langmuir, 2009. **26**(5): p. 3453-3461.
146. Meng, F., Abedini, A., Plesner, A., Middleton, C., Potter, K. J., Zanni, M. T., Verchere, C. B., and Raleigh, D. P., *The sulfated triphenyl methane derivative acid fuchsin is a potent inhibitor of amyloid formation by human islet amyloid polypeptide and protects against the toxic effects of amyloid formation.* Journal of Molecular Biology, 2010. **400**(3): p. 555-566.
147. Rigacci, S., Guidotti, V., Bucciantini, M., Parri, M., Nediani, C., Cerbai, E., Stefani, M., and Berti, A., *Oleuropein aglycon prevents cytotoxic amyloid aggregation of human amylin.* Journal of Nutritional Biochemistry, 2010. **21**(8): p. 726-735.
148. Buzea, C., Blandino, I.I.P., and Robbie, K., *Nanomaterials and nanoparticles: sources and toxicity.* Biointerphases, 2007. **2**(4): p. MR17 - MR172.
149. El-Ansary, A., and Al-Daihan, S., *On the toxicity of therapeutically used nanoparticles: an overview.* Journal of Toxicology, 2009. **2009**: p. 1-9.
150. Soto, C., Castano, E. M., Kumar, R. A., Beavis, R. C., and Frangione, B., *Fibrillogenesis of synthetic amyloid-beta peptides is dependent on their initial secondary structure.* Neuroscience Letters, 1995. **200**(2): p. 105-108.
151. Muthusamy, K., Albericio, F., Arvidsson, P. I., Govender, P., Kruger, H. G., Maguire, G. E. M., and Govender, T., *Microwave assisted SPPS of amylin and its toxicity of the pure product to RIN-5F cells.* Biopolymers, 2010. **94**(3): p. 323-330.
152. Hou, L.M., Kang, I., Marchant, R. E., and Zagorski, M. G., *Methionine 35 oxidation reduces fibril assembly of the amyloid A beta-(1-42) peptide of Alzheimer's disease.* Journal of Biological Chemistry, 2002. **277**(43): p. 40173-40176.
153. Uversky, V.N., Yamin, G., Souillac, P. O., Goers, J., Glaser, C. B., and Fink, A. L., *Methionine oxidation inhibits fibrillation of human alpha-synuclein in vitro.* Febs Letters, 2002. **517**(1-3): p. 239-244.
154. Raleigh, D.P., and Abedini, A., *Incorporation of pseudoproline derivatives allows the facile synthesis of human IAPP, a highly amyloidogenic and aggregation-prone polypeptide.* Orgnic Letters, 2005. **7**(4): p. 693-696.
155. Raleigh, D.P., Abedini, A., and Singh, G., *Recovery and purification of highly aggregation-prone disulfide-containing peptides: application to islet amyloid polypeptide.* Analytical Biochemistry 351 (2006) 181–186, 2006. **351**: p. 181-186.
156. Park, J.H., Page, K., Hood, C.A., Patel, H., Fuentes, G., Menakuru, M., *Fast Fmoc synthesis of hAmylin1–37 with pseudoproline assisted on-resin disulfide formation.* Journal of Peptide Science, 2007. **13**: p. 833-838.
157. Park, J.H., Hood, C.A., Fuentes, G., Patel, H., Page, K., Menakuru, M., *Fast conventional Fmoc solid-phase peptide synthesis with HCTU.* Journal of Peptide Science 2008. **14**: p. 97-101.

158. Marek, P., Woys, A. M., Sutton, K., Zanni, M. T., and Raleigh, D. P., *Efficient microwave-assisted synthesis of human islet amyloid polypeptide designed to facilitate the specific incorporation of labeled amino acids.* Organic Letters, 2010. **12**(21): p. 4848-4851.

CHAPTER 3

RESEARCH RESULTS I

Microwave assisted SPPS of amylin and toxicity of the pure product to RIN-5F cells

This manuscript was published in
Peptide Science (2010)

Microwave assisted SPPS of amylin and toxicity of the pure product to RIN-5F cells

Karen Muthusamy,[a] Fernando Albericio,[b,c,d] Per I. Arvidsson,[e,f] Patrick Govender,[a] Hendrik G. Kruger,[g] Glenn E. M. Maguire,[g] Thavendran Govender[h]

[a] School of Life Sciences, University of KwaZulu Natal, South Africa
[b] Institute for Research in Biomedicine, Barcelona, Spain
[c] CIBER-BBN, Networking Centre on Bioengineering, Biomaterials and Nanomedicine, Barcelona, Spain
[d] Department of Organic Chemistry, University of Barcelona, Spain
[e] Department of Biochemistry and Organic Chemistry, Uppsala University, Sweden
[f] Discovery CNS and Pain Control, AstraZeneca R&D, Sweden
[g] School of Chemistry, University of KwaZulu Natal, South Africa
[h] School of Pharmacy and Pharmacology, University of KwaZulu Natal, South Africa

3.1 Abstract

The 37-amino acid polypeptide amylin, is found as amyloid aggregates in the islets of Langerhans in patients with type II diabetes. Herein, we report an efficient microwave assisted solid phase peptide synthesis of amylin. The most efficient synthesis used double and triple couplings and 10 equivalents of amino acids. Double couplings were used for most amino acids, whereas triple couplings were utilized for amino acids in selected regions. The most effective method for formation of the disulfide bond in amylin was found to be iodine oxidation. Amylin with the highest purity was obtained when the crude peptide was purified with high performance liquid chromatography (HPLC) before formation of the disulfide bond. The cytotoxicity of the synthesized amylin product to RIN-5F cells was determined and it was found that the chemically synthesized amylin exhibits an exponential increase of cytotoxicity at concentrations >35 μM. Transmission electron microscopy studies illustrated that chemically synthesized amylin spontaneously formed insoluble typical amyloid fibrils after an incubation time of 24 hours in a suitable buffer. Thus, chemically synthesized amylin is suitable to use for screening potential inhibitors of fibril formation and cytotoxicity.

3.2 Introduction

Islet amyloid polypeptide (IAPP), also referred to as amylin, is a 37-amino acid polypeptide that is secreted by pancreatic *β*-cells together with insulin.[1] It is found in the pancreas, blood plasma, and gastrointestinal tract. Although little is known about the exact function of amylin in the human body, its soluble form is believed to play a role in glucose homeostasis.[1-5]

From as early as 1901, a link between the deposition of fibrillar material in the islets of Langerhans in the pancreas and manifestation of type II diabetes had been established.[6] Because these deposits consisted mainly of amylin aggregated into fibrils, type II diabetes was classified as an amyloid disease.[6-8]

Relatively large quantities of amylin are required to study the mechanism of aggregation or to screen for potential inhibitors of toxicity. However, the peptide is extremely expensive to purchase, and in our opinion, the quality varies greatly between suppliers possibly due to the difficulties associated with its synthesis and its tendency to form fibrils once synthesized and purified. Of note, a previous study reported that amyloidogenic peptides from different suppliers have diverse properties.[9] The highly hydrophobic sequence, which is the cause of its rapid aggregation, and the presence of a disulfide bridge between residues 2 and 7 are the factors that have made amylin difficult to synthesize efficiently.

Raleigh and Abedini (2005) were the first to describe the use of pseudoproline derivatives for the solid phase peptide synthesis (SPPS) of amylin.[10] Raleigh *et al.* (2006) thereafter reported an improvement to the synthesis with air oxidation in dimethylsulfoxide (DMSO) or 1,1,1,3,3,3-hexafluoro-2-propanol (HFIP) to form the Cys-2 to Cys-7 disulfide bond.[10] The use of the solvent DMSO was reported as more efficient with a reaction time of just five hours as opposed to HFIP which required 24 hours.[11] They obtained an overall yield of 25–28% based on the weight of the oxidized pure product compared with the weight of the crude material.[11] Park *et al.* (2008) also reported on the efficiency of using pseudoproline derivatives in synthesizing the linear peptide but described the formation of the disulfide bridge before cleavage of the peptide from the resin.[12] It was also reported that 1H-benzotriazolium 1-[bis(dimethylamino) methylene]-5-chloro-hexa-fluorophosphate [1-], 3-oxide (HCTU) is a superior coupling reagent if amylin is to be synthesized with faster coupling times using pseudoproline derivatives.[13] Kelly *et al*. (2008) improved the method of Raleigh and Abedini (2005) by successfully using single coupling of the pseudoproline derivatives and achieved a yield of 20 mg from a 0.1 mmol scale reaction.[10, 14] Although these methods are successful, they are not cost effective because pseudoproline derivatives are expensive to purchase or synthesize.

The recent introduction of microwave assisted SPPS has revolutionized this field. It has been reported to not only increase coupling efficiency but also to overcome near impossible coupling steps.[15-19] The use of 2-(1H-benzotriazole-1-yl)-1,1,3,3-tetramethyluronium hexafluorophosphate (HBTU) or HCTU with temperatures of up to 95°C (via microwave SPPS) was shown to be beneficial for the synthesis of peptides that were previously reported as difficult with conventional methods.[18, 19]

In addition, the introduction of ChemMatrix (CM) [20] resin, a total polyethyleneglycol (PEG) based resin comprised of primary ether bonds, has been reported to minimize some of the aggregation problems associated with polystyrene resins during the synthesis.[21-23] This resin swells efficiently in all of the common solvents and is therefore useful for a broad range of organic chemistries. CM resin performs extremely well compared with polystyrene resins in the solid-phase synthesis of hydrophobic, highly structured peptides such as poly-Arg peptide and *β*-amyloid(1–42) [21-23], showing that the presence of PEG chains impair the aggregation of the growing peptide chain, thereby facilitating the solid-phase synthesis of complex peptides. Thus, CM resins have been reported as the resin of choice for synthesis of hydrophobic peptides.[21, 22, 24]

This communication describes for the first time the synthesis of amylin with the use of microwave assisted SPPS, using a CM resin, and without the use of pseudoproline derivatives. We also compared the reported efficiency of DMSO and/or HFIP for air oxidation and formation of the disulfide bridge, to that of oxidation with iodine. In a manner that mimics the biological activity of naturally occurring amylin, the newly synthesized amylin was also observed to form typical amyloid fibrils and was found to be cytotoxic to the RIN-5F cell line.

3.3 Materials and Methods

3.3.1 Reagents

All 9-fluorenylmethoxycarbonyl (Fmoc) protected amino acids and coupling reagents were purchased from GLS Biochem Systems, Inc. (China). The following protecting groups were used for the side chains of the amino acids: trityl (Trt) for asn, cys, gln, and his, *t*-butyl ether (*t*Bu) for ser and thr, 2,2,4,6,7-pentamethyl-dihydrobenzofuran-5-sulfonyl (Pbf) for arg, and *t*-butyloxycarbonyl (Boc) for lys. The Wang-CM resin was kindly donated by Matrix Innovation (Quebec, Canada). All solvents for synthesis and purification were of high performance liquid chromatography (HPLC) grade and were purchased from Sigma-Aldrich (U.S.A.). The CellTiter 96® nonradioactive cell proliferation assay was purchased from Promega Corporation (U.S.A.).

3.3.2 Linear peptide synthesis

Peptides were synthesized on a 0.1 mmol scale using a CEM microwave peptide synthesizer. Deprotection was performed using 20% piperidine/DMF (v/v). Coupling was performed using 1:1:1 amino acid/HBTU/*N*, *N*-diisopropyl ethylamine (DIPEA) in dimethylformamide (DMF). Three different synthetic strategies were tested. Strategy A made use of five molar equivalents (eq.) of all amino acids and double couplings for each, strategy B used ten molar equivalents of amino acids that proved to be problematic during synthesis and again double couplings, whereas strategy C used ten molar equivalents for the problematic amino acids and triple couplings for these. DMF top and bottom washes were performed between deprotection and coupling steps. The standard microwave settings from the manufacturer were modified according to Table 3.1. This method now includes 900 seconds of coupling without microwave heating in order to reduce racemization associated with excessive heating.

Table 3.1 Microwave conditions for coupling and deprotection

	Microwave power (Watts)	**Temperature (°C)**	**Time (sec)**
Double coupling			
30 minute coupling	0	73	900
	35	73	900
6 minute coupling	35	90	360
Triple coupling			
30 minute coupling	0	73	900
	35	73	900
6 minute coupling*	35	90	360
Arginine coupling			
60 minute coupling*	0	73	2700
	35	73	900
Deprotection	40	73	180

* Double couplings.

3.3.3 Cleavage

Peptides were cleaved from the resin using 5% tri-isopropylsilane in trifluoroacetic acid (TFA) for two hours.

3.3.4 Oxidation to form the cys-2 to cys-7 disulfide bridge

Methods 1 and 2 used air oxidation in DMSO and HFIP, respectively, as described by Raleigh *et al*. (2006) to form the disulfide bridge.[11] Briefly, method 1 involved dissolving crude amylin (± 20 mg) in 100% DMSO (10 mL) and subjecting it to air oxidation (five hours), whereas method 2 involved dissolving crude amylin (± 20 mg) in HFIP (10 mL) and 12 mL of 50 mM Tris buffer (pH 8.5), followed by air oxidation (24 hours). For method 3, crude amylin (± 20 mg) was dissolved in a large volume of methanol (400 mL). Iodine dissolved in methanol (10 mL) was then added drop-wise with continuous stirring until a faint yellow color was observed. The solvent was then evaporated and the crude product dissolved in DMSO before purification. This method was also applied to purified unoxidized amylin (16 mg), by dissolving it in an excess of methanol (400 mL) and adding methanolic iodine drop-wise (over 20 minutes) until a faint yellow color developed. The solvents were evaporated under reduced pressure at 40°C and residual iodine was removed by azeotropic distillation with methanol. This amylin sample was lyophilized without further purification.

3.3.5 Purification of unoxidized and oxidized amylin

The unoxidized and oxidized amylin were purified directly via an ACE C18 preparative column (250 mm x 22 mm, Scotland). A dual-buffer system was employed, with TFA serving as the ion-pairing agent. The first buffer consisted of 0.1% TFA/H_2O (v/v) and the second buffer was composed of 0.1% TFA/acetonitrile (v/v). The peptides were eluted using a gradient of 0-90% of the second buffer over 60 minutes with a flow rate of 20 mL/minute. The solvent from pooled peptide-containing fractions was evaporated to 20 mL and the samples were snap-frozen in liquid nitrogen and lyophilized.

3.3.6 Peptide analysis

Peptides were analyzed with an Agilent 1100 HPLC system fitted with a Waters XBridge C18 column, 250 × 3.6 mm. Chromatography was performed over 90 minutes using a gradient of 0-90% of 0.1% TFA/acetonitrile (v/v) at a flow rate of 0.3 mL/minute and the eluent was monitored at a UV wavelength of 215 nm. A Bruker electrospray ionization time-of-flight spectroscope (ESI-QTOF) in positive mode was used to obtain mass spectra (MS) and matrix assisted laser desorption ionization time-of-flight mass spectroscopy (MALDI-TOF MS) was performed with an Autoflex III instrument (Bruker) operated in positive mode with cyano-4-hydroxycinnamic acid being used as the matrix.

3.3.7 Disaggregation method

Before any testing could be performed, it was essential to start with completely disaggregated amylin. Although previous studies have recommended the use of either DMSO or HFIP alone for the purpose of amylin disaggregation [25-28], in the current study the following optimal procedure was established using transmission electron microscopy (TEM) studies. Amylin was dissolved in 200 µL hexafluoroisopropanol (HFIP):TFA solution (50:50, v/v) and the sample was sonicated for 10 minutes. Samples were then left to stand overnight at room temperature and the solvents removed under vacuum using a centrifugal evaporator for approximately 1-2 hours. Approximately 100 µL HFIP was added to the amylin, followed by vortexing and the solvent was removed by rotary evaporation for 1-2 hours. To remove all traces of TFA, the latter process was repeated twice using HFIP (100 µL).

3.3.8 Transmission electron microscopy (TEM)

Amylin was disaggregated as described earlier, and thereafter, dissolved in 10 mM sodium phosphate buffer, pH 7.4 containing 50 mM NaCl (Buffer A) to give a final concentration of 45 µM. Aggregation was followed by TEM immediately following preparation as well as after 24 hours of incubation at 37°C. At each time-point, aliquots (2 µL) of the sample were applied onto formvar coated carbon-stabilized grids. After drying for one minute, excess liquid was blot dried and samples were stained with 2% (w/v) uranyl acetate for 30 seconds. Samples were blot dried again before being analyzed with a CM120 Biotwin Philips TEM at a voltage of 100 V.

3.3.9 Cytotoxicity assay

The RIN-5F cell line (European Collection of Cell Cultures, Sigma-Aldrich, U.S.A.) was cultured in RPMI 1640 growth medium containing 10% heat-inactivated fetal bovine serum, 2 mM glutamine, 1 mM sodium pyruvate, 25 mM 2-[4-(2-hydroxyethyl)-1-piperazinyl] ethanesulfonic acid (HEPES), and 0.1 mg/mL penicillin/streptomycin. Cells were plated at a density of 7.5 x 10^5 cells/mL (100 µL/well) into poly-D-lysine pre-coated 96 well plates (Sigma-Aldrich, U.S.A.) and incubated at 37°C for 24 hours.

Thereafter, spent medium was removed from all wells and fresh fully constituted medium was added (60 µL). Serial dilutions of amylin were prepared initially in 100 µL of Buffer A to which an equal volume of RPMI 1640 was then added. Thereafter, 40 µL samples containing varying concentrations of amylin were added to each well. Untreated control cells received 40

μL amylin-free samples that were disaggregated as described earlier and that were reconstituted in a solution containing equal volumes of Buffer A and RPMI 1640. Subsequently, plates were incubated at 37°C for a further 24 hours. The CellTiter 96® nonradioactive cell proliferation assay was used as per manufacturer's instructions to assess cell viability by measuring the cellular reduction of 3-(4,5-dimethylthiazol-2-yl)-2,5-diphenyltetrazolium bromide (MTT).[29, 30] Absorbance readings for the MTT assay were performed using an Automated Microplate Reader (ELx800) from Bio-Tek Instruments. All assays were performed in quintuplicate and repeated twice. Statistical analysis was performed using the One-way Analysis of Variance (ANOVA) and Tukey-Kramer Multiple comparisons test (GraphPad InStat version 3 for Windows XP, U.S.A), and results were considered significantly different if p values were less than 0.05.

3.4 Results

Initially, amylin fragments 26–37, 18–37, 9–37, and then 2–37 were synthesized with double coupling of each amino acid. The major deletion products that contributed to the inefficient synthesis and purification were identified and are illustrated in Figure 3.1. Synthesis of the 26–37 region of amylin was successful without any deletion products. However, when the 18–37 region was synthesized, it was found that several amino acids in the 18–23 region were missing. Subsequent synthesis of the 9–37 and 2–37 regions identified difficult coupling sequences with amino acids in the 11–14 and 3–6 segments. The identified difficult sequences were in accordance with predictions from the peptide companion software.[31]

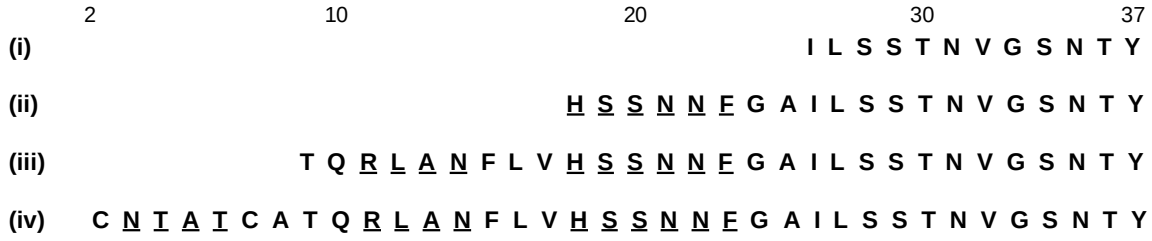

Figure 3.1 Sequence of amylin fragments homologous to the 26-37 (i), 18-37 (ii), 9-37 (iii), and 2-37 (iv) regions. Missing amino acids are underlined.

Three different synthetic strategies were then used to synthesize full length amylin and the HPLC trace of each strategy can be observed in Figures 3.2 and 3.3. Strategy C (Figure 3.3) indicates that a more pure product is present than that achieved with either strategy A (Figure

3.2A) or strategy B (Figure 3.2B). In addition, the desired product from strategy C would elute independently during HPLC purification.

Three different methods were then tested for the formation of the disulfide bridge between residues 2 and 7. The first two strategies involved air oxidation in DMSO and HFIP, respectively, as described by Raleigh *et al*. (2006).[11] However, air oxidation in DMSO only reached completion after five days, whereas the use of HFIP in Tris buffer resulted in formation of a precipitate and proved unsuccessful for formation of the disulfide bridge. A third method involved the use of iodine for oxidation. The reaction reached completion quickly (approimately 20 minutes) and the oxidized peptide was then purified. As illustrated in Figures 3.4, it is clear that this method still yields a large fraction of impurity. However, as seen in Figure 3.5, oxidation after purification results in presence of a pure peptide. The latter synthetic strategy resulted in a yield of 8% (32 mg), based on using a 0.1 mmol scale for synthesis.

As determined by MALDI-TOF MS analysis (Figure 3.6), the molecular weight of commercially available amylin (m/z ± 3905.5) is comparable with that of chemically synthesized amylin (m/z ± 3905.4). Unlike chemically synthesized amylin, a substantial impurity (m/z ± 2926.0) was present in commercially supplied amylin (Figure 3.6B). The contaminants in both samples could be as a result of deletion products which are known to form during the chemical synthesis of amylin.

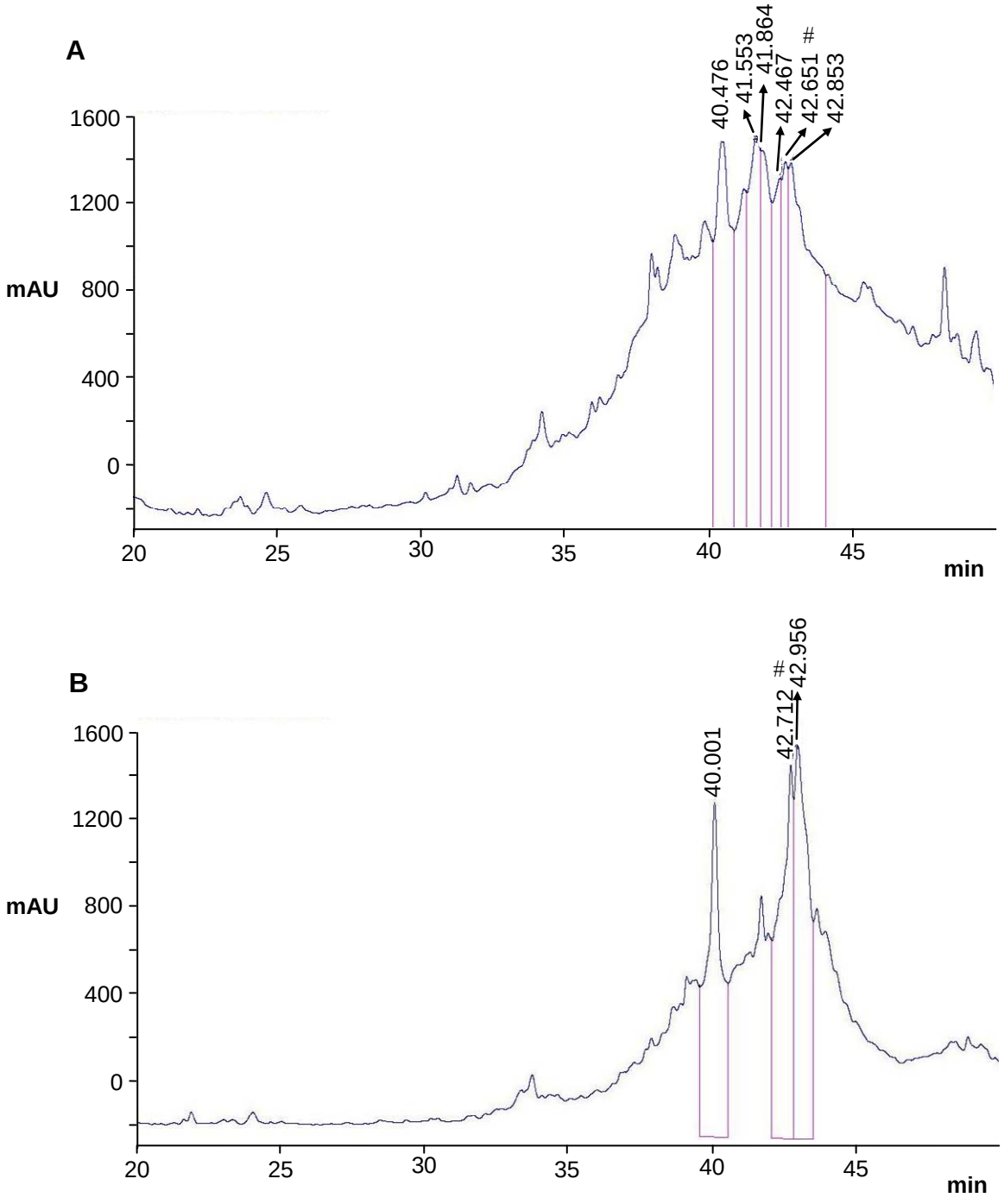

Figure 3.2 Analytical reverse-phase HPLC traces of crude samples of amylin using different synthetic strategies: (A) double couplings and 5 eq. of all amino acids (strategy A); and (B) double couplings and 10 eq. of specific amino acids (strategy B). All HPLC traces were run at a gradient of 0-90% of 0.1% TFA in acetonitrile (v/v) over 90 minutes. # indicates the elution position of the desired product.

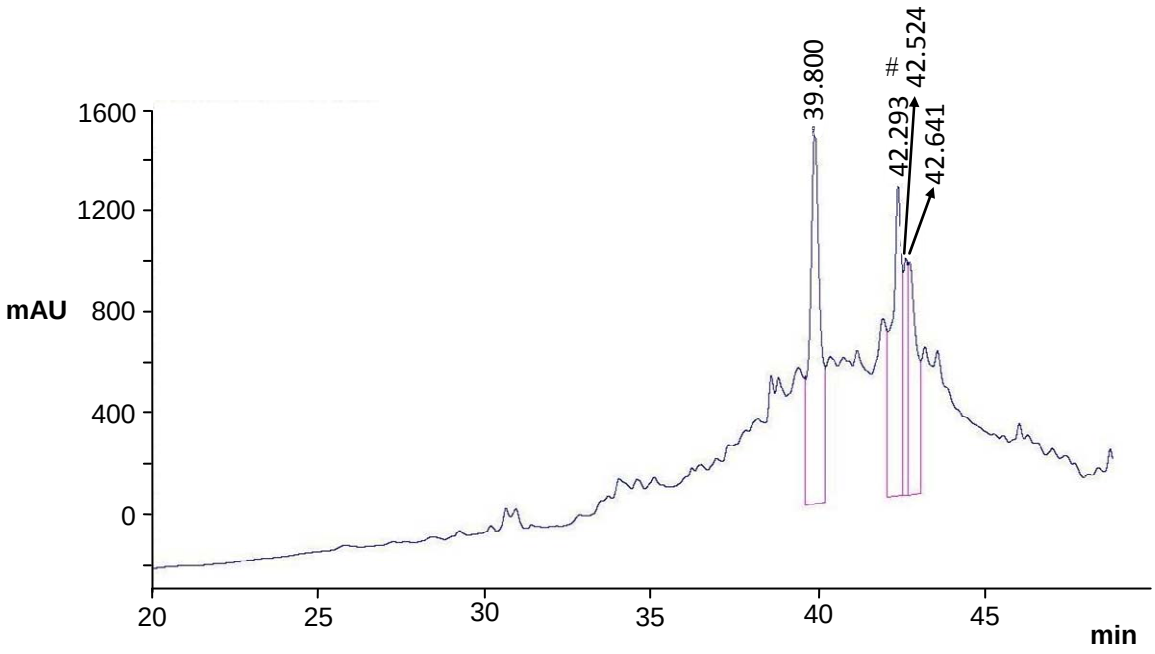

Figure 3.3 Analytical reverse-phase HPLC trace of crude samples of amylin using strategy C (triple couplings and 10 eq. of specific amino acids). All HPLC traces were run at a gradient of 0-90% of 0.1% TFA in acetonitrile (v/v) over 90 minutes. # indicates the elution position of the desired product.

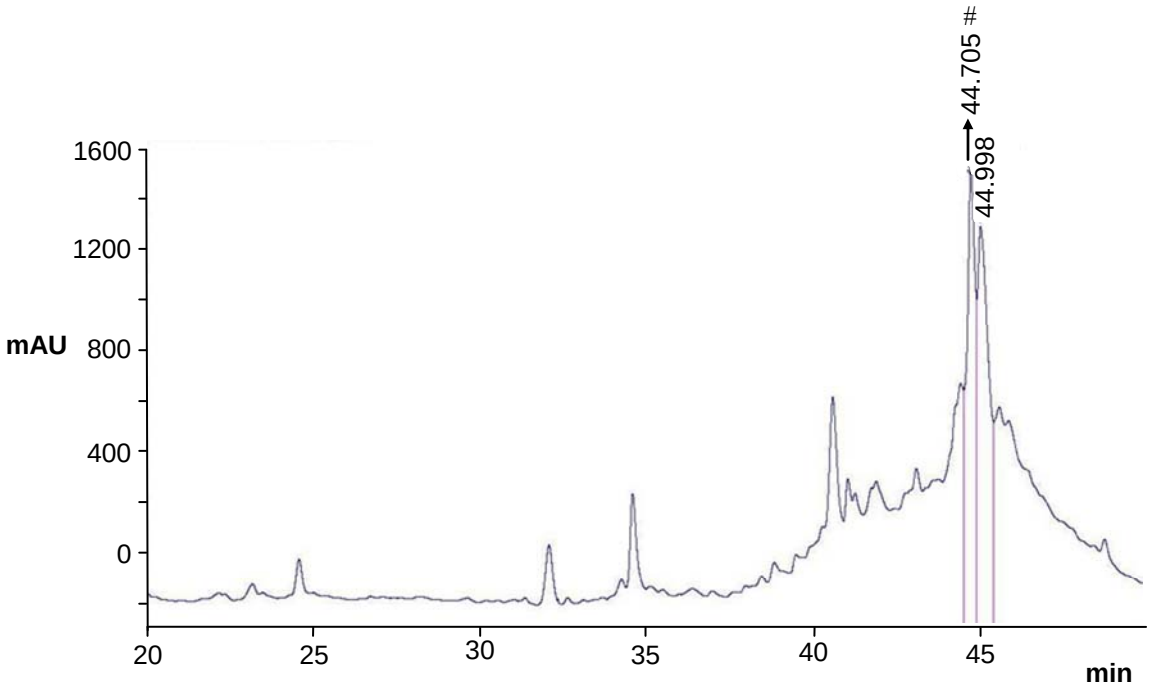

Figure 3.4 Analytical reverse-phase HPLC traces of crude samples of amylin after iodine oxidation. HPLC traces were run at a gradient of 0-90% of 0.1% TFA in acetonitrile (v/v) over 90 minutes. # indicates the elution position of the desired product.

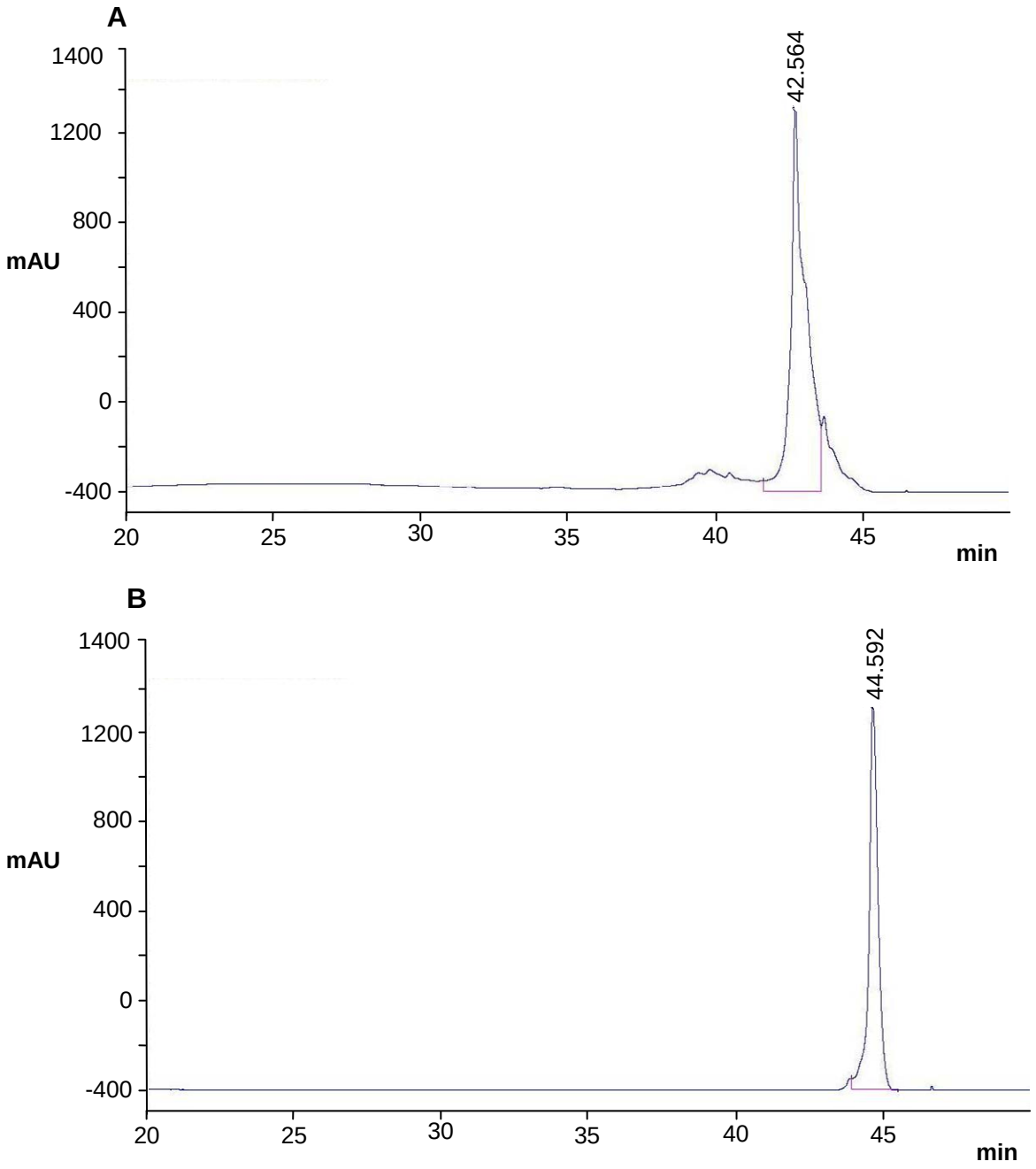

Figure 3.5 Analytical reverse-phase HPLC traces of (A) purified unoxidized amylin; and (B) amylin after oxidation using iodine. HPLC traces were run at a gradient of 0-90% of 0.1% TFA in acetonitrile (v/v) over 90 minutes.

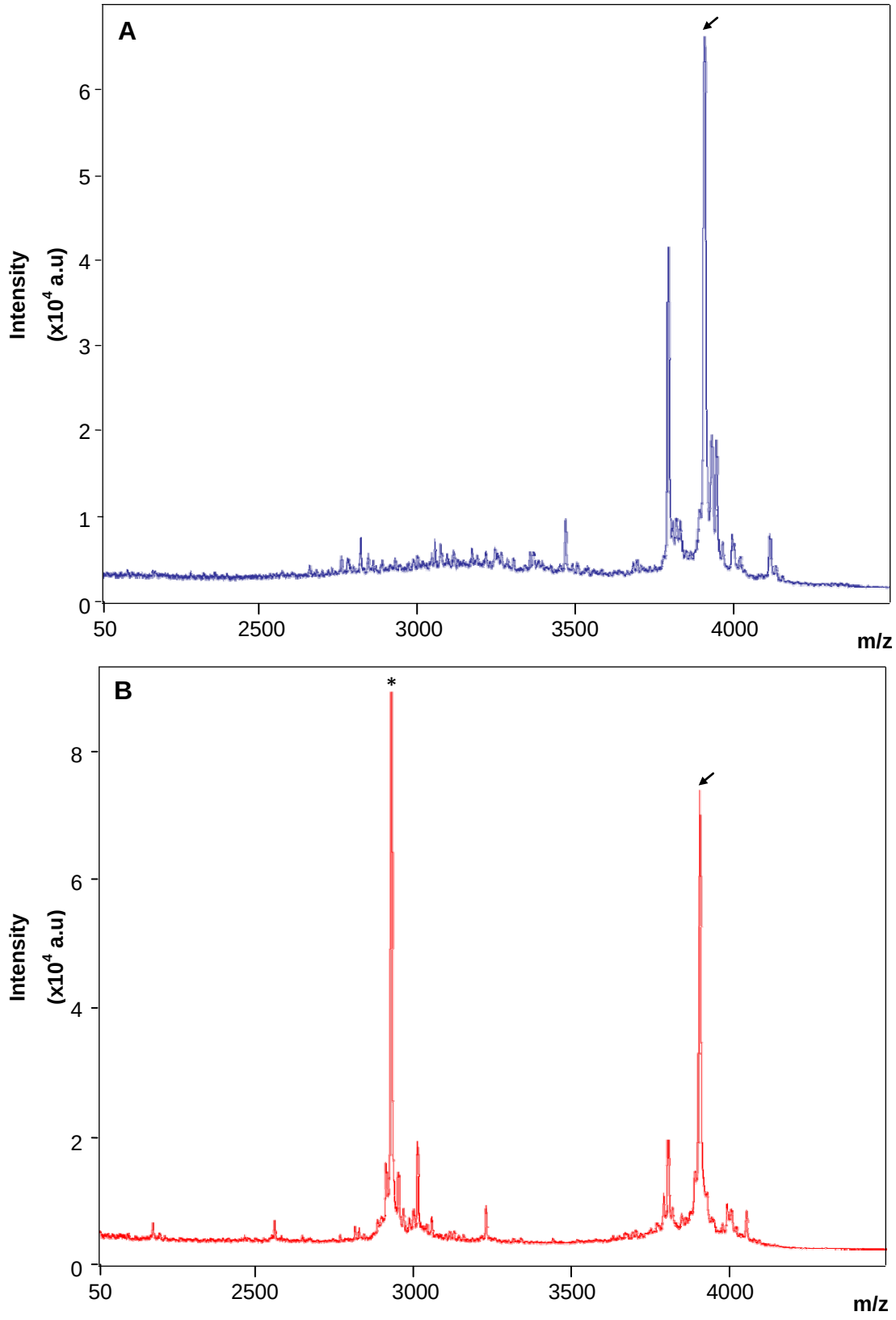

Figure 3.6 MALDI-TOF MS analysis of (A) chemically synthesized amylin and the best commercially available amylin (B). Arrows in (A) and (B) indicates the correct mass of amylin (m/z = 3905.4 and 3905.5 respectively). * indicates the impurity (m/z = 2926.0).

TEM was performed to determine the amyloidogenic nature of the chemically synthesized amylin and as observed in Figure 3.7, the synthesized amylin forms typical amyloid fibrils. Figure 3.8 illustrates a lag phase in cytotoxicity when 5–35 µM of amylin was used. Thereafter, an exponential increase in cytotoxicity was observed.

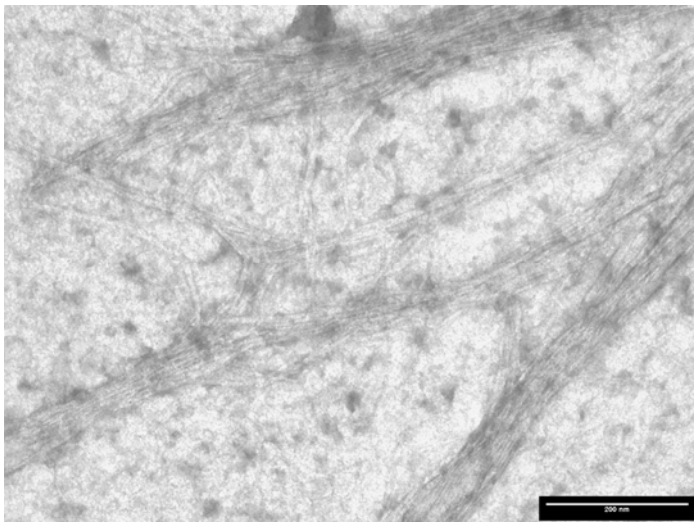

Figure 3.7 Electron micrograph illustrating spontaneously formed amyloid fibrils in a 45 µM sample of chemically synthesized amylin after 24 hours of incubation in 10 mM sodium phosphate buffer, pH 7.4 containing 50 mM NaCl. Scale bar = 200 nm.

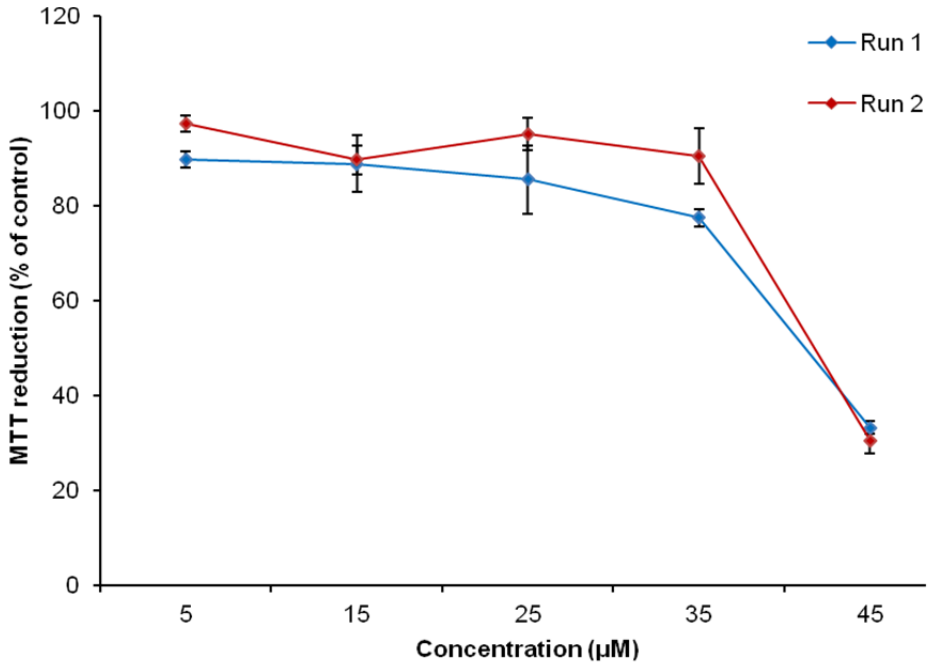

Figure 3.8 The cytotoxic effect of various concentrations of amylin on RIN-5F cells (7.5 × 10^4 cells/well after 24 hours incubation with amylin). Data are percentages of control, with

run 1 and run 2 being two independent experiments, each of which was performed with multiple replicates (n=5). When compared to the control, p values for 45 μM amylin were < 0.001 for both runs.

3.5 Discussion

In the synthesis of amylin, strategy A made use of a five-fold excess of all amino acids with double couplings for each residue. Although the desired peptide was obtained (m/z ± 3905), large amounts of two deletion peptides (m/z ± 3438 and m/z ± 2595) were also present. Deletion peptide 1 (m/z ± 3438) was attributed to the absence of amino acids in the 18–23 region, whereas the other major deletion peptide 2 (m/z ± 2595) was present due to inefficient coupling of residues in the 3–6, 11–14, and 18–23 regions. There are several other deletion products but they would not affect the purification of the desired peptide. Strategy B involved using five equivalents of each amino acid with double couplings, whereas ten equivalents were utilized for the 3–6, 11–14, and 18–23 regions. This approach proved to be a more successful strategy by significantly reducing the peak corresponding to deletion peptide 2. Deletion peptide 1 (m/z ± 3438) forms as a result of inefficient coupling of the two asn, phe and ser residues belonging to the 18–23 region. Relying on the findings of the first 2 strategies, strategy C was then performed using a ten-fold excess of amino acids for the difficult regions as in strategy B but with triple couplings for amino acids in the 18–23 region. This approach proved more efficient in reducing the amount of deletion peptide 1 and the analytical HPLC profile indicated an easier isolation of the desired linear amylin.

Of the three methods tested for the formation of the disulfide bridge between residues 2 and 7, iodine oxidation was the most successful when performed after purification of the unoxidized peptide since there was no need for purification after oxidation. The retention times of reduced and oxidized amylin differed by approximately two minutes, which is in agreement with previously reported data.[10] Using our best synthetic strategy, this study reported a yield of 32 mg on a 0.1 mmol scale which is similar to that obtained by Kelly *et al*. (2008) (yield of 20 mg).[14] However, in this study the pseudoproline derivatives were replaced with normal Fmoc amino acids and a 10 molar excess with triple couplings were used for the assigned difficult regions. This synthetic strategy is thus far cheaper than the strategy using pseudoprolines when prices for commercially available pseudoproline derivatives are taken into account. As indicated by MALDI-TOF MS, chemically synthesized amylin had a similar molecular weight as that of commercially available amylin. In addition, the chemically

synthesized amylin had a similar aggregating potential as both commercially available as well as naturally occurring amylin since it formed typical amyloid fibrils.[32-34]

Considering the variations reported in both the concentrations of amylin used and the percentage cytotoxicity observed in previous studies, a range of amylin concentrations (5–45 μM) were screened in this study. It seems from literature that commercial samples of isolated amylin lead to dramatic variations in toxicity toward the same cell line (RIN-5F). Bai *et al*. (1999) found that 5 μM amylin was 20% toxic [35] whilst subsequent studies reported a 20% toxicity arising from lower concentrations of amylin, 100 nM [31], 10 nM [27] and even 1 nM [28]. It was also reported that 280 nM amylin was approximately 8% toxic.[36] In the present study, an exponential increase in cytotoxicity of chemically synthesized amylin was observed which correlates with that observed in previously published studies that made use of commercially available amylin.[27, 28] Thus, the chemically synthesized amylin also exhibits a similar cytotoxic potential as that of commercially available amylin, thereby allowing it to be used to screen potential inhibitors of amylin-mediated aggregation and cytotoxicity.

3.6 Conclusion

Linear amylin can be efficiently synthesized without the use of pseudoproline derivatives. This is the first report of amylin synthesis by using microwave assisted SPPS with CM resin and it seems to generate fewer impurities in comparison with previously published strategies. Furthermore, we have shown that iodine is a fast, efficient, and facile method for disulfide bond formation. The oxidation process was proven to be successful on both impure and pure amylin product. We propose that this approach is a cost-effective improvement on the reported synthesis of amylin thus far. The cytotoxicity of pure amylin was determined on the RIN-5F cell line and it was shown that amylin concentrations of >35 μM exhibit an exponential increase in toxicity, making chemically synthesized amylin suitable for screening potential inhibitors of amylin-mediated cytotoxicity.

3.7 Acknowledgements

This work was made possible through financial support from the National Research Foundation and UKZN.

3.8 References

1. Martin, C., *The physiology of amylin and insulin: maintaining the balance between glucose secretion and glucose uptake.* The Diabetes Educator, 2006. **32**: p. 101-104.
2. Cooper, G.J.S., *Amylin compared with calcitonin-gene-related peptide - structure, biology, and relevance to metabolic disease.* Endocrine Reviews, 1994. **15**(2): p. 163-201.
3. Kruger, D.F., Gatcomb, P. M., and Owen, S. K., *Clinical implications of amylin and amylin deficiency.* Diabetes Educator, 1999. **25**(3): p. 389-397.
4. Silvestre, R.A., Rodriguez-Gallardo, J., Jodka, C., Parkes, D. G., Pittner, R. A., Young, A. A., and Marco, J., *Selective amylin inhibition of the glucagon response to arginine is extrinsic to the pancreas.* American Journal of Physiology-Endocrinology and Metabolism, 2001. **280**(3): p. E443-E449.
5. Akesson, B., Panagiotidis, G., Westermark, P., and Lundquist, I., *Islet amyloid polypeptide inhibits glucagon release and exerts a dual action on insulin release from isolated islets.* Regulatory Peptides, 2003. **111**(1-3): p. 55-60.
6. Opie, E., *The relation of diabetes mellitus to lesions of the pancreas. Hyaline degeneration of the islands of Langerhans.* The Journal of Experimental Medicine, 1901. **5**: p. 528-540.
7. Cooper, G.J.S., Willis, A.C., Clark, A., Turner, R.C., Sim, R.B. and Reid, K.B.M., *Purification and characterization of a peptide from amyloid-rich pancreases of type 2 diabetic patients.* Proceedings of the National Academy of Science, 1987. **84**: p. 8628-8632.
8. Cooper, G.J.S., Leighton, B., Dimitriadis, G. D., Parry-Billings, M., Kowalchuk, J. M., Howland K., Rothbard, J. B., Willis, A. C., and Reid, K. B. M, *Amylin found in amyloid deposits in human type 2 diabetes mellitus may be a hormone that regulates glycogen metabolism in skeletal muscle.* Proceedings of the National Academy of Science, 1988. **85**: p. 7763-7766.
9. Soto, C., Castano, E. M., Kumar, R. A., Beavis, R. C., and Frangione, B., *Fibrillogenesis of synthetic amyloid-beta peptides is dependent on their initial secondary structure.* Neuroscience Letters, 1995. **200**(2): p. 105-108.
10. Raleigh, D.P., and Abedini, A., *Incorporation of pseudoproline derivatives allows the facile synthesis of human IAPP, a highly amyloidogenic and aggregation-prone polypeptide.* Orgnic Letters, 2005. **7**(4): p. 693-696.
11. Raleigh, D.P., Abedini, A., and Singh, G., *Recovery and purification of highly aggregation-prone disulfide-containing peptides: application to islet amyloid polypeptide.* Analytical Biochemistry 351 (2006) 181–186, 2006. **351**: p. 181-186.
12. Park, J.H., Page, K., Hood, C.A., Patel, H., Fuentes, G., and Menakuru, M., *Fast Fmoc synthesis of hAmylin1–37 with pseudoproline assisted on-resin disulfide formation.* Journal of Peptide Science, 2007. **13**: p. 833-838.
13. Park, J.H., Hood, C.A., Fuentes, G., Patel, H., Page, K., Menakuru, M., *Fast conventional Fmoc solid-phase peptide synthesis with HCTU.* Journal of Peptide Science 2008. **14**: p. 97-101.
14. Kelly, J.W., Yonemoto, I. T., Kroon, G. J. A., Dyson, H. J., and Balch, W. E., *Amylin proprotein processing generates progressively more amyloidogenic peptides that initially sample the helical state.* Biochemistry, 2008. **47**: p. 9900–9910.
15. Yu, H., Chen, S., and Wang, K., *Enhanced coupling efficiency in solid-phase peptide synthesis by microwave irradiation.* The Journal of Organic Chemistry, 1992. **57**(18): p. 4781-4784.
16. Erdélyi, M., and Gogoll, A., *Rapid microwave-assisted solid phase peptide synthesis.* Synthesis, 2002. **11**: p. 1592-1596.
17. Bacsa, B., Desai, D., Dibo, G., and Kappe, C.O., *Rapid solid-phase peptide synthesis using thermal and controlled microwave irradiation.* Journal of Peptide Science, 2006. **12**: p. 633-638.
18. Collins, J., Collins Jr., M.J., Singh, S.K., Vanier, G., Merriweather, H., Douglas, A., and Cox, Z.J. *Recent developments in microwave enhanced solid phase peptide synthesis*. in *4th International Peptide Symposium*. 2007. Australia.
19. Collins, J.M., and Leadbeater, N.E., *Microwave energy: a versatile tool for the biosciences.* Organic & Biomolecular Chemistry, 2007. **5**: p. 1141–1150.
20. Côté, S. *New polyether based monomers, cross-linkers, and highly cross-linked amphiphile polyether resins.* (2005). Patent no.
21. Garcia-Martin, F., Quintanar-Audelo, M., Garcia-Ramos, Y., Cruz, L.J., Gravel, C., Furic, R., Cote, S., Tulla-Puche, J., and Albericio, F., *ChemMatrix, a poly(ethylene glycol)-based support for the solid-phase synthesis of complex peptides.* Journal of Combinatorial Chemistry 2006. **8**: p. 213-220.

22. Garcia-Martin, F., White, P., Steinauer, R., Cote, S., Tulla-Puche, J., Albericio, F., *The synergy of ChemMatrix resin and pseudoproline building blocks renders RANTES, a complex aggregated chemokine.* Biopolymers, 2006. **84**(6): p. 566-575.
23. de la Torre, B.G., Jakab, A., and Andreu, D., *Polyethyleneglycol-based resins as solid supports for the synthesis of difficult or long peptides.* International Journal of Peptide Research and Therapeutics 2007. **13**(1-2): p. 265–270.
24. Albericio, F., Bayo, N., Camperi, S.A., Cascone, O., Côté, S., Cruz, L.J., Errachid, A., Furic, R., García-Martín, F., García-Ramos, Y., Iannucci, N.B., Marani, M. M., Pla-Roca, M., Quintanar-Audelo, M., Samitier, J., and Tulla-Puche, J., *Solid-phase peptide synthesis using ChemMatrix®, a polyethylenglycol (PEG)-based solid*, in *Understanding Biology Using Peptides*, S.E. Blondelle, 2005, American Peptide Society. p. 114.
25. Larson, J.L., Ko, E., and Miranker, A.D., *Direct measurement of islet amyloid polypeptide fibrillogenesis by mass spectrometry.* Protein Science, 2000. **9**: p. 427–431.
26. Tenidis, K., Waldner, M., Bernhagen, J., Fischle, W., Bergmann, M., Weber, M., Merkle, M., Voelter, W., Brunner, H., and Kapurniotu, A., *Identification of a penta- and hexapeptide of islet amyloid polypeptide (IAPP) with amyloidogenic and cytotoxic properties.* Journal of Molecular Biology, 2000. **295**: p. 1055-1071.
27. Tatarek-Nossol, M., Yan, L., Schmauder, A., Tenidis, K., Westermark, G., and Kapurniotu, A., *Inhibition of hIAPP amyloid-fibril formation and apoptotic cell death by a designed hiapp amyloid-core-containing hexapeptide.* Chemistry & Biology, 2005. **12**: p. 797–809.
28. Yan, L., Tatarek-Nossol, M., Velkova, A., Kazantzis, A. and Kapurniotu, A., *Design of a mimic of nonamyloidogenic and bioactive human islet amyloid polypeptide (IAPP) as nanomolar affinity inhibitor of IAPP cytotoxic fibrillogenesis.* Proceedings of the National Academy of Science, 2006. **103**(7): p. 2046–2051.
29. Shearman, M.S., Ragan, C.I., and Iversen, L.L., *Inhibition of PC12 cell redox activity is a specific, early indicator of the mechanism of 1-amyloid-mediated cell death.* Proceedings of the National Academy of Science, 1994. **V91**: p. 1470-1474.
30. Kapurniotu, A., Bernhagen, J., Greenfield, N., Al-Abed, Y., Teichberg, S., Frank, R.W., Voelter, W., and Bucala, R., *Contribution of advanced glycosylation to the amyloidogenicity of islet amyloid polypeptide.* European Journal of Biochemistry, 1998. **251**: p. 208-216.
31. Krampert, M., Bernhagen, J., Schmucker, J., Horn, A., Schmauder, A., Brunner, H., Voelter, W., and Kapurniotu, A., *Amyloidogenicity of recombinant human pro-islet amyloid polypeptide (ProIAPP).* Chemistry & Biology, 2000. **7**: p. 855-871.
32. Westermark P, *Fine-structure of islets of Langerhans in insular amyloidosis.* Virchows Archiv Abteilung a Pathologische Anatomie, 1973. **359**(1): p. 1-18.
33. Westermark, P., Engstrom, U., Johnson, K. H., Westermark, G.T., and Betsholtz, C., *Islet amyloid polypeptide: pinpointing amino acid residues linked to amyloid fibril formation.* Proceedings of the National Academy of Science, 1990. **87**: p. 5036-5040.
34. Charge, S.B.P., Dekoning, E. J. P., and Clark, A., *Effect of pH and insulin on fibrillogenesis of islet amyloid polypeptide in-vitro.* Biochemistry, 1995. **34**(44): p. 14588-14593.
35. Bai, J., Saafi, E.L., Zhang, S. and Cooper, G.J.S., *Role of Ca2+ in apoptosis evoked by human amylin in pancreatic islet b-cells.* Biochem. J., 1999. **343**: p. 53-61.
36. Aitken, J.F., Loomes, K.M., Konarkowska, B., and Cooper, G.J.S, *Suppression by polycyclic compounds of the conversion of human amylin into insoluble amyloid.* Biochemical Journal, 2003. **374**: p. 779–784.

Chapter 4

RESEARCH RESULTS II

Design and study of peptide-based inhibitors of amylin cytotoxicity

This manuscript was published in
Bioorganic and Medicinal Chemistry Letters (2010)

Design and study of peptide-based inhibitors of amylin cytotoxicity

Karen Muthusamy,[a] Per I. Arvidsson,[b,c] Patrick Govender,[a] Hendrik G. Kruger,[d] Glenn E. M. Maguire,[d] and Thavendran Govender[e]

[a] *School of Life Sciences, University of KwaZulu Natal, South Africa*
[b] *Department of Biochemistry & Organic Chemistry, Uppsala University, Sweden*
[c] *Discovery CNS & Pain Control, AstraZeneca R&D, Sweden*
[d] *School of Chemistry, University of KwaZulu Natal, South Africa*
[e] *School of Pharmacy and Pharmacology, University of KwaZulu Natal, South Africa*

4.1 Abstract

As the world moves towards a more Westernized diet, type II diabetes, a disease that debilitates by its many secondary complications, has been shown to be on the increase each year. Deposits consisting mainly of a small protein, called islet amyloid polypeptide (amylin), which aggregates into oligo-/polymeric β-sheet structures are responsible for toxicity to the pancreatic *beta* cells, thus leading to this disease. Hence inhibition of the aggregation process has been explored as a potential prevention or treatment of type II diabetes. *N*-methylated and non-methylated peptides spanning the length of amylin were synthesized and evaluated for their inhibition of full length amylin-mediated cytotoxicity to RIN-5F cells. The non-methylated peptides were very effective in inhibiting the cytotoxicity of amylin while the *N*-methylated peptides were not. Both the *N*-methylated and non *N*-methylated versions of the 29-34 region of amylin were equally effective.

4.2 Introduction

The incidence of type II diabetes also referred to as non-insulin dependent diabetes mellitus is on the increase each year and the World Health Organization (WHO) predicts there to be over 360 million diabetic patients worldwide by the year 2030.[1] From as early as 1901, a link between the deposition of fibrillar material in the Islets of Langerhans in the pancreas and manifestation of type II diabetes had been established.[2] It was found that the deposits consisted mainly of a small protein, called amylin, which aggregates into amyloid fibrils and type II diabetes was thus classified as an amyloid disease.[2-4] Amylin is a 37-amino acid long polypeptide and is released from the *β*-granules of pancreatic *beta* cells together with insulin in a constant molar ratio of 20:1 (insulin/amylin). It is believed to play a role in maintaining glucose homeostasis and was found to be released by the body following an increase in blood glucose levels, as is the case after a meal.[5, 6] Soluble monomeric amylin is stabilized when it self-associates via hydrogen bonding into *β*-sheet oligomeric states and can further associate into insoluble amyloid fibrils.[7, 8] The exact nature of the toxic species is controversial with some researchers arguing that amyloid fibers are toxic [9-17] whilst others have shown that the pre-amyloid intermediates (oligomers) exert the toxic effect.[18-22]

In 2002, it was found that the introduction of *N*-alkylated amino acids or ester functionalities into peptide sequences allowed the peptide to act as *β*-sheet inhibitors and prevented toxicity.[23] Single strands form *β*-sheets by hydrogen bonding between *NH*- and *O* moieties that point out of the peptide backbone. Peptides containing *N*-alkylated amino acids are able to bind to the native protein and prevent the attachment of any further peptide strands by disrupting the hydrogen-bonding capacity and by providing steric hindrance. In 1990, Westermark *et al.* found that the 20–29 region alone was able to form amyloid fibrils and for many years it was believed that this was the only region that was crucial for aggregation into cytotoxic fibrils.[24] This hypothesis was further supported when it was found that the 22–27 region is the shortest fragment of amylin that could form the typical cytotoxic amyloid fibrils.[25] However, a later study demonstrated that the 8–20 fragment is capable of forming fibrils that have the *β*-sheet conformation.[26] More recently, Abedini and Raleigh (2006) synthesized the 8–37 region of amylin, substituting residues at positions 17, 19 and 30 for proline and showed that the modified peptide had a significant lack of aggregating potential as compared to its wild type peptide.[27]

The sequence SNNF(N-Me)GA(N-Me)ILSS was reported as one of the first peptide-based inhibitors that reduced toxicity of the 20–29 region of amylin.[15] It was also reported that the presence of *N*-methylated amino acids allowed the peptide to exist in an ordered *β*-sheet structure which was crucial if the peptide was to be used as an inhibitor.[15] However, to date only two other modified peptides were shown to inhibit the aggregation of full length amylin and its subsequent cytotoxicity. The first of these two peptides made use of the full length amylin with *N*-methylations in positions 24 and 26 and the second was a hexapeptide homologous to the 22–27 region with *N*-methylated amino acids in the 23 and 25 positions.[16, 28]

In addition, there is only a limited number of studies that describe the evaluation of unmodified amylin derivatives as inhibitors of full length amylin-mediated cytotoxicity. Scrocchi *et al.* (2002) focused on the 20–29 region of amylin and observed that amylin$_{20–25}$ reduced amylin-mediated toxicity by 25% whereas amylin$_{24–29}$ did not.[29] However, it should be noted that amylin alone was only 35-40% toxic to RIN-1056 cells. In a later report, the 12-17 and 15-20 regions of amylin were tested as potential inhibitors of toxicity on the RIN-1056 cell line and it was reported that neither of the two peptides were successful.[30] Amylin$_{13–18}$ was observed to completely prevent amylin-mediated cytotoxicity on RIN-1056A cells and when freshly cultured human islets were exposed to full length amylin, this derivative reduced the amount of apoptotic cells from 25% to 12.5%.[31] The 20-25 region of amylin was also observed to reduce amylin toxicity by 50%.[31]

When working with amyloid proteins, it is difficult to compare results between reports. In this communication we thus report the synthesis of ten short *N*-methylated and non-methylated amylin derivatives spanning the full length of amylin and evaluated these via a cytotoxicity assay in a single study. It was also decided to use as many *N*-methylated amino acids in each peptide as synthetically possible since it was recently reported by Arvidsson *et al.* (2009) that a hexapeptide with five *N*-methylations was effective in inhibiting toxicity mediated by A$\beta_{1–42}$ protein.[32] Interestingly, the general trend observed was that the non-methylated peptides were better inhibitors of amylin-induced cytotoxicity than their *N*-methylated counterparts, with the exception of the *N*-methylated derivative of the 29-34 region of amylin which displayed an equal inhibitory effect as its non-methylated counterpart.

4.3 Materials and methods

4.3.1 Reagents

Rink amide resin, and all 9-fluorenylmethoxycarbonyl (Fmoc) protected amino acids and coupling reagents were purchased from GLS Biochem Systems, Inc. (China). The following protecting groups were used for the side chains of the amino acids: trityl (Trt) for asn, cys, gln, and his, *t*-butyl ether (*t*Bu) for ser and thr, 2,2,4,6,7-pentamethyl-dihydrobenzofuran-5-sulfonyl (Pbf) for arg, and *t*-butyloxycarbonyl (Boc) for lys. The Wang-CM resin was kindly donated by Matrix Innovation (Quebec, Canada). All solvents for synthesis and purification were of high performance liquid chromatography (HPLC) grade and were purchased from Sigma-Aldrich (U.S.A.). The CellTiter 96® nonradioactive cell proliferation assay was purchased from Promega Corporation (U.S.A.).

4.3.2 Peptide synthesis

Human amylin (1–37) was synthesized as described in Chapter 3. Amino acids were *N*-methylated as described by Zhang *et al.* (2005).[33] Synthetic peptides spanning the length of amylin (Figure 4.1) were synthesized on a CEM microwave peptide synthesizer using rink amide resin and standard Fmoc-based solid phase peptide synthesis methodology. Deprotection was performed using 20% piperidine in dimethyl formamide (DMF). The activator used in the synthesis was 0.5 M 2-(1H-benzotriazole-1-yl)-1, 1, 3, 3-tetramethyluronium hexafluorophosphate (HBTU) in DMF, with 1 M *N*, *N*-diisopropylethylamine (DIPEA) in DMF serving as the activator base. The peptides were cleaved from the resin using 5% tri-isopropylsilane in trifluoroacetic acid (TFA) (v/v) for one hour. They were then purified by reverse phase preparative HPLC on an ACE C18 preparative column (250 × 22 mm, Scotland) using a dual-buffer system. The first buffer consisted of 0.1% trifluoroacetic acid (TFA) in water (v/v) whilst the second buffer was composed of 0.1% TFA/acetonitrile (v/v). The peptides were eluted using a gradient from 10-60% acetonitrile over 45 minutes. The solvent from pooled peptide-containing fractions was evaporated and the samples were snap-frozen in liquid nitrogen and lyophilized. The purified peptides were analyzed with an Agilent 1100 HPLC system fitted with a Waters XBridge C18 column, 250 × 3.6 mm. A Bruker electrospray ionization time-of-flight spectroscope (ESI-QTOF) in positive mode was used to obtain mass spectra (MS) and matrix assisted laser desorption ionization time-of-flight mass spectroscopy (MALDI-TOF MS) was performed with an Autoflex III instrument (Bruker) operated in positive mode with cyano-4-hydroxycinnamic acid being used as the matrix.

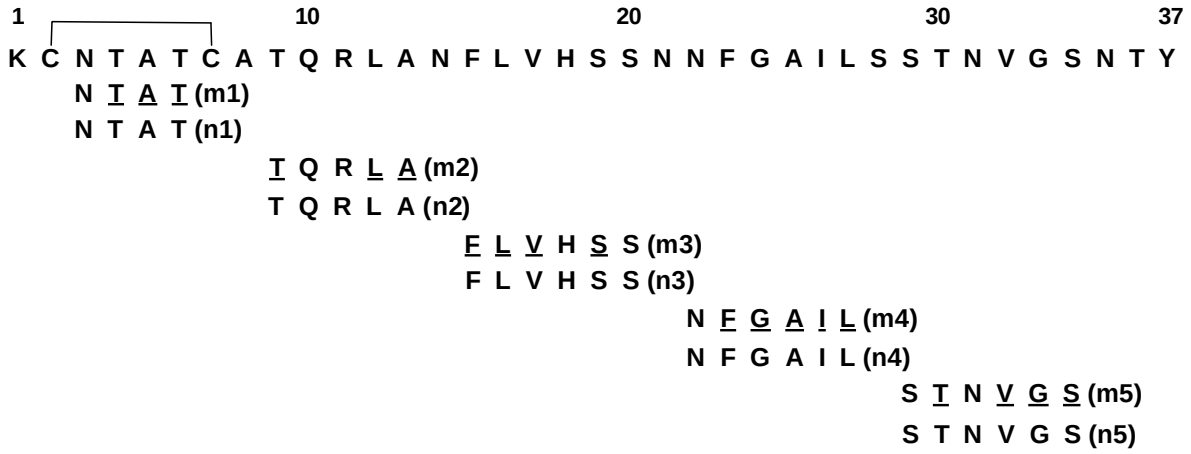

Figure 4.1 Primary structure of full length human amylin and the *N*-methylated and non-methylated amylin derivatives that were synthesized as potential inhibitors. Single letter notation used for amino acids and *N*-methylated amino acids are underlined. m1-m5 and n1-n5 are shorthand notations that are used to denote the *N*-methylated amylin derivatives and their non-methylated counterparts respectively.

4.3.3 Circular dichroism spectroscopy (CD)

CD measurements were carried out using a Jasco J-810 spectropolarimeter (c = 0.1 mmol, 25°C). Wavelength scans were performed with a minimum of five repeats.

4.3.4 Disaggregation method

Before any testing could be performed, it was essential to start with completely disaggregated amylin. As described in Chapter 3, disaggregation was achieved by solubilizing amylin in 200 µL hexafluoroisopropanol (HFIP):TFA solution (50:50, v/v) and sonicating for 10 minutes. Samples were left overnight and solvents were then removed under vacuum using a centrifugal evaporator for approximately 1-2 hours. Thereafter, approximately 100 µL HFIP was added to the peptide, followed by vortexing and the solvent was removed by rotary evaporation for 1-2 hours. To remove all traces of TFA, the latter process was repeated twice using HFIP (100 µL).

4.3.5 Transmission electron microscopy (TEM)

To monitor fibril formation, amylin was disaggregated as described above and solubilized in 10 mM sodium phosphate buffer, pH 7.4 containing 50 mM NaCl (Buffer A) by sonicating for five minutes to give a final concentration of 45 µM. TEM was performed as follows immediately

following preparation as well as after 24 hours of incubation at 37°C. At each time point, 2 µl aliquots of sample were transferred onto formvar coated carbon-stabilized copper grids. After drying for one minute, excess liquid was blot dried and samples were stained with 2% (w/v) uranyl acetate for 30 seconds. Samples were blot dried again before being analyzed with a CM120 Biotwin Philips transmission electron microscope at a voltage of 100 V.

To evaluate the effect of each amylin derivative on amylin fibrillogenesis, each amylin derivative was added to lyophilized samples of disaggregated amylin to yield a final ratio of 50 µM:250 µM (amylin:amylin derivative). Mixtures of amylin and each of the amylin derivatives were sonicated for five minutes before TEM was performed as described above.

4.3.6 Cytotoxicity assay

The RIN-5F cell line (European Collection of Cell Cultures, Sigma-Aldrich) was cultured in RPMI 1640 growth medium containing 10% heat-inactivated fetal bovine serum, 2 mM glutamine, 1 mM sodium pyruvate, 25 mM 2-[4-(2-hydroxyethyl)-1-piperazinyl] ethanesulfonic acid (HEPES), and 0.1 mg/mL penicillin/streptomycin. Cells were plated at a density of 7.5×10^5 cells/mL (100 µL/well) into poly-D-lysine precoated 96 well plates (Sigma-Aldrich) and incubated at 37 °C for 24 hours. Thereafter, spent media were removed from all wells and fresh fully constituted media were added (60 µL). Samples containing disaggregated amylin only (45 µM), amylin derivatives only (50-1000 µM) or mixtures of disaggregated amylin (45 µM) and each of its derivatives (225 µM), were prepared as described for TEM. Thereafter, 40 µL of each sample was added to each well whilst untreated control cells received 40 µL amylin-free samples that were disaggregated as described above and reconstituted in buffer solution. Plates were incubated at 37 °C for a further 24 hours before the CellTiter 96® non-radioactive cell proliferation assay was performed. This assay was carried out as per manufacturer's instructions to assess cell viability by measuring the cellular reduction of 3-(4,5-dimethylthiazol-2-yl)-2,5-diphenyltetrazolium bromide (MTT).[20, 22] Absorbance readings for the MTT assay were performed using an Automated Microplate Reader (ELx800) from Bio-Tek Instruments. Statistical analysis was performed using the One-way Analysis of Variance (ANOVA) and Tukey-Kramer Multiple comparisons test (GraphPad InStat version 3 for Windows XP, U.S.A) and results were considered significantly different if p values were less than 0.05.

4.4 Results

As illustrated in Table 4.1, all amylin derivatives were synthesized with a high yield and all peptides had a purity of >95%.

Table 4.1 Yield and purity of peptides synthesized

Amylin derivative	Expected Mass (g/mol)	Observed Mass (g/mol)	Yield (%)
NTAT (n1)	405.2	406.2	96
TQRLA (n2)	587.6	588.2	88
FLVHSS (n3)	688.4	689.2	90
NFGAIL (n4)	633.4	634.4	93
STNVGS (n5)	563.3	564.3	92
N<u>TAT</u> (m1)*	488.5	489.3	93
<u>T</u>QR<u>LA</u> (m2)*	629.4	630.2	70
<u>FLV</u>H<u>S</u>S (m3)*	785.9	786.4	85
N<u>FGAIL</u> (m4)*	744.8	745.4	88
S<u>T</u>N<u>VGS</u> (m5)*	660.7	661.3	90

* *N*-methylated amino acids are underlined

Circular dichroism (CD) spectroscopy measurements were taken of each peptide to determine its secondary structure. CD is based on the ability of optically active molecules ability preferentially absorbs either left- or right-handed circularly polarized light. The non-methylated amylin derivatives appear to be primarily unstructured in solution since the entire spectra exhibit a minimum around 200 nm and lack significant intensity between 210 and 230 nm (Figure 4.2). However, all of the amylin derivatives containing *N*-methylated amino acids displayed a β-sheet secondary structure since its maxima is at approximately 200 nm with a minima just after 220 nm (Figure 4.3).

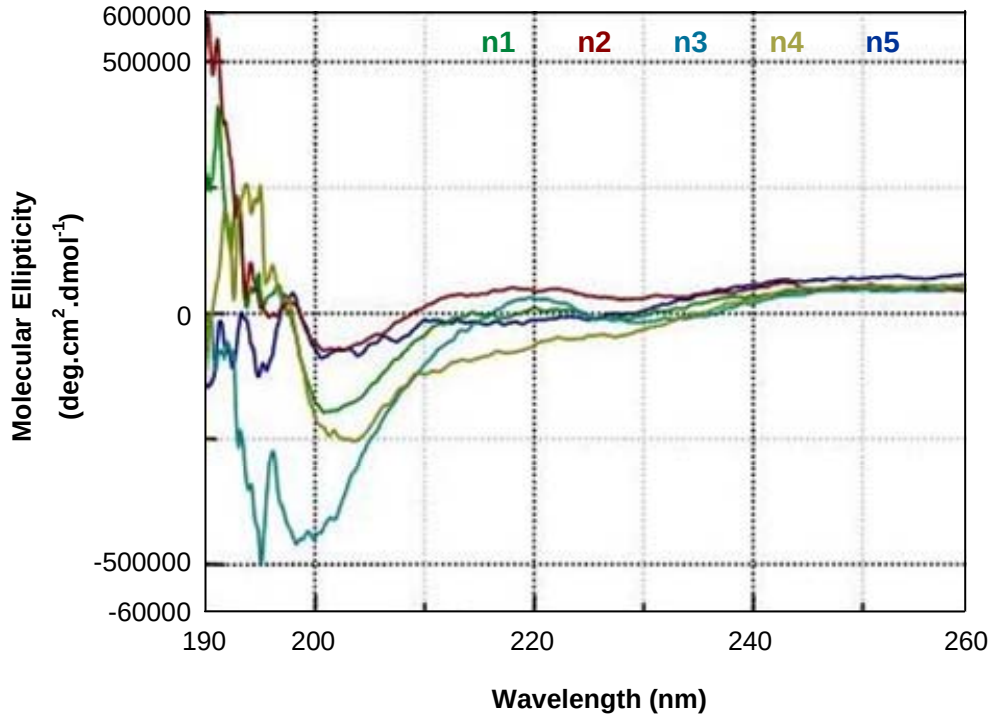

Figure 4.2 CD spectra of the non-methylated amylin derivatives n1-n5 indicating that these peptides are unstructured in solution.

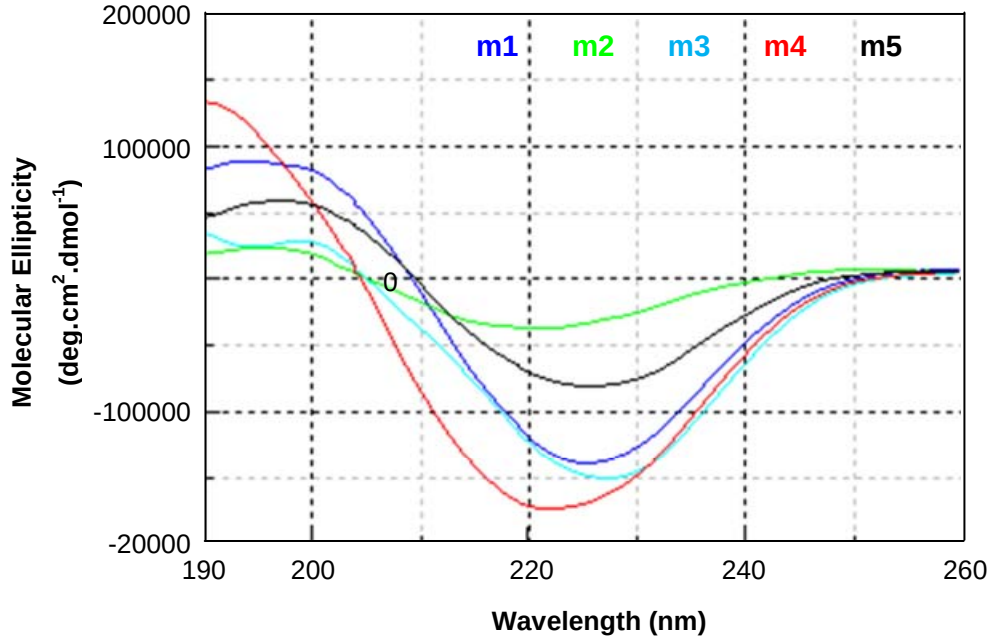

Figure 4.3 CD spectra of the *N*-methylated amylin derivatives m1-m5 indicating that these peptides are in a typical *β*-sheet conformation.

Transmission electron microscopy was performed to determine the effect of each amylin derivative on amylin fibril formation. TEM of all samples immediately after preparation revealed that no fibrils were present. After an incubation time of 24 hours, typical amyloid fibrils was observed in the sample containing amylin only (Figure 4.4). TEM analysis of samples containing amylin and each of its derivatives illustrated that with the exception of n1 and m5, all the other amylin derivatives (n2-n5 and m1-m4) did not prevent amylin aggregation into a typical fibrillar structure (Figures 4.5 and 4.6) after an incubation time of 24 hours. Amylin derivatives n1 and m5 appears to delay fibril formation as very few amorphous aggregates (Figure 4.7) were observed after an incubation time of 24 hours.

The cytotoxicity assay was performed to ascertain if any of the amylin derivatives were cytotoxic to the RIN-5F cell line and if they could reduce amylin-mediated cytotoxicity to these cells. The control studies indicated that the amylin derivatives were non-toxic to the RIN-5F cell line. As seen in Figure 4.8, amylin was approximately 70% toxic to RIN-5F cells. However, in the presence of the non-methylated amylin derivatives n1, n2, n4, and n5, the toxic effect of amylin was drastically reduced with p values less than 0.001. Amylin derivative n1 reduced the toxic effect of amylin from 70% to 25%, while derivatives n2 and n4 decreased toxicity by approximately 50%. Of the non-methylated amylin derivatives, n5 seems to be the best inhibitor and resulted in a decrease in toxicity from 70% to approximately 18% whereas derivative n3 decreased toxicity by only 20% ($p < 0.01$). It was found that the *N*-methylated peptide fragments m1–m4 did not reduce the toxic effect of amylin ($p > 0.05$) while, m5 (which is homologous to amylin$_{29–34}$ and contains four *N*-methylated amino acids) proved to be just as effective as its non-methylated derivative and decreased cytotoxicity from 70% to just 18% ($p < 0.001$).

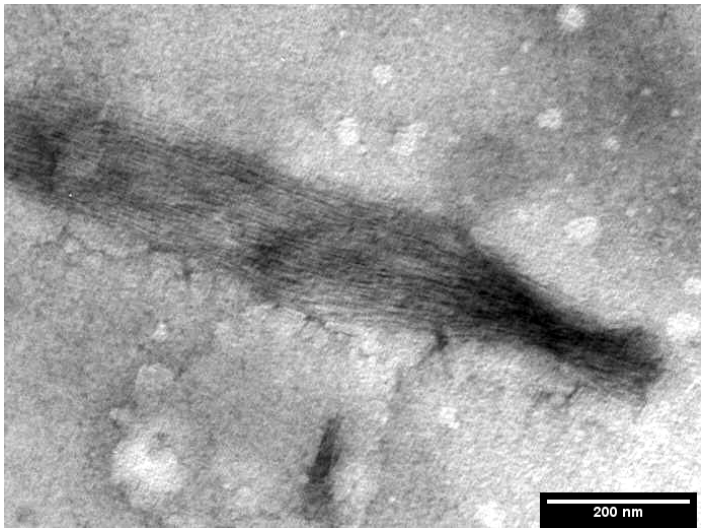

Figure 4.4 TEM analysis of samples containing amylin only after 24 hours incubation at 37°C in 10 mM sodium phosphate buffer, pH 7.4 containing 50 mM NaCl. Typical amyloid fibrils are observed in the electron micrograph of the sample containing amylin only. Scale bar = 200 nm.

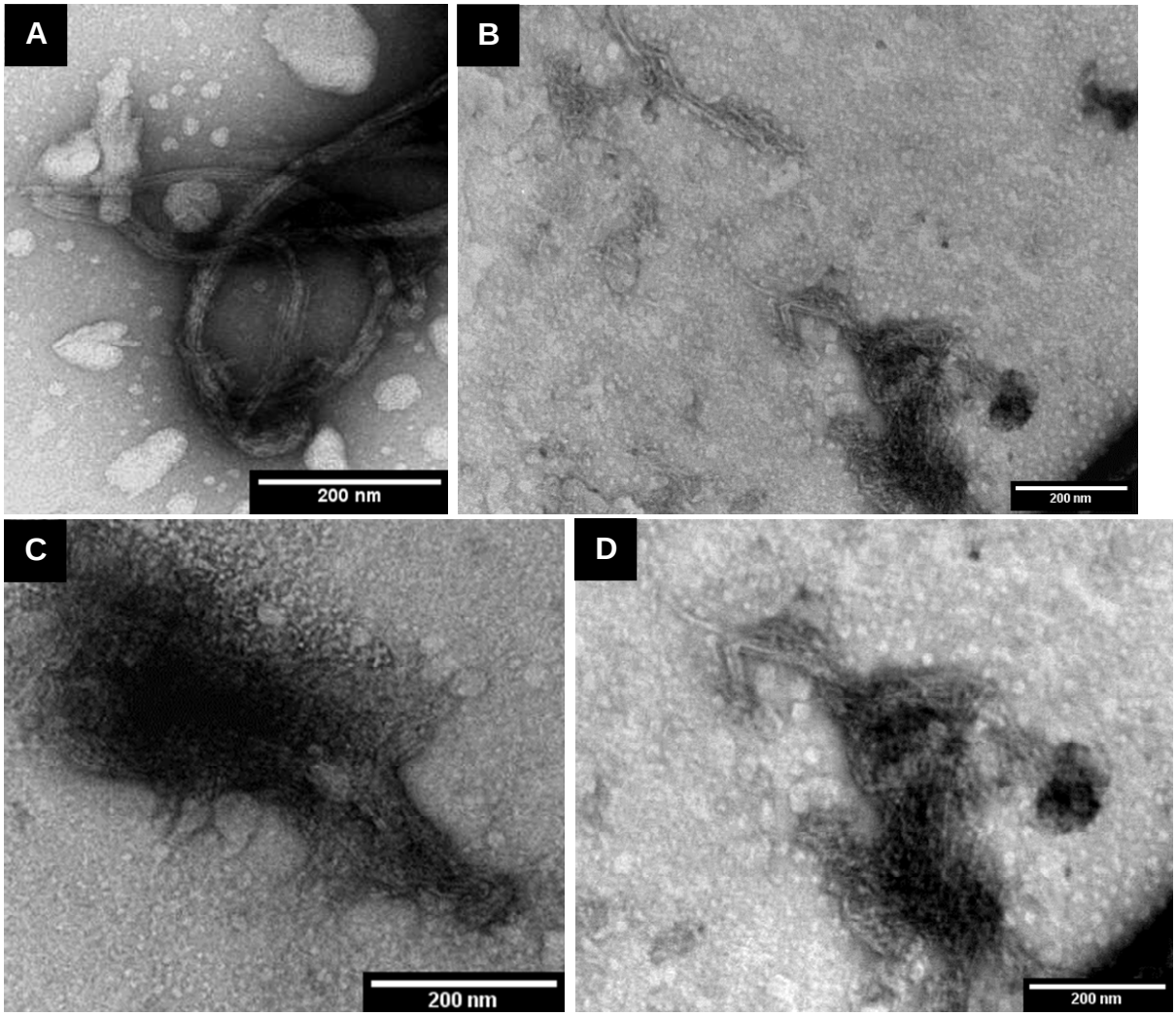

Figure 4.5 TEM analysis of samples containing a mixture of amylin and each of its derivatives after 24 hours incubation at 37°C in 10 mM sodium phosphate buffer, pH 7.4 containing 50 mM NaCl. Typical amyloid fibrils are observed in the electron micrographs of samples containing amylin its derivatives n2 (A), n3 (B), n4 (C), and n5 (D) respectively. Scale bar = 200 nm.

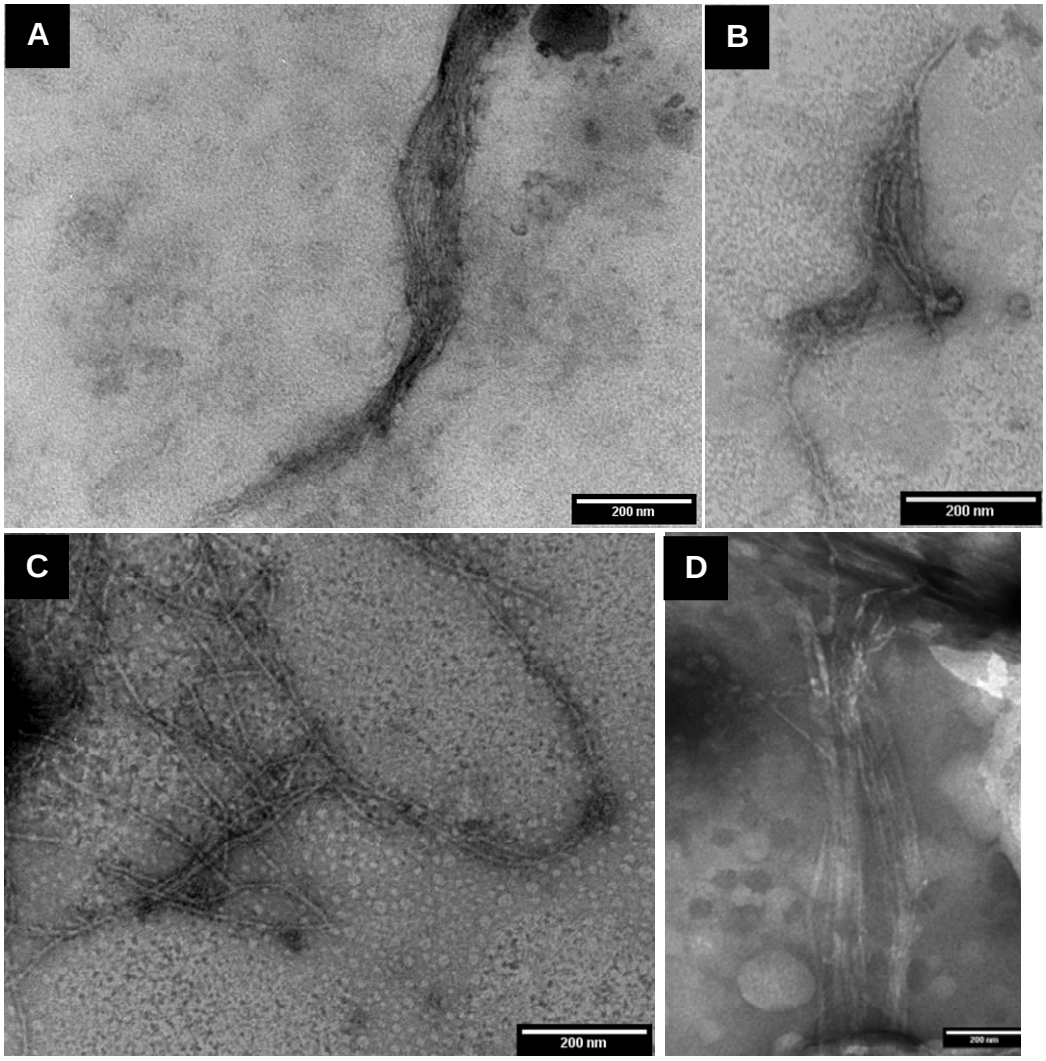

Figure 4.6 TEM analysis of samples containing a mixture of amylin and each of its derivatives after 24 hours incubation at 37°C in 10 mM sodium phosphate buffer, pH 7.4 containing 50 mM NaCl. Typical amyloid fibrils are observed in the electron micrographs of samples containing amylin its derivatives m1 (A), m2 (B), m3 (C), and m4 (D) respectively. Scale bar = 200 nm.

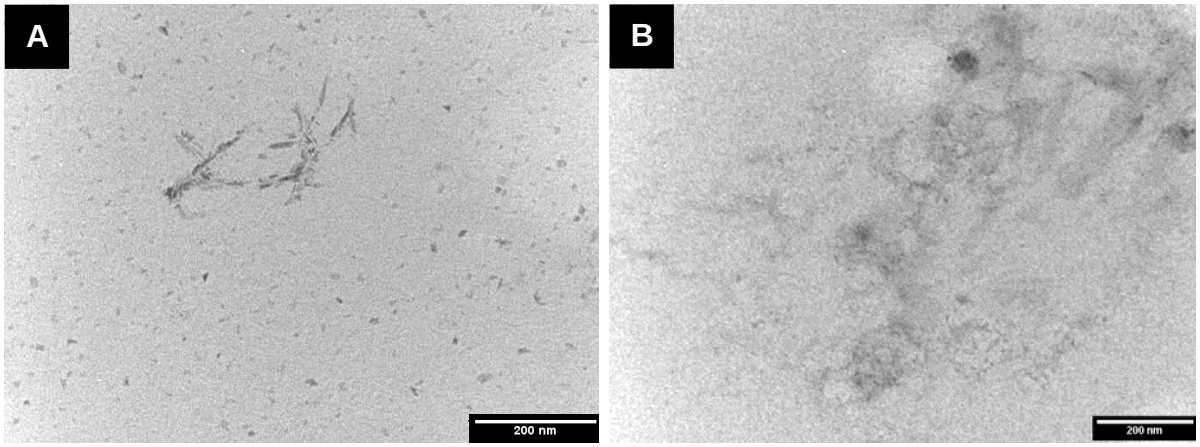

Figure 4.7 TEM analysis of samples containing a mixture of amylin and each of its derivatives after 24 hours incubation at 37°C in 10 mM sodium phosphate buffer, pH 7.4 containing 50 mM NaCl. Amorphous aggregates are present in samples containing amylin and derivatives n1 (A) and m5 (B) respectively. Scale bar = 200 nm.

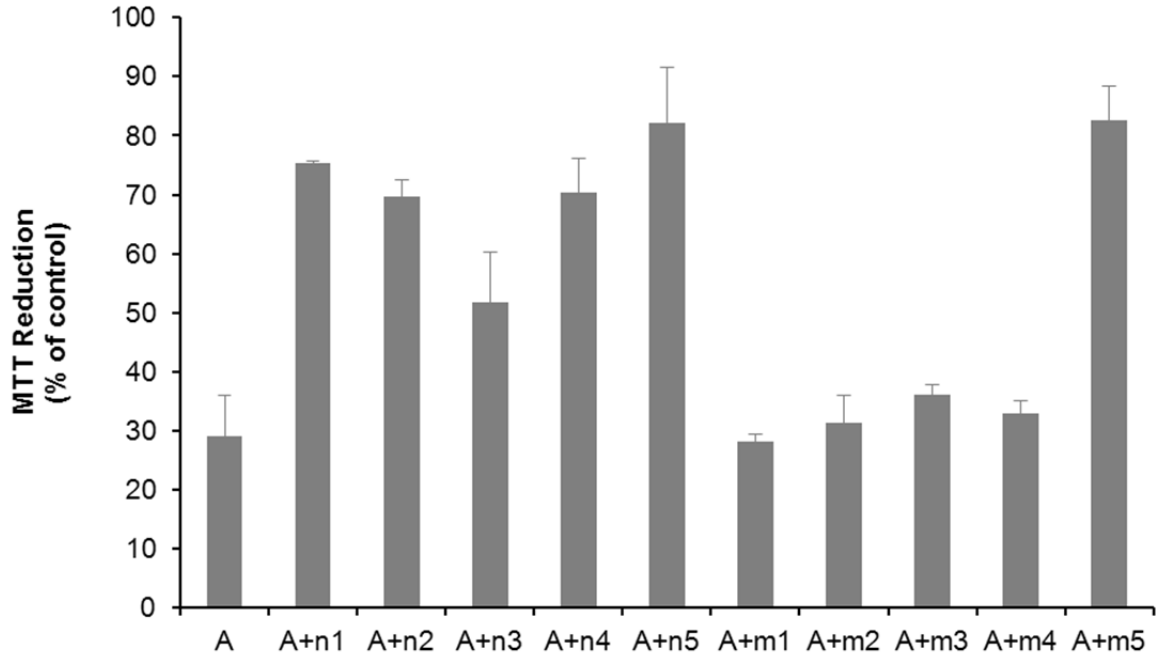

Figure 4.8 The cytotoxic effect of amylin (45 μM) on RIN-5F cells (7.5×10^4 cells/well after 24 hours incubation with amylin) in the presence or absence of its derivatives (225 μM), as determined by the MTT assay. Data are percentages of control values and are the mean (±SD) of five determinants. A = amylin, n1-n5 = non-methylated and m1-m5 = *N*-methylated derivatives of amylin. When compared to A, $p < 0.001$ for A+n1, A+n2, A+n4, A+n5 and A+m5; $p<0.01$ for A+n3; and $p>0.05$ for A+m1, A+m2, A+m3 and A+m4.

4.5 Discussion

As mentioned previously, derivatives of amylin have potential as inhibitors of amylin-mediated cytotoxicity and hence could be developed into therapeutic agents for type II diabetes. This study thus aimed to synthesize tetra- and hexa-peptide amylin derivatives spanning the length of amylin to evaluate their effect on fibril formation and amylin-mediated cytotoxicity. Analogs of these amylin derivatives were also synthesized with some of its constituent amino acids being substituted by *N*-methylated amino acids to assess if the presence of methyl groups could improve the ability of each amylin derivative to inhibit fibrillogenesis and/or amylin-mediated cytotoxicity.

As previously mentioned, the non-methylated amylin derivatives n2-n5 did not prevent fibrillogenesis. This observation is in agreement with other reports that have shown with the exception of amylin$_{3\text{-}6}$, that all other non-methylated amylin derivatives (n2-n5) were constituents of the amyloidogenic region of amylin.[8, 24-26, 29, 30, 35-40] In addition, amylin derivatives n2-n5 each contain at least one of the proposed nucleation sites for amylin aggregation.[41] It is noteworthy that amylin derivative n1 appears to delay fibril formation which is supportive of the hypothesis that the 1-7 region of amylin is in a random coil conformation and could have a modulating effect on amylin aggregation, that is the amyloidogenic nature of amylin is increased if this region is excluded from the amylin sequence.[26] However, all of the non-methylated amylin derivatives significantly reduced amylin-mediated cytotoxicity. Thus, it could be suggested that the non-methylated amylin derivative n1 retards amylin aggregation into toxic aggregates whilst the derivatives n2-n5 could potentially increase fibrillogenesis of amylin into non-toxic fibrils and thus our data supports the theory that the oligomer is the toxic species of amylin.[18-20, 22, 42-44] Of all the amylin derivatives analyzed in this study, only derivative n3 was previously evaluated as an inhibitor of amylin-mediated cytotoxicity.[30] Although it was found that this derivative did not reduce cytotoxicity, it should be noted that the previous study did not report on whether amylin was completely disaggregated prior to it being used in the cytotoxicity assay which could have a major impact on data generated.[30]

Contrary to expectations, the *N*-methylated amylin derivatives m1–m4 did not reduce fibrillogenesis and neither did they inhibit the toxic effect of amylin. It can therefore be suggested that the introduction of *N*-methylated amino acids into peptides does not always result in inhibition of fibril formation, an observation that has previously been reported.[45] In addition, further testing is necessary to probe amylin-amylin aggregation and to determine why *N*-methylated peptides in general do not prevent fibril formation.

However, amylin derivative m5 (which is homologous to amylin$_{29–34}$ and contains four *N*-methylated amino acids) proved to be just as effective as its non-methylated analog and also resulted in a 60% reduction of amylin-mediated cytotoxicity. Since both versions of amylin$_{29–34}$ could significantly reduce toxicity; this could be interpreted as a critical region for designing peptides as potential therapeutic agents of type II diabetes.

This is the first report describing the effect of peptides spanning the length of amylin for their ability to inhibit cytotoxicity of full length amylin. Amylin$_{3–6}$, amylin$_{9–13}$, amylin$_{22–27}$, amylin$_{29–34}$, and amylin derivative m5 which contains the sequence ST(N-Me)NV(N-Me)G(N-Me)S(N-Me) were identified as potential inhibitors of amylin-mediated cytotoxicity. The only drawback to the non-methylated amylin derivatives would be their biological instability and for this reason the *N*-methylated peptide corresponding to the 29–34 region becomes significant. The next step in finding a potential therapeutic agent for type II diabetes would be further testing to evaluate the biodegradability of the *N*-methylated amylin derivative m5 followed by *in vivo* testing.

In addition, a peptoid molecule that is based on the 29-34 region of amylin could also be evaluated as a potential inhibitor of amylin-mediated cytotoxicity. Peptoids are peptide analogs that contain *N*-substituted glycines and the R-groups on the amino group of each residue can be chosen to mimic a specific peptide sequence.[46] Sequence homology to amylin and in particular the 29-34 region, could allow association with full length amylin but since the R-groups are present on the amino group, the hydrogen bonding capacity of the peptide would be retarded, thus possibly preventing amylin aggregation. In addition, it has been suggested that peptoids may have reduced immunogenicity and good biostability [47], thus these modified peptides could be evaluated as potential inhibitors of amylin-mediated toxicity.

4.6 Conclusion

This is the first study that has synthesized amylin derivatives spanning the length of amylin and evaluated their effect on amylin-mediated cytotoxicity. It was observed that in general, the non-methylated peptides were better inhibitors of amylin-mediated cytotoxicity than their *N*-methylated counterparts. Interestingly, inhibition of amylin fibril formation did not correlate to inhibition of cytotoxicity which further supports the hypothesis that the oligomer is the toxic species of amylin. Due to its biostability, it can be suggested that the *N*-methylated amylin derivative ST(N-Me)NV(N-Me)G(N-Me)S(N-Me) has potential as a therapeutic agent of type II diabetes and further testing will be conducted using this derivative.

4.7 Acknowledgements

This work was made possible through financial support from the National Research Foundation and UKZN.

4.8 References

1. World Health Organisation. *Country and regional data-prevalence of diabetes worldwide*. Accessed: 14 March 2008. Available from: http://www.who.int/entity/diabetes/facts/en/.
2. Opie, E., *The relation of diabetes mellitus to lesions of he pancraes. hyaline degeneration of the islands of langerhans.* The Journal of experimental medicine, 1901. **5**: p. 528-540.
3. Cooper, G.J.S., Willis, A.C., Clark, A., Turner, R.C., Sim, R.B. and Reid, K.B.M., *Purification and characterization of a peptide from amyloid-rich pancreases of type 2 diabetic patients.* Proceedings of the National Academy of Science, 1987. **84**: p. 8628-8632.
4. Cooper, G.J.S., Leighton, B., Dimitriadis, G. D., Parry-Billings, M., Kowalchuk, J. M., Howland K., Rothbard, J. B., Willis, A. C. and Reid, K. B. M. , *Amylin found in amyloid deposits in human type 2 diabetes mellitus may be a hormone that regulates glycogen metabolism in skeletal muscle.* Proceedings of the National Academy of Science, 1988. **85**: p. 7763-7766.
5. Grant, A.D., and Brain, S.D., *Vascular Actions of Calcitonin Gene-Related Peptide and Adrenomedullin.* Physiological Review, 2004. **84**: p. 903-934.
6. Martin, C., *The physiology of amylin and insulin: maintaining the balance between glucose secretion and glucose uptake.* The Diabetes Educator, 2006. **32**: p. 101-104.
7. Kayed, R., Bernhagen, J., Greenfield, N., Sweimeh, K., Brunner, H., Voelter, W. and Kapurniotu, A., *Conformational transitions of islet amyloid polypeptide (IAPP) in amyloid formation in vitro.* Journal of Molecular Biology, 1999. **287**: p. 781-796.
8. Luca, S., Yau, W., Leapman, R., and Tycko, R., *Peptide conformation and supramolecular organization in amylin fibrils: constraints from solid-state NMR.* Biochemistry, 2007. **46**(47): p. 13505-13522.
9. Mattson, M.P., and Goodman, Y., *Different arrlyloidogenic peptides share a similar mechanism of neurotoxicity involving reactive oxygen species and calcium.* Brain Research, 1995. **676**: p. 219-224.
10. Mirzabekov, T.A., Lin, M. and Kagan, B.L., *Pore Formation by the Cytotoxic Islet Amyloid Peptide Amylin.* The Journal of Biological Chemistry, 1996. **Vol. 271**: p. 1988–1992.
11. Tomiyama, T., Kaneko, H., Kataoka, K., Asano, S. and Endo, N., *Rifampicin inhibits the toxicity of pre-aggregated amyloid peptides by binding to peptide fibrils and preventing amyloid-cell interaction.* Biochemical Journal, 1997. **322**: p. 859-865.
12. Kapurniotu, A., Bernhagen, J., Greenfield, N., Al-Abed, Y., Teichberg, S., Frank, R.W., Voelter, W. and Bucala, R., *Contribution of advanced glycosylation to the amyloidogenicity of islet amyloid polypeptide.* Eur. J. Biochem., 1998. **251**: p. 208-216.
13. Bai, J., Saafi, E.L., Zhang, S. and Cooper, G.J.S., *Role of Ca2+ in apoptosis evoked by human amylin in pancreatic islet b-cells.* Biochem. J., 1999. **343**: p. 53-61.
14. Hiddinga, H.J., and Eberhardt, N.L., *Intracellular amyloidogenesis by human islet amyloid polypeptide induces apoptosis in COS-1 cells.* American Journal of Pathology, 1999. **154**(4): p. 1077-1088.
15. Kapurniotu, A., Schmauder, A. and Tenidis, K., *Structure-based design and study of non-amyloidogenic, double n-methylated IAPP amyloid core sequences as inhibitors of IAPP amyloid formation and cytotoxicity.* Journal of Molecular Biology, 2002. **315**: p. 339-350.
16. Tatarek-Nossol, M., Yan, L., Schmauder, A., Tenidis, K., Westermark, G., and Kapurniotu, A., *Inhibition of hIAPP amyloid-fibril formation and apoptotic cell death by a designed hiapp amyloid-core-containing hexapeptide.* Chemistry & Biology, 2005. **12**: p. 797–809.
17. Yan, L., Velkova, A., Tatarek-Nossol, M., Andreetto, E. and Kapurniotu, A., *IAPP mimic blocks Ab cytotoxic self-assembly: cross-suppression of amyloid toxicity of Ab and IAPP suggests a molecular link between Alzheimers disease and type II diabetes.* Angew. Chem. Int. Ed., 2007. **46**: p. 1246 –1252.
18. Janson, J., Ashley, R.H., Harrison, D., McIntyre, S. and Butler, P.C., *The mechanism of islet amyloid polypeptide toxicity is membrane disruption by intermediate-sized toxic amyloid particles.* Diabetes, 1999. **48**: p. 491–498.
19. Anguiano, M., Nowak, R.J. and Lansbury, P.T., *Protofibrillar islet amyloid polypeptide permeabilizes synthetic vesicles by a pore-like mechanism that may be relevant to type II diabetes.* Biochemistry, 2002. **41**: p. 11338-11343.

20. Kayed, R., Sokolov, Y., Edmonds, B., McIntire, T.M., Milton, S.C., Hall, J.E. and Glabe, G.C., *Permeabilization of lipid bilayers is a common conformation-dependent activity of soluble amyloid oligomers in protein misfolding diseases.* The Journal of Biological Chemistry, 2004. **279**(45): p. 46363–46366.
21. Meier, J.J., Kayed, R., Lin, C., Gurlo, T., Haataja, L., Jayasinghe, S., Langen, R., Glabe, C.G., and Butler, P.C., *Inhibition of human IAPP fibril formation does not prevent -cell death: evidence for distinct actions of oligomers and fibrils of human IAPP.* Am J Physiol Endocrinol Metab, 2006. **291**: p. E1317–E1324.
22. Ritzel, R.A., Meier, J. J., Lin, C., Veldhuis, J. D., and Butler, P. C., *Human islet amyloid polypeptide oligomers disrupt cell coupling, induce apoptosis, and impair insulin secretion in isolated human islets.* Diabetes, 2007. **56**: p. 65-71.
23. Rijkers, D.T.S., Hoppener, J.W.M., Posthuma, G., Lips, C.J.M. and Liskamp, R.M.J, *Inhibition of amyloid fibril formation of human amylin by N-alkylated amino acid and α-hydroxy acid residue containing peptides.* Chemistry: A European Journal, 2002. **8**(18): p. 4285-4291.
24. Westermark, P., Engstrom, U., Johnson, K. H., Westermark, G.T., and Betsholtz, C., *Islet amyloid polypeptide: pinpointing amino acid residues linked to amyloid fibril formation.* Proceedings of the National Academy of Science, 1990. **87**: p. 5036-5040.
25. Tenidis, K., Waldner, M., Bernhagen, J., Fischle, W., Bergmann, M., Weber, M., Merkle, M., Voelter, W., Brunner, H., and Kapurniotu, A., *Identification of a penta- and hexapeptide of islet amyloid polypeptide (IAPP) with amyloidogenic and cytotoxic properties.* Journal of Molecular Biology, 2000. **295**: p. 1055-1071.
26. Jaikaran, E.T.A.S., Higham, C.E., Serpell, L.C., Zurdo, J., Gross, M., Clark, A. and Fraser, P.E., *Identification of a novel human islet amyloid polypeptide b-sheet domain and factors influencing fibrillogenesis.* Journal of Molecular Biology, 2001. **308**: p. 515-525.
27. Abedini, A., and Raleigh, D.P., *Destabilization of human IAPP amyloid fibrils by proline mutations outside of the putative amyloidogenic domain: is there a critical amyloidogenic domain in human IAPP?* J. Mol. Biol., 2006. **355**: p. 274–281.
28. Yan, L., Tatarek-Nossol, M., Velkova, A., Kazantzis, A., and Kapurniotu, A., *Design of a mimic of nonamyloidogenic and bioactive human islet amyloid polypeptide (IAPP) as nanomolar affinity inhibitor of IAPP cytotoxic fibrillogenesis.* Proceedings of the National Academy of Science, 2006. **103**(7): p. 2046–2051.
29. Scrocchi, L.A., Chen, Y., Waschuk, S., Wang, F., Cheung, S., Darabie, A.A., McLaurin, J. and Fraser, P.E., *Design of peptide-based inhibitors of human islet amyloid polypeptide fibrillogenesis.* Journal of Molecular Biology, 2002. **318**: p. 697–706.
30. Scrocchi, L.A., Ha, K., Chen, Y., Wu, L., Wang, F., and Fraser, P. E., *Identification of minimal peptide sequences in the (8-20) domain of human islet amyloid polypeptide involved in fibrillogenesis.* Journal of Structural Biology, 2003. **141**(3): p. 218-227.
31. Potter, K.J., Scrocchi, L. A., Warnock, G. L., Ao, Z., Younker, M. A., Rosenberg, L., Lipsett, M., Verchere, C. B., and Fraser, P. E., *Amyloid inhibitors enhance survival of cultured human islets.* Biochimica Et Biophysica Acta-General Subjects, 2009. **1790**(6): p. 566-574.
32. Bose, P.P., Chatterjee, U., Nerelius, C., Govender, T., Norstrom, T., Gogoll, A., Sandegren, A., Gothelid, E., Johansson, J., and Arvidsson, P. I., *Poly-N-methylated amyloid beta-peptide (A beta) C-terminal fragments reduce A beta toxicity in vitro and in Drosophila melanogaster.* Journal of Medicinal Chemistry, 2009. **52**(24): p. 8002-8009.
33. Zhang, S., Govender, T., Norstrom, T. and Arvidsson, P.I., *An improved synthesis of Fmoc-N-methyl-r-amino acids.* Journal of Organic Chemistry, 2005. **70**: p. 6918-6920.
34. Yan, L., Velkova, A., Tatarek-Nossol, M., Andreetto, E., and Kapurniotu, A., *IAPP mimic blocks Ab cytotoxic self-assembly: cross-suppression of amyloid toxicity of Ab and IAPP suggests a molecular link between Alzheimers disease and type II diabetes.* Angewandte Chemie International Edition, 2007. **46**: p. 1246 –1252.
35. Nilsson, M.R., and Raleigh, D.P., *Analysis of amylin cleavage products provides new insights into the amyloidogenic region of human amylin.* Journal of Molecular Biology, 1999. **294**: p. 1375-1385.
36. Goldsbury, C., Goldie, K., Pellaud, J., Seelig, J., Frey, P., Muller, S. A., Kistler, J., Cooper, G. J. S., and and U. Aebi, *Amyloid fibril formation from full-length and fragments of amylin.* Journal of Structural Biology, 2000. **130**(2-3): p. 352-362.
37. Azriel, R., and Gazit, E., *Analysis of the structural and functional elements of the minimal active fragment of islet amyloid polypeptide (IAPP) - An experimental support for the key role of the phenylalanine residue in amyloid formation.* Journal of Biological Chemistry, 2001. **276**(36): p. 34156-34161.
38. Kajava, A.V., Aebi, U., and Steven, A. C., *The parallel superpleated beta-structure as a model for amyloid fibrils of human amylin.* Journal of Molecular Biology, 2005. **348**(2): p. 247-252.
39. Galzitskaya, O.V., Garbuzynskiy, S. O., and Lobanov, M. Y., *Is it possible to predict amyloidogenic regions from sequence alone?* Journal of Bioinformatics and Computational Biology, 2006. **4**(2): p. 373-388.

40. Zhang, Z., Chen, H., and Lai, L., *Identification of amyloid fibril-forming segments based on structure and residue-based statistical potential.* Bioinformatics, 2007. **23**(17): p. 2218-2225.
41. Shim, S.H., Gupta, R., Ling, Y. L., Strasfeld, D. B., Raleigh, D. P., and Zanni, M. T., *Two-dimensional IR spectroscopy and isotope labeling defines the pathway of amyloid formation with residue-specific resolution.* Proceedings of the National Academy of Sciences of the United States of America, 2009. **106**(16): p. 6614-6619.
42. Konarkowska, B., Aitken, J. F., Kistler, J., Zhang, S. P., and Cooper, G. J. S., *The aggregation potential of human amylin determines its cytotoxicity towards islet beta-cells.* Febs Journal, 2006. **273**(15): p. 3614-3624.
43. Meier, J.J., Kayed, R., Lin, C., Gurlo, T., Haataja, L., Jayasinghe, S., Langen, R., Glabe, C.G., and Butler, P.C., *Inhibition of human IAPP fibril formation does not prevent beta-cell death: evidence for distinct actions of oligomers and fibrils of human IAPP.* American Journal of Physiology, Endocrinology and Metabolism, 2006. **291**: p. E1317–E1324.
44. Aitken, J.F., Loomes, K. M., Scott, D. W., Reddy, S., Phillips, A. R. J., Prijic, G., Fernando, C., Zhang, S. P., Broadhurst, R., L'Huillier, P., and Cooper, G. J. S., *Tetracycline treatment retards the onset and slows the progression of diabetes in human amylin/islet amyloid polypeptide transgenic mice.* Diabetes, 2010. **59**(1): p. 161-171.
45. Gordon, D.J., K.L. Sciarretta, and S.C. Meredith, *Inhibition of beta-amyloid(40) fibrillogenesis and disassembly of beta-amyloid(40) fibrils by short beta-amyloid congeners containing N-methyl amino acids at alternate residues.* Biochemistry, 2001. **40**(28): p. 8237-8245.
46. Simon, R.J., Kania, R. S., Zuckermann, R. N., Huebner, V. D., Jewell, D. A., Banville, S., Ng, S., Wang, L., Rosenberg, S., Marlowe, C. K., Spellmeyer, D. C., Tan, R. Y., Frankel, A. D., Santi, D. V., Cohen, F. E., and Bartlett, P. A., *Peptoids - a modular approach to drug discovery.* Proceedings of the National Academy of Sciences of the United States of America, 1992. **89**(20): p. 9367-9371.
47. Patch, J.A. and A.E. Barron, *Mimicry of bioactive peptides via non-natural, sequence-specific peptidomimetic oligomers.* Current Opinion in Chemical Biology, 2002. **6**(6): p. 872-877.

Chapter 5

RESEARCH RESULTS III

Novel insights into amylin aggregation

This manuscript was submitted for publication in
Biotechnology and Biotechnological Equipment
(Submitted on 12/12/12)

Novel insights into amylin aggregation

Karen Pillay,[a] and Patrick Govender[a]

[a]*School of Life Sciences, University of KwaZulu-Natal, South Africa*

5.1 Abstract

Amylin is a peptide that aggregates into species that are toxic to pancreatic *beta* cells, leading to type II diabetes. This study has for the first time quantified amylin association and dissociation kinetics (association constant (k_a) = 28.7 ± 5.1 $M^{-1}s^{-1}$ and dissociation constant (k_d) = 2.8 ± 0.6 x 10^{-4} s^{-1}) using surface plasmon resonance (SPR). Thus far, techniques used for the sizing of amylin aggregates do not cater for the real time monitoring of unconstrained amylin in solution. In this regard we evaluated recently innovated nanoparticle tracking analysis (NTA). In addition, both SPR and NTA were used to study the effect of previously synthesized amylin derivatives on amylin aggregation and to evaluate their potential as a cell-free system for screening potential inhibitors of amylin-mediated cytotoxicity. Results obtained from NTA highlighted a predominance of 100-300 nm amylin aggregates and correlation to previously published cytotoxicity results suggests the toxic species of amylin to be 200-300 nm in size. The results seem to indicate that NTA has potential as a new technique to monitor the aggregation potential of amyloid peptides in solution and also to screen potential inhibitors of amylin-mediated cytotoxicity.

5.2 Introduction

Full length human amylin (amylin) is a 37 amino acid long peptide which is released together with insulin from pancreatic *beta* cells.[1, 2] Accumulation of amylin can result in its soluble monomeric form aggregating into toxic oligomers and eventually fibrils [3-5], allowing it to be classified as an amyloidogenic peptide and implicating it in the development of type II diabetes.[2, 6-9] Inhibition or prevention of amylin aggregation and subsequent cytotoxicity has always relied on compounds that could bind to amylin [10-15], and numerous studies have investigated the multi-faceted dynamics of amylin aggregation.

Techniques that have been used to elucidate the conformational change from a random coil or helical structure to a β-sheet structure and to provide a model for the secondary structure of amylin include circular dichroism spectroscopy [16, 17], Fourier transform infrared (FT-IR) spectroscopy [18], two-dimensional (2D) spectroscopy [19, 20], and solid state nuclear magnetic resonance (NMR).[21] Filtration assays [5, 16] were used to monitor the time-dependent change in aggregate size but does not allow for real time monitoring of the aggregation process. For observation of the aggregation process in real time, atomic force microscopy (AFM) [22, 23] can be employed which generates quantitative data on the diameter as well as the growth rate of amylin aggregates. The latter mentioned amylin aggregation dynamics were also elucidated using scanning transmission electron microscopy (STEM).[17, 24, 25]

Two other techniques that have been used to monitor amylin aggregation dynamics include, electrochemical analysis [26] which is based on the oxidation of tyrosine, and tryptophan triplet quenching [27] which as its name implies monitors the quenching of the triplet state of tryptophan by cysteine or disulfides. Although no quantitative data were presented, these techniques were used to study the rate of interaction between the chain termini of amylin and the kinetics of amylin aggregation respectively. A more recent study made use of the thioflavin T (ThT) dye and total internal reflection fluorescence microscopy to visualize amylin aggregation.[28] Although AFM and STEM data can be combined to generate association kinetics, none of the techniques mentioned above are independently capable of generating quantitative data on the association and dissociation kinetics of amylin. In addition, no study to date has monitored the change in size of aggregates that formed from unconstrained amylin in solution over real time.

From as early as 1994, surface plasmon resonance (SPR) technology has been used to determine the aggregation kinetics of amyloidogenic proteins.[29-31] Surface plasmon resonance can monitor protein-protein interaction and is based on the principle that the refractive index at a surface changes proportionally to the amount of molecules present on it which can be measured using an optical system.[32] Some of the advantages of SPR are that it allows for fibril growth to be monitored over minutes or even seconds, very low sample concentrations are required, and no peptide-labeling strategy is necessary thus permitting direct analysis of unmodified peptide sequences.[33] Moreover, quantitative data can be generated to express the rate of association as well as the dissociation kinetics.

Of all the amyloidogenic proteins, amyloid *beta* (Aβ) interactions have been the most extensively studied using SPR [30, 33-46] followed by prion protein (PrP), which have been implicated in Alzheimer's disease and transmissible spongiform encephalopathy (Prion diseases) respectively.[47-50] Initially Myszka *et al.* (1999) reported SPR as a suitable technique to assess the association and dissociation kinetics of Aβ aggregation.[51] Thereafter, SPR was employed to extensively characterize the aggregation kinetics of Aβ [33, 37], and a SPR-based assay was subsequently developed to allow identification of small molecules that bind to Aβ and which could act as potential therapeutic agents against Alzheimer's disease.[36] It was also reported that SPR could be used as a potential assay for screening anti-prion molecules.[48] For more details with respect to SPR investigations into Aβ aggregation an extensive review by Aguilar and Small (2005) is recommended.[52] However, up until now SPR-based studies into amylin aggregation are limited to the attachment of biotinylated-amylin derivatives to strepavidin-coated sensor chips.[53, 54]

Jaikaran *et al.* (2004) evaluated the interaction of rat amylin and compounds present in the secretory granule of pancreatic *beta* cells such as insulin, somatostatin and proinsulin, with the sensor chip-bound biotinylated-amylin.[53] A similar SPR-based approach was employed by Wei *et al.* (2009) and in both of these studies, it was suggested that insulin inhibits formation of β-sheet structures by binding to biotinylated-amylin.[53, 54] The most recent study immobilized nanoparticles on a sensor chip and used SPR to evaluate the binding affinity of amylin for these particles.[55] However, the generated data was not indicative of the kinetics of amylin association and dissociation. In addition, a SPR-based strategy is yet to be evaluated as a potential cell-free selection system for inhibitors of amylin-mediated cytotoxicity.

Elucidation of the aggregation dynamics of amylin could also involve monitoring the change in size of the amylin aggregates. As mentioned earlier, other studies that have monitored the size of amylin aggregates made use of STEM or AFM which involves adsorption of aggregates onto copper grids or mica surfaces respectively.[5, 16, 17, 24, 25] Although these studies provided valuable insight into amylin aggregate structure, they did not allow for unconstrained real time monitoring of amylin aggregation. In addition, it has been observed that fibrils formed from unconstrained amylin in solution exhibit distinctly different morphologies from those propagated on a mica surface.[22, 23] It was suggested that the mica surface used in AFM could possibly impede coiling of fibrils around each other and thereby prevent formation of higher order fibrils.[22, 23]

Another commonly used particle sizing technique but which does not involve attachment of the molecule to a solid support is dynamic light scattering (DLS). This technique is easy to perform and has been proven to produce accurate results in a short time.[56] Dynamic light scattering relies on the phenomenon that Brownian motion of particles causes fluctuations in their scattered light intensity which is proportional to the particle size. An alternative technique that makes use of the Brownian motion of particles for size determination is nanoparticle tracking analysis (NTA) which was developed by Malloy and Carr (2006).[57] The NTA technology makes use of a laser light scattering microscope and charge-coupled device (CCD) camera that visualizes and records nanoparticles. Thereafter NTA-based software is able to track nanoparticles that move under Brownian motion and relate the movement to its size using a formula (Equation 1) as derived by Filipe *et al.* (2010) [58] from the Stokes-Einstein equation [59], as follows:

$$\overline{(x,y)^2} = \frac{2k_BT}{3r_h\pi\eta} \qquad (1)$$

where k_B is the Boltzmann constant, and $\overline{(x,y)^2}$ is the mean-squared speed of a particle at temperature T, in a medium of viscosity η with a hydrodynamic radius of r_h. Thus, NTA can estimate the size of particles in a poly-disperse sample and was shown to be a suitable technique for monitoring protein aggregation.[58]

To date, DLS has been used to size the monomeric form of amylin and the aggregated form of amylin derivatives.[60, 61] However, it should be mentioned that DLS and NTA technologies are yet to be employed to evaluate the oligomeric and fibrillar forms of amylin.

It is also noteworthy that cell-free systems such as circular dichroism (CD) [11, 13, 14, 62, 63], FT-IR spectroscopy [11], transmission electron microscopy [11-13, 62-65], the ThT assay [12-14, 64-67] and sedimentation assays [12, 14, 62] cannot differentiate between the toxic oligomeric and non-toxic fibrillar forms of amylin and thus are used together with cell-based assays for screening potential inhibitors of amylin-induced cytotoxicity. However, cell-based systems can be time-consuming and extremely expensive as it is dependent on the growth rate of a particular cell line and is also labor-intensive, thus highlighting the need for a cell-free system for efficient routine screening of potential inhibitors of amylin-mediated cytotoxicity.

In the present study we employ DLS, NTA and SPR strategies to evaluate the aggregation dynamics of amylin. Moreover the potential of these techniques as a new screening technology for inhibitors of amylin-mediated cytotoxicity was assessed by monitoring the effect of chemically synthesized human amylin derivatives on amylin-amylin interaction and correlating results to previously published cytotoxicity data.[68] NTA was also used to identify the size of the amylin aggregates that are probably responsible for amylin-mediated cytotoxicity.

SPR-derived data indicates that the association kinetics of amylin is similar to that of A$\beta_{1\text{-}40}$ whilst it appears that amylin dissociates slower than A$\beta_{1\text{-}40}$. Data generated from NTA of amylin samples co-incubated with each of its derivatives were found to correlate well with the ability of each amylin derivative to inhibit amylin-mediated cytotoxicity. In addition, NTA seemingly indicates that the size range of the toxic species of amylin is 200-300 nm. It can be tentatively suggested that NTA could be employed as a novel cell-free approach to monitor the aggregation of amyloidogenic peptides and for the screening of potential inhibitors of amylin aggregation and cytotoxicity.

5.3 Materials and Methods

5.3.1 Reagents

All 9-fluorenylmethoxycarbonyl (Fmoc) protected amino acids and coupling reagents were purchased from GLS Biochem Systems, Inc. (China). The following protecting groups were used for the side chains of the amino acids; trityl (Trt) for asn, cys, gln, and his, t-butyl ether (tBu) for ser and thr, 2,2,4,6,7-pentamethyl-dihydrobenzofuran-5-sulfonyl (Pbf) for arg, and t-butyloxycarbonyl (Boc) for lys. The PAL-ChemMatrix resin was purchased from Matrix Innovation (Canada) and all solvents for synthesis and purification were of high performance liquid chromatography (HPLC) grade and were purchased from Sigma-Aldrich (U.S.A.). The CM5 sensor chip and the thiol coupling kit were purchased from BIAcore AB (Sweden).

5.3.2 Peptide synthesis

For the SPR experiment, a modified version of human amylin (MA) was synthesized, wherein the first seven residues at the *N*-terminal of human amylin was replaced by the linker sequence CRKRK (Figure 5.1). This modification contains a cysteine residue at the *N*-terminus to enable thiol coupling to the BIAcore sensor chip, thus allowing MA to be used as the ligand for the SPR-based experiment. Chemically synthesized human amylin (amylin) [69] was used as the analyte for the SPR experiments, as well as for the DLS and NTA experiments.

Figure 5.1 Primary sequences of chemically synthesized full length human amylin and modified amylin (MA).

Modified amylin was synthesized on a 0.1 mmol scale using a CEM microwave peptide synthesizer as described previously.[69] Briefly, deprotection was performed using 20% piperidine in dimethyl formamide (DMF). The activator used in the synthesis was 0.5 M 2-(1H-benzotriazole-1-yl)-1, 1, 3, 3-tetramethyluronium hexafluorophosphate (HBTU) in DMF, with 1 M *N*, *N*-diisopropylethylamine (DIPEA) in DMF serving as the activator base. The peptide was cleaved from the resin using 5% tri-isopropylsilane in trifluoroacetic acid (TFA) (v/v) for two hours.

Amylin derivatives (Table 5.1) were synthesized as potential inhibitors of amylin-mediated cytotoxicity as previously reported [68] and their impact on amylin aggregation dynamics were investigated.

Table 5.1 Sequence of chemically synthesized non-methylated and *N*-methylated amylin derivatives

Amylin segment	Non-methylated sequence	*N*-methylated sequence
$Amylin_{3-6}$	NTAT (n1[#])	N<u>TAT</u>[*] (m1[#])
$Amylin_{9-13}$	TQRLA (n2[#])	<u>TQRLA</u>[*] (m2[#])
$Amylin_{15-20}$	FLVHSS (n3[#])	<u>FLVHSS</u>[*] (m3[#])
$Amylin_{22-27}$	NFGAIL (n4[#])	N<u>FGAIL</u>[*] (m4[#])
$Amylin_{29-34}$	STNVGS (n5[#])	S<u>TNVGS</u>[*] (m5[#])

[#]n1-n5 and m1-m5 are shorthand notations that are used to denote amylin derivatives.

[*]*N*-methylated amino acids are underlined.

5.3.3 Peptide purification

The modified amylin was purified on an ACE C18 preparative column (250 × 22 mm, Scotland) as previously described.[69] A dual-buffer system was employed, with TFA serving as the ion-pairing agent. The first buffer consisted of 0.1 % TFA/H_2O (v/v) whilst the second buffer was composed of 0.1% TFA/acetonitrile (v/v). The peptides were eluted using a gradient of 0-90% of 0.1% TFA/acetonitrile (v/v) over 90 minutes with a flow rate of 20 mL/min. The solvent from pooled peptide-containing fractions was evaporated to 20 mL and the samples were snap-frozen in liquid nitrogen and lyophilized.

5.3.4 Peptide analysis

The purified peptide was analyzed with an Agilent 1100 HPLC system fitted with a Waters XBridge C18 column, 250 × 3.6 mm as previously described.[69] Chromatography was performed over 90 minutes using a gradient of 0-90% of 0.1% TFA/acetonitrile (v/v) at a flow rate of 0.3 mL/min and the eluent was monitored at a UV wavelength of 215 nm. A Bruker electrospray ionization time-of-flight spectroscope (ESI-QTOF) in positive mode was used to obtain mass spectra (MS) and matrix assisted laser desorption ionization time-of-flight mass spectroscopy (MALDI-TOF MS) was performed with an Autoflex III instrument (Bruker) operated in positive mode with cyano-4-hydroxycinnamic acid being used as the matrix.

5.3.5 Disaggregation method

Disaggregation of amylin and its derivative MA were performed as previously described.[68] Pre-weighed amylin samples were solubilized in 200 µL hexafluoroisopropanol (HFIP):TFA solution (50:50, v/v), sonicated for 10 minutes and left overnight. The solvents were then removed under vacuum using a centrifugal evaporator for approximately 1-2 hours. Approximately 100 µL HFIP was added to the peptide, followed by vortexing and the solvent was removed by rotary evaporation for 1-2 hours. To remove all traces of TFA, the latter process was repeated twice using HFIP (100 µL).

5.3.6 Amylin immobilization for surface plasmon resonance (SPR)

All sensorgrams for SPR were performed on a BIAcoreX biosensor and analyzed using BIAevaluation version 4.1.1 software (BIAcore AB, Sweden). The running buffer for all SPR-based experiments were adapted from Jaikaran *et al.* (2004) [53] and contained 10 mM 4-(2-hydroxyethyl)-1-piperazineethanesulfonic acid (HEPES), 4 mM EDTA, 150 mM NaCl, 0.005% Tween 20, and 5% dimethylsulfoxide (DMSO), pH 7.4. The following solutions were adapted from Liu *et al.* (2004) and Takahashi *et al.* (2010) [44, 70] for the regeneration/washing steps. Solution 1 contained 6 M guanidine hydrochloride (Gdn-HCl) in 10 mM Tris-HCl (pH 8.0), solution 2 was made up of 5% DMSO in water (v/v), and solution 3 was composed of 100 mM NaOH.

Attachment of MA to the CM5 sensor chip followed standard ligand thiol coupling conditions as suggested by the manufacturer. A flow rate of 10 µL/min was maintained for all immobilization steps, unless otherwise stated. The carboxymethyl dextran matrix on the CM5 sensor chip was activated by injecting 40 µL of a 1:1 mixture of 200 mM *N*-ethyl-*Nα*-[(dimethylamino)propyl]-carbodiimide (EDC) and 50 mM *N*-hydroxysuccinimide (NHS), followed by the addition of 40 µL of 80 mM 2-(2-Pyridinyldithio)-ethaneamine hydrochloride (PDEA) in 50 mM sodium borate buffer (pH 8.5). A 20 µL aliquot of 1 µM MA in 10 mM sodium acetate buffer (pH 5.0) was then injected into the activated flow cell. An aliquot (40 µL) of 50 mM L-cysteine in 0.1 M sodium acetate and 1.0 M NaCl, pH 4.0 was then injected to eliminate free, unreacted maleimide groups so as to prevent non-specific binding. To remove non-covalently associated MA, the surface of the chip was washed sequentially with 15 µL of each of the three wash solutions described above, whilst maintaining a flow rate of 20 µL/min. The control flow cell was setup using the protocol described above with elimination of the MA attachment step and the three subsequent wash steps.

5.3.7 Surface plasmon resonance analysis of amylin and its derivatives

A flow rate of 5 µL/min was maintained for all subsequent SPR experiments, unless otherwise stated. To determine amylin aggregation kinetics, a concentration series (40-120 µM) of disaggregated amylin samples were solubilized in filter sterilized (0.22 µm, nylon) running buffer by sonication for five minutes and injected onto the sensor chip-immobilized amylin for 3 minutes. Dissociation kinetics was monitored for 360 seconds by allowing running buffer only to pass over the sensor chip surface. Whilst maintaining a flow rate of 20 µL/min, regeneration was achieved using 15 µL of solution 1 and solution 3 respectively. Triplicate injections of 40, 50, 60, 80 and 120 µM disaggregated amylin were analyzed in a random order with two regeneration steps being performed between each concentration. Curve fitting of each data set at varying concentrations were performed using BIAevaluation version 4.1.1 software.

To evaluate the effect of each amylin derivative on amylin-amylin interaction, stock solutions (1 mM) of each derivative was prepared in running buffer. Each amylin derivative was then added to lyophilized samples of disaggregated amylin to yield a final ratio of 50 µM:250 µM (amylin:amylin derivative). Mixtures of amylin and each of the amylin derivatives were sonicated for 5 minutes before 15 µL of each sample was injected onto sensor chip-immobilized amylin. Dissociation was once again monitored for 360 seconds by allowing running buffer to flow over the sensor chip surface. Between each sample, regeneration was performed as described above.

All sensorgrams were double referenced, that is, responses were corrected with both blank buffer injections and the response from the reference flow cell. Double referencing was performed to remove system artifacts as recommended by Myszka (1999).[51] For samples containing a mixture of amylin and each of its derivatives, responses were also corrected with sensorgrams obtained from 15 μL injections of samples containing each amylin derivative only (250 μM).

5.3.8 Dynamic light scattering (DLS)

Dynamic light scattering experiments were performed in a Zetasizer NanoZS (Malvern Instruments Ltd., United Kingdom). To monitor the change in size of amylin aggregates during aggregation, a sample of disaggregated amylin was solubilized by sonication for five minutes in filter sterilized 10 mM sodium phosphate buffer, pH 7.4 containing 50 mM NaCl (Buffer A) to a final concentration of 50 μM and analyzed at various time points. To determine if lower concentrations of the sample affected the poly-dispersity index, serial dilutions of the 50 μM amylin sample were prepared in Buffer A and analyzed. Zetasizer version 6.30 software (Malvern Instruments Ltd., United Kingdom) was used to analyze and convert data sets obtained to apparent hydrodynamic diameters.

5.3.9 Nanoparticle tracking analysis (NTA)

NTA measurements were performed with a NanoSight LM20 instrument (NanoSight, United Kingdom) equipped with a 640 nm laser and a temperature controlled sample chamber. To monitor the change in size of amylin aggregates during aggregation, disaggregated amylin was solubilized by sonication for five minutes in Buffer A to a final concentration of 50 μM. The peptide was then injected into the sample chamber and allowed to equilibrate to 37°C (approximately one minute) before 60 second video recordings were captured at ten minute intervals for the first hour and then at 24 hours. The sample temperature was maintained at 37°C for the entire duration of the experiment. These experimental conditions were similar to that used for a previously reported cytotoxicity experiment [68] thus allowing correlation of results obtained from the two techniques.

To assess the effect of the amylin derivatives on amylin aggregation, stock solutions (1 mM) of each amylin derivative was prepared in Buffer A. Each amylin derivative was then added to lyophilized samples of disaggregated amylin to give a final ratio of 50 μM:250 μM (amylin:amylin derivative). Mixtures of amylin and each of its derivatives were sonicated for 5 minutes before being injected into the sample chamber. Once again, samples were maintained at 37°C and 60 second video footage were recorded every ten minutes for the first hour and then at 24 hours. All videos were captured with the single shutter and gain modes. Analysis was performed using NanoSight NTA version 2.2 software with a viscosity setting of 0.70. All determinations were performed in duplicate with standard deviations displayed as error bars on the NTA graphs.

5.3.10 Statistical analysis

In this study, the means and standard deviations were employed in the unpaired t test to statistically compare the concentration of 100-150 nm, 150-200 nm and 200-300 nm aggregates in samples containing amylin only to that formed in samples containing a mixture of amylin and each of its derivatives. GraphPad InStat version 3 for Windows XP (GraphPad Software, U.S.A) was used for the statistical analysis and results were considered significantly different if p values were less than 0.05.

5.4 Results

5.4.1 Peptide synthesis

As observed by MALDI-TOF analysis (Figure 5.2), MA was synthesized with high purity and a yield of 9% (35 mg). The linker sequence CRKRK in MA was selected and incorporated since the basic R-groups of the arginyl and lysinyl residues will repel each other under physiological conditions. Upon binding of MA to the sensor chip for SPR-based experiments, this linker region ensures that the 8-37 region of amylin will be a sufficient distance away from the surface of the chip and from each other, thereby allowing it to freely interact with the analyte. The linker sequence in MA replaced the 1-7 region of amylin since the 8-37 region alone was previously shown to exhibit a typical amyloidogenic β-sheet structure and formed fibrils with the same morphology as fibrils formed from full length amylin.[17, 71] In addition, solid state NMR models have revealed that the 1-7 region of amylin is not involved in the formation of β-sheet structures.[20, 21, 71] Moreover, a peptide analog of the 8-37 region of amylin exhibited fibrillogenesis kinetics that was comparable to full length amylin.[72] Thus, it was strategized that MA would have a similar binding affinity as full length amylin thereby being suitable to study amylin-amylin interactions.

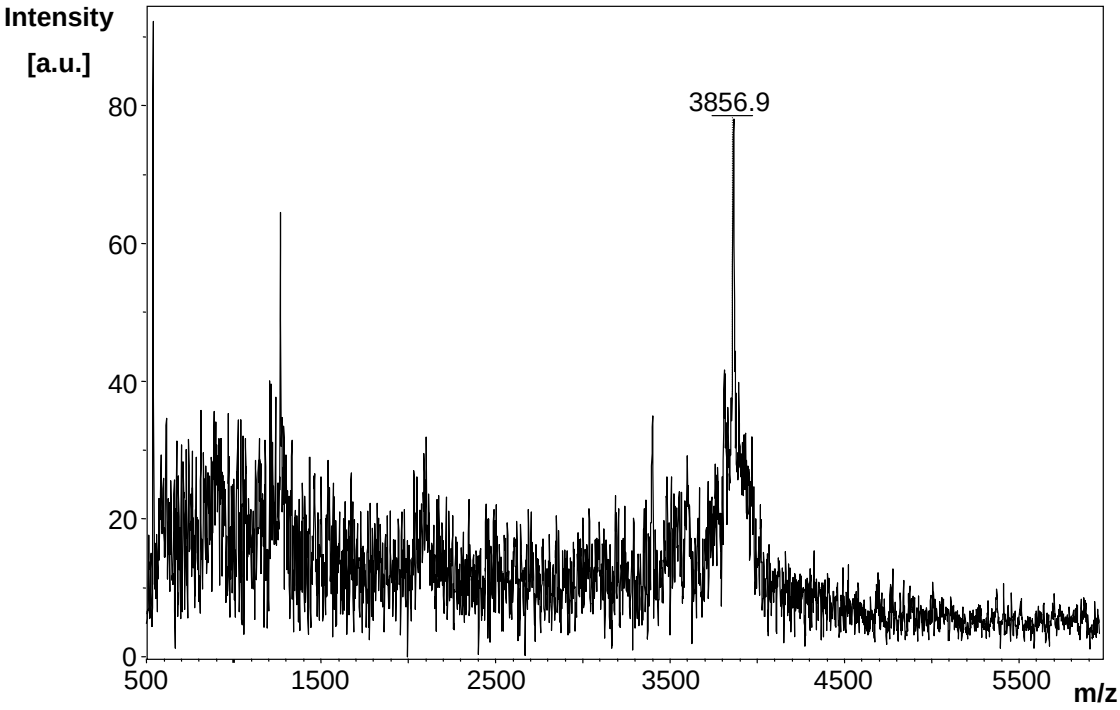

Figure 5.2 MALDI-TOF spectrum of modified amylin (MA).

5.4.2 Surface plasmon resonance

When disaggregated amylin was immobilized, a change of 640 response units (RU) was recorded, indicating that amylin attachment to the sensor chip was efficient since a similar immobilization density was observed during previous SPR-based kinetic studies of Aβ.[37] Once this was established, further experiments were performed to determine the kinetic rate constants of amylin aggregation. Samples of disaggregated amylin at various concentrations (40-120 μM) were analyzed and global fitting of the data using different types of interactions was performed using BIAevaluation version 4.1.1 software to determine the kinetic rate constants which include the association constant (k_a) and dissociation constant (k_d) (Table 5.2). The three sets of data were fitted independently to verify reproducibility and it should be noted that all three replicates followed a similar trend (representative plot in Figure 5.3).

Table 5.2 Binding kinetics of amylin obtained from SPR BIAevaluation data fitting software

k_a ($M^{-1}s^{-1}$)	28.7 ± 5.1 *
k_d (s^{-1})	$2.8 \pm 0.6 \times 10^{-4}$ *

* The kinetic data represents averages ± SD of triplicate samples.

The 1:1 Langmuir interaction (equation 1) was found to fit the generated data very well since the curves created from this type of interaction fit the observed plots very well (representative residual plots and fitted curves in Figure 5.3). This type of interaction could thus give the best representation of the kinetic data generated for amylin. In this interaction, one ligand (L) molecule interacts with one analyte (A) molecule and the resultant complex (LA) follows pseudo first-order kinetics. The rate equation 2 indicates that the amount of complex formed over time is proportional to k_a and k_d in the presence of excess analyte.[73, 74] As observed from the residual plots in Figure 5.3A, the chi^2 values are less than 10 which is an acceptable value for good fitting of data as suggested by the BIAevaluation handbook. This confirms an alignment of the observed and expected data since they are within the noise range of the sensorgrams.[73]

$$[L] + [A] \underset{k_d}{\overset{k_a}{\rightleftharpoons}} [LA] \qquad (1)$$

$$\frac{d[LA]}{dt} = k_a \,.\, [L] \,.\, [A] - k_d \,.\, [LA] \qquad (2)$$

Where L=immobilized ligand, A=analyte, LA=ligand-analyte complex, and t=time.

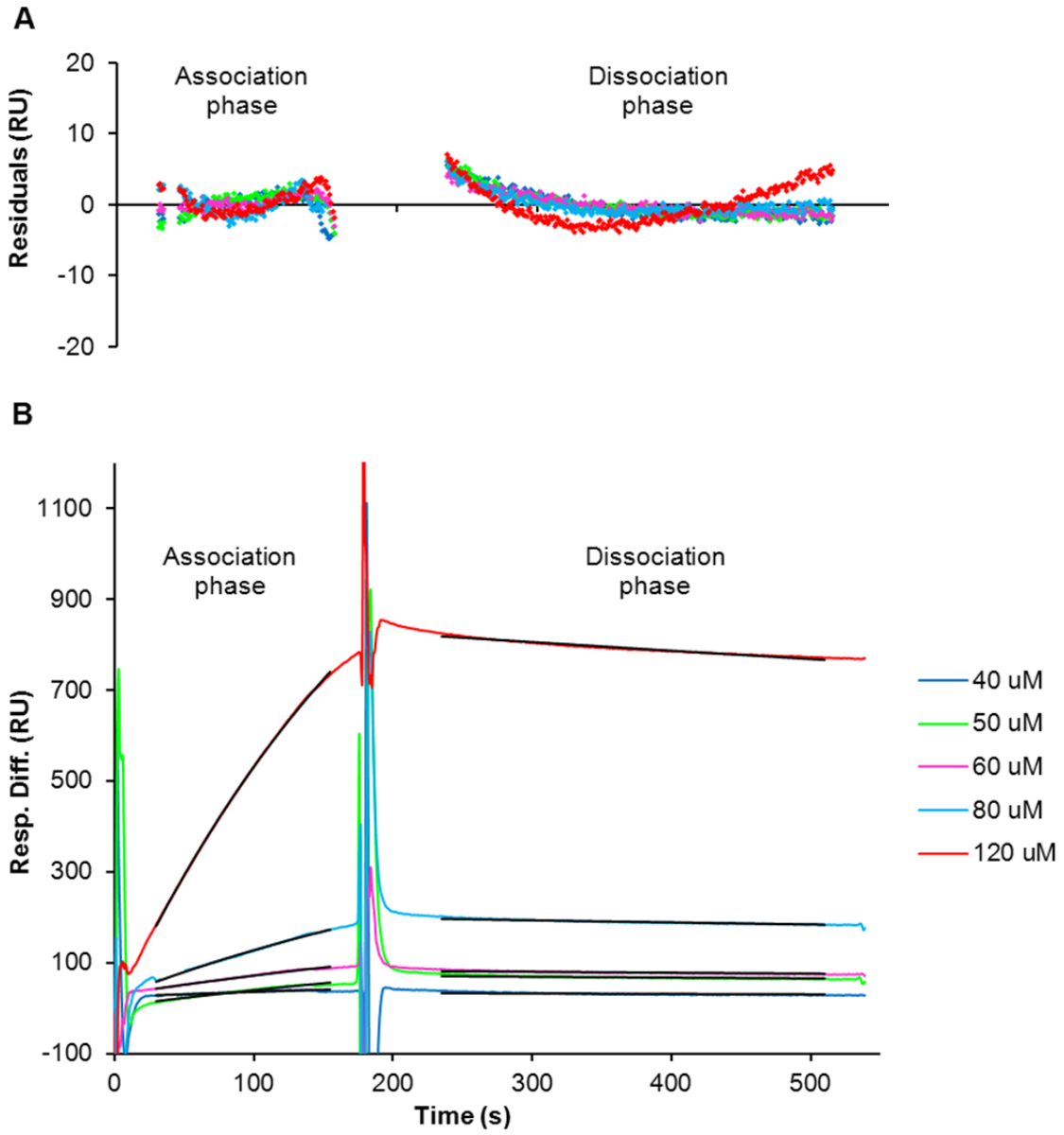

Figure 5.3 Kinetic analysis of amylin aggregation as generated from SPR-based experiments. (B) Sensorgram plots of various concentrations (40-120 μM) of disaggregated amylin that were injected for three minutes to observe association and with dissociation being monitored for six minutes, whilst maintaining a flow rate of 5 μL/min. The black lines represent the global fit for association (30-155 s) and dissociation (235-510 s). (A) The residual plots of curve fitting, that is, the difference between the observed and calculated values for association and dissociation. The chi^2 value for association was observed to be 3 whilst the chi^2 value for dissociation was 3.7.

Analysis via SPR was used to establish the effect of the amylin derivatives on amylin-amylin interaction. The sensorgrams for the association and dissociation phases of amylin in the presence and absence of its *N*-methylated and non-methylated derivatives are illustrated in Figures 5.4 and 5.5. Of the non-methylated amylin derivatives, n1 appears to increase binding of amylin to sensor chip-bound amylin without having an appreciable effect on dissociation, whilst amylin derivatives n2, n3 and n5 displayed negligible effects on association of amylin to immobilized amylin and marginally increased dissociation (Figure 5.4A). The amylin derivative n4 was observed to markedly increase amylin association and decrease dissociation (Figure 5.4B). It is noteworthy that this derivative alone interacted strongly with surface-bound amylin as evidenced by an increase in response units during association which decreased marginally during the dissociation phase (data not shown). Evaluation of the *N*-methylated amylin derivatives show that m1, m2, m3, m4 and m5 do not have a significant effect on amylin association but rather appear to slightly increase dissociation of amylin from the sensor chip-immobilized amylin (Figure 5.5). However, it is noteworthy that SPR-generated data on the effect of the amylin derivatives on amylin-amylin interaction did not correlate to previously published results of these derivatives as potential inhibitors of amylin-mediated cytotoxicity.[68]

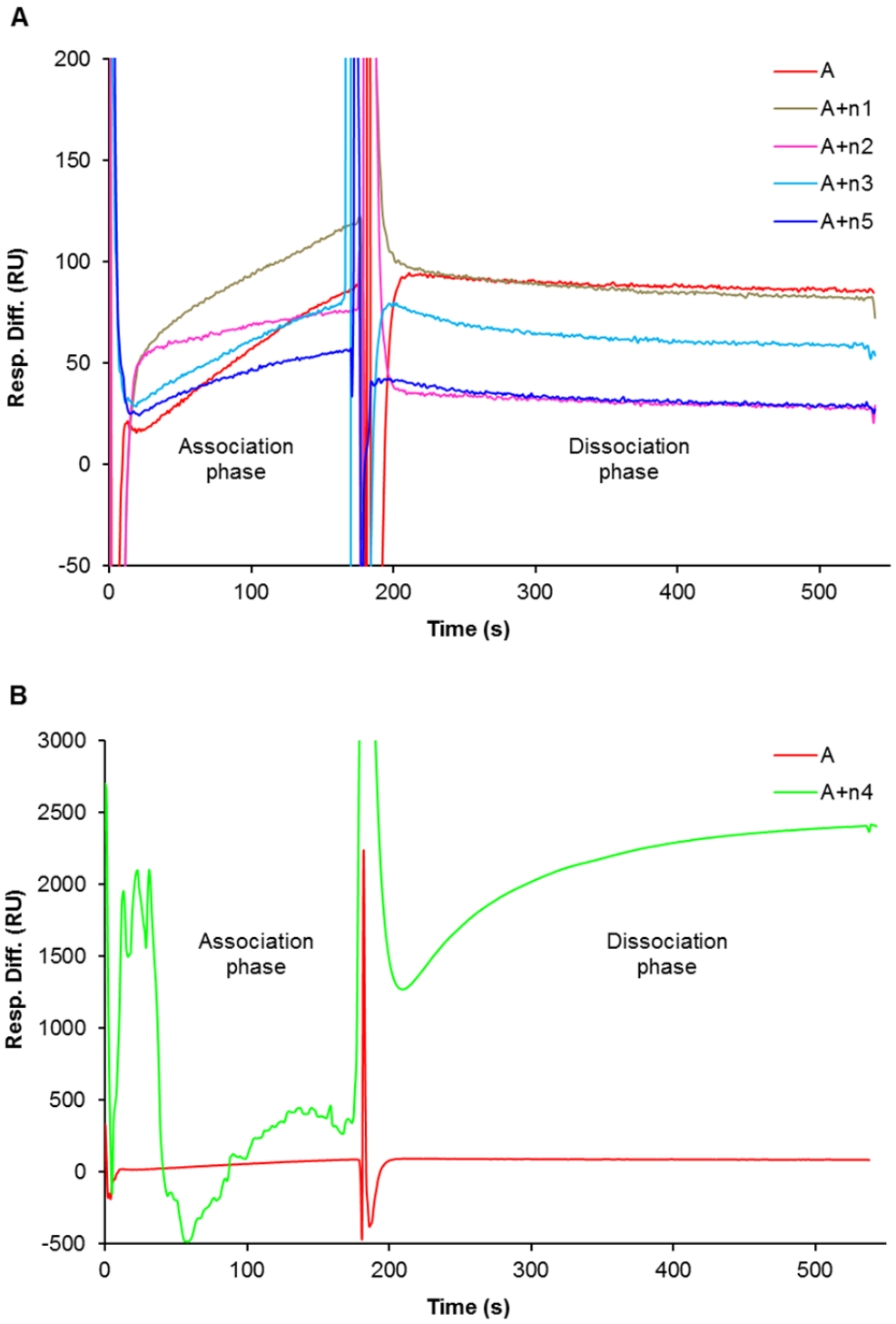

Figure 5.4 SPR generated sensorgrams showing the effect of non-methylated (n1-n5) amylin derivatives on amylin interaction with sensor chip-immobilized amylin. Sample A is disaggregated amylin that was prepared in running buffer to a final concentration of 50 μM, whilst A+n1, A+n2, A+n3, A+n4, and A+n5 are samples containing a mixture of disaggregated amylin (50 μM) and a five times molar excess of each of the amylin derivatives respectively. The samples were injected onto the sensor chip for three minutes to observe association and dissociation was monitored for six minutes, whilst maintaining a flow rate of 5 μL/min.

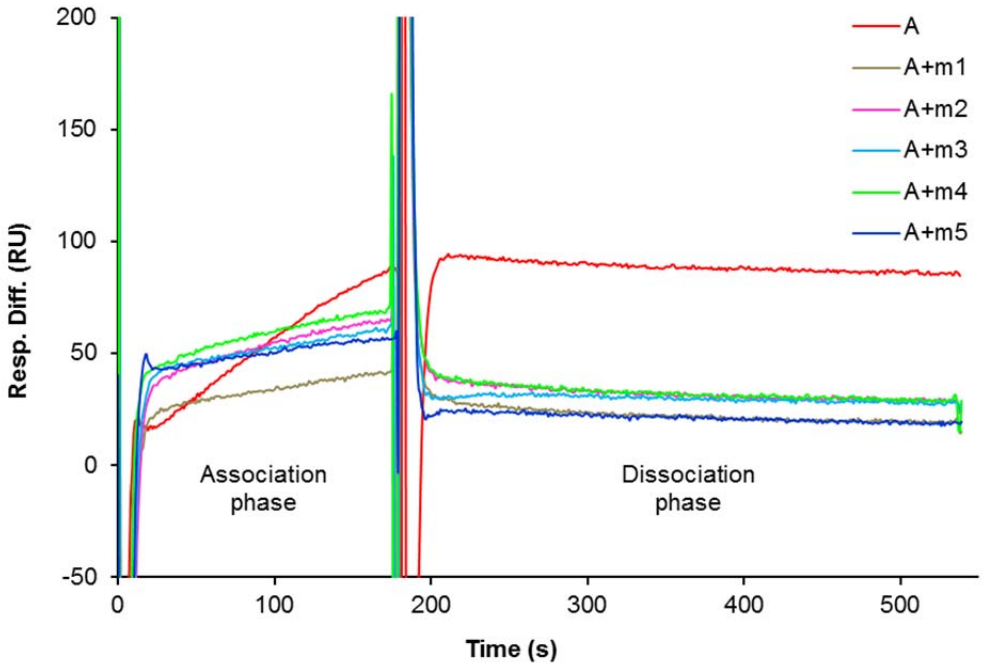

Figure 5.5 SPR generated sensorgrams showing the effect of the *N*-methylated (m1-m5) amylin derivatives on amylin interaction with sensor chip-immobilized amylin. Sample A is disaggregated amylin that was prepared in running buffer to a final concentration of 50 µM, whilst A+m1, A+m2, A+m3, A+m4 and A+m5 are samples containing a mixture of disaggregated amylin (50 µM) and a five times molar excess of each of the amylin derivatives respectively. The samples were injected onto the sensor chip for three minutes to observe association and dissociation was monitored for six minutes, whilst maintaining a flow rate of 5 µL/min.

5.4.3 Dynamic light scattering

Dynamic light scattering analysis of disaggregated amylin (50 µM) was performed after resuspension in Buffer A. Reports generated by the Zetasizer version 6.30 software recorded a poly-dispersity index of greater than 0.7, indicating that the sample is very poly-disperse and therefore reported no data. A similar outcome was observed during DLS analysis of samples containing lower concentrations of disaggregated amylin.

5.4.4 Nanoparticle tracking analysis

Nanoparticle tracking analysis was employed to evaluate the size of amylin aggregates that form in real time when disaggregated amylin samples are unconstrained in solution. Initial NTA of a 50 µM amylin sample established that a total concentration of 3.12 x 10^8 aggregates/mL was present which is within the ideal concentration range (1-25 x 10^8 aggregates/mL) for accurate NTA.[75] This concentration was thus selected for all further NTA experiments.

Taking resuspension, injection and equilibration times into consideration, the time lapse from addition of buffer to analysis was approximately ten minutes, making analysis of a zero time-point impractical. Figures 5.6 and 5.7 illustrate that aggregates are present at the ten minute time-point, suggesting that amylin starts to aggregate almost immediately upon resuspension in buffer. The three major peaks indicate that the predominant aggregates are within the following size ranges, 100-150 nm, 150-200 nm and 200-300 nm which are represented by arrows a, b and c respectively (Figure 5.6). During the first 50 minutes, peaks in the size range 100-200 nm are not well defined indicating that there is a range of aggregates with sizes between 100-200 nm. As time progresses, the amylin aggregates clearly resolves into two distinct peaks that are indicated by arrows a and b (Figure 5.6). Further analysis on these size ranges were performed and are depicted in Figure 5.7. During the first hour, the number of 100-150 nm, 150-200 nm and 200-300 nm aggregates decreased by more than 50% to a concentration of 2.5-3.0 x 10^7 aggregates/mL and thereafter remained stable up until 24 hours.

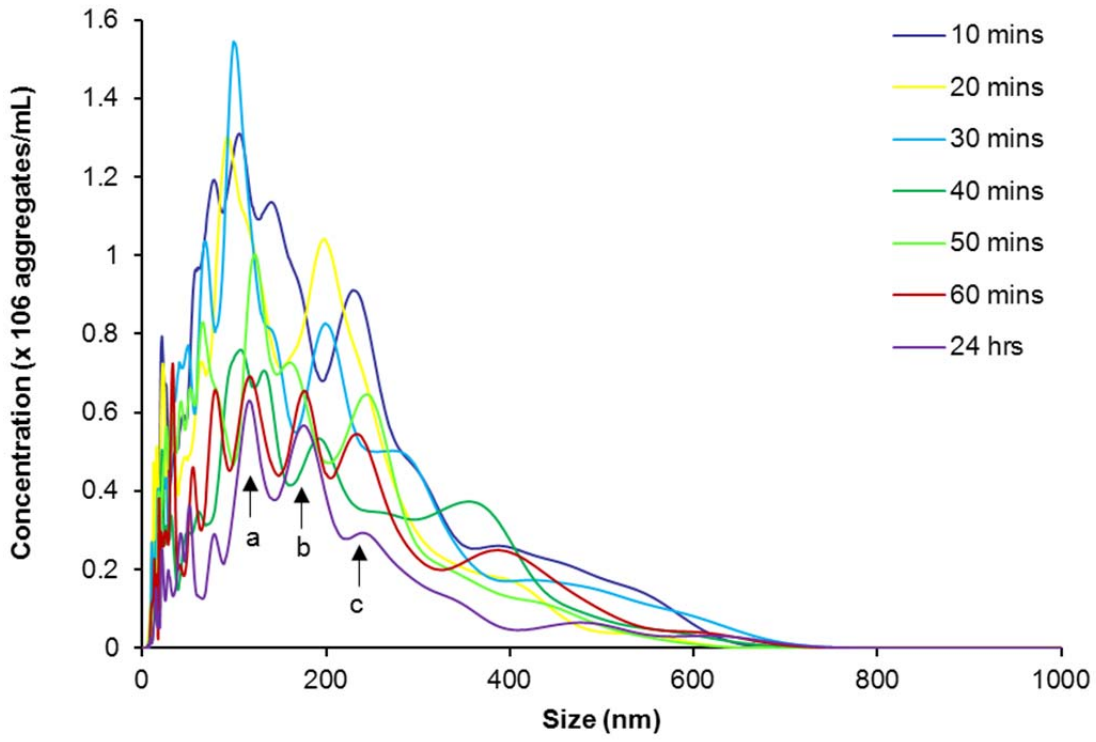

Figure 5.6 NTA size distribution profile of disaggregated amylin (50 μM) in 10 mM sodium phosphate buffer, pH 7.4 containing 50 mM NaCl. The sample was maintained at 37°C for the duration of the experiment. Video recordings (duration of 60 seconds) for NTA were taken at each time point using the single shutter and gain mode. Arrows labeled a, b and c indicates the predominant size range over 24 hours.

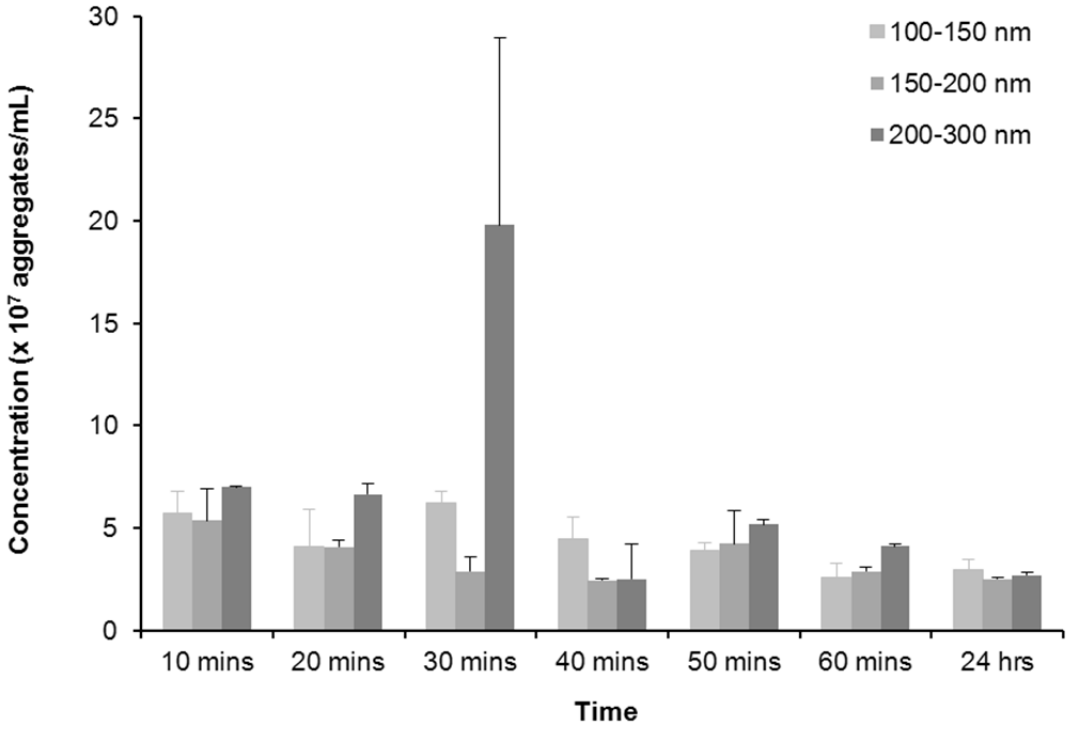

Figure 5.7 NTA distribution of 100-150 nm, 150-200 nm and 200-300 nm aggregates that formed over time from disaggregated amylin (50 μM) in 10 mM sodium phosphate buffer, pH 7.4 containing 50 mM NaCl. Samples were maintained at 37°C for the duration of the experiments. Video recordings (duration of 60 seconds) for NTA were taken at each time point using the single shutter and gain mode.

Each of the ten amylin derivatives were then individually co-incubated with disaggregated amylin and NTA was performed to evaluate their effect on amylin aggregation to the predominant sizes (Table 5.3). It appears that some of the non-methylated and *N*-methylated derivatives of amylin do exert a significant impact on the observed particle sizes at the 10 minute and 24 hour time intervals.

Table 5.3 Aggregate size distribution of amylin in the presence and absence of each of its derivatives

	Concentration of aggregates (x 10^7 aggregates/mL)					
	100-150 nm		**150-200 nm**		**200-300 nm**	
	10 minutes	24 hours	10 minutes	24 hours	10 minutes	24 hours
A[#]	5.7	2.9	5.4	2.5	7.0	2.7
A+n1[#]	0.5[*]	0.9[*]	0.5[*]	1.1[*]	0.4[*]	0.8[*]
A+n2[#]	4.3	1.5[*]	2.5	1.5[*]	3.4	2.1[*]
A+n3[#]	2.0	3.4	1.2	2.1	1.4[*]	1.9[*]
A+n4[#]	3.8	1.7	2.3	1.8	5.1	1.7[*]
A+n5[#]	0.1[*]	2.4	0.1[*]	1.4[*]	0.5[*]	2.0[*]
A+m1[#]	4.0	2.2	2.2	2.8	2.4[*]	4.3
A+m2[#]	3.9	3.6[**]	2.4	7.9	2.6[*]	4.6
A+m3[#]	2.1	5.9	1.6	3.9	2.1[*]	4.7
A+m4[#]	2.7	4.1	1.5	2.8	1.6[*]	3.3
A+m5[#]	0.9[*]	1.6[*]	0.8[*]	1.3[*]	0.8[*]	1.4[*]

[#] A denotes amylin whilst A+n1, A+n2, A+n3, A+n4, A+n5, A+m1, A+m2, A+m3, A+m4 and A+m5 denote amylin plus each of its derivatives.

[*] Statistical analysis showed that this concentration of aggregates was significantly less ($p<0.05$) than that of samples containing amylin only.

[**] Statistical analysis showed that this concentration of aggregates was significantly more ($p<0.05$) than that of samples containing amylin only.

When disaggregated amylin was co-incubated with its derivative n1, the concentration of aggregates in the three size ranges for the entire duration of the experiment was significantly less than that observed in samples containing disaggregated amylin only. At the ten minute time interval, the concentration of 100-150 nm, 150-200 nm and 200-300 nm aggregates in the presence of derivatives n2 and n4 were not significantly different from that of samples containing disaggregated amylin only. However, after a 24 hour period it was found that the concentration of 200-300 nm aggregates were significantly less in samples containing disaggregated amylin and either derivative n2 or n4 than that of amylin only samples. Analysis of samples containing disaggregated amylin and the derivative n3 illustrate that at the start of the experiment there is a small amount of aggregates of all size ranges which increases only marginally over 24 hours. A similar trend was observed in samples containing amylin and its derivative n5.

When compared to samples containing disaggregated amylin only, the derivatives m1, m2, m3 and m4 were found to have no significant effect on amylin aggregation since after 24 hours, the amount of 100-150 nm, 150-200 nm and 200-300 nm aggregates formed in the presence of each of these derivatives were similar to or more than the number of aggregates present in samples containing disaggregated amylin only. In the presence of derivative m5, there are significantly fewer amylin aggregates of all size ranges that form over the entire duration of the experiment when compared to samples containing amylin only.

5.5 Discussion

Whilst the kinetics of Aβ interactions are known, only limited data regarding human amylin-based aggregation is available. Although previous microscopy-based studies (AFM and STEM) have reported on the size of amylin oligomers, there currently exists no information with respect to the magnitude of free fibrillar structures formed by amylin in solution. The data presented herein sheds some light on the above mentioned amylin parameters thereby promoting a greater understanding of amylin aggregation, a potential causative agent of type II diabetes.

Data fitting of results from SPR-based studies using various concentrations of disaggregated amylin illustrate that amylin association and dissociation kinetics follow a 1:1 Langmuir association trend which is the simplest model for a 1:1 interaction between analyte and an immobilized ligand. The observed amylin association constant (k_a) of 28.7 ± 5.1 $M^{-1}s^{-1}$ can be interpreted as 0.035 complexes of amylin being formed per second in a one molar solution of amylin. An observed amylin dissociation constant (k_d) of $2.8 \pm 0.6 \times 10^{-4}$ s^{-1} suggests that under experimental conditions, it takes approximately 60 minutes for the complete dissociation of free amylin from sensor chip-immobilized amylin.

Previous quantitative studies using STEM postulated that the mass-per-length (MPL) of an amylin protofibril is 10 kDa/nm [24] and AFM studies have shown that amylin grows at a rate of 1.1 nm/minute.[22] From these studies by Goldsbury *et al.* (1997 and 1999) it can be estimated that the approximate rate of amylin aggregation is 11 kDa/minute.[22, 24] As indicated by SPR-generated data of this study, 0.035 complexes of amylin form per second which translates to 2.1 complexes being formed per minute. This implies an aggregation rate of 8.2 kDa/minute (wherein a single amylin molecule of 3.9 kDa is added per complex). The SPR-derived amylin association kinetics generated in this study seemingly correlates to that previously reported by Goldsbury *et al.* (1997 and 1999) [22, 24] whom employed a similar strategy of pre-binding amylin to a solid support and monitoring association kinetics of amylin that is free in solution.

Since amylin and Aβ share similar structural properties of amyloidosis [5] it is opportune in this study to compare their association and dissociation kinetics. Aβ kinetics generated from previous SPR-based experiments revealed an association rate of 0.01 complexes per second.[37] Global fitting of the SPR data also found that Aβ dissociation follows the first order kinetic model with a k_d of 2.23 x 10^{-3} s^{-1}.[37] This was further supported by a recent SPR-based Aβ study that determined a k_a of 0.01 complexes per second for Aβ association following first order kinetics, whilst the k_d was 9.2 ± 1.3 x 10^{-4} s^{-1}.[76] It is noteworthy that the former SPR-based evaluation of Aβ was performed under similar conditions to those used in the present study.[37] Both SPR-based studies on Aβ kinetics have established that fewer complexes of Aβ are formed over time.[37, 76] In addition, Aβ was revealed to have a faster dissociation time than amylin (7.5 and 18 minutes versus 60 minutes).[37, 76]

The data presented herein complements previously published association kinetics of amyloid aggregation whilst differences were observed in the dissociation kinetics. This could indicate that even though amylin and Aβ share similarities in their conformational properties of aggregation, having non-identical sequences could result in different interactions being responsible for stabilizing the aggregated structure, thereby accounting for differences in their dissociation kinetics. According to a model developed by Petkova *et al*. (2006), the 12-21 and 30-40 regions of the Aβ peptide form the β-sheet structure whilst the 22-29 region is responsible for forming the β-strand turn.[77] These regions contain predominantly hydrophobic amino acids and it has been suggested that the only hydrophilic interaction could be present between the oppositely charged side chains of asp and lys, thereby implying that only hydrophobic interactions are responsible for stabilizing the structure of aggregated Aβ.[21, 77] In contrast, NMR studies on amylin propose that there are hydrophobic interactions between the 15-17 and 23-27 region of amylin whilst inter-chain hydrophilic (electrostatic) interactions could be present between the 28-31 regions of amylin.[21] It is thus probable that both hydrophobic and hydrophilic interactions contribute to stabilization of the β-sheet structure of amylin and since hydrophilic interactions are stronger than hydrophobic interactions, this could most likely account for the longer dissociation time of amylin as observed in the present study. In addition, the SPR-derived aggregation kinetics of Aβ that have been described above was generated using the 1-40 form of Aβ which was previously shown to aggregate much more slowly than the 1-42 form of Aβ.[78]

In a previous study, we reported on *N*-methylated and non-methylated derivatives of amylin as potential inhibitors of *in vitro* amylin-mediated cytotoxicity.[68] In this SPR-based study these derivatives were co-incubated with disaggregated amylin so as to evaluate the effect of the amylin derivatives on the binding affinity of free amylin in solution to sensor chip-bound amylin and to subsequently determine if SPR could be used as a screening technique for inhibitors of amylin-mediated cytotoxicity. Of the non-methylated amylin derivatives only derivative n4 was found to associate with surface-bound amylin and hence had a significant effect on amylin:immobilized amylin interaction by increasing association and decreasing dissociation. Interestingly, this peptide is an analog of the 22-27 region of amylin that was previously observed to increase fibril formation [62] and to associate into *β*-sheet structures that coil around each other to form typical amyloid fibrils.[18] This region also covers the 25-29 and 22-29 regions of amylin, which have been described as the most amyloidogenic region of amylin.[60, 79] A predictive model of amylin fibril formation also suggests that the 22-27 region could be involved in formation of *β*-sheets.[80] Hence, it can be tentatively implied that the constituent amino acids of this region promote inter-chain hydrogen bonding interactions between carbonyl-imino dipoles, thereby facilitating binding of free amylin to the n4 derivative. It seems plausible that these aggregates containing amylin and its derivative n4 would then interact with surface-immobilized amylin resulting in the observed higher association kinetics.

Based on analysis of the SPR-generated data, it appears that the *N*-methylated amylin derivatives facilitate dissociation of amylin from sensor chip-bound amylin. A probable suggestion is that the introduction of the bulky methyl group onto the amide nitrogen of an amino acid prevents inter-chain hydrogen bonding interactions between carbonyl-imino dipoles and also provides steric hindrance, thereby destabilizing the *β*-sheet structure of amylin. This scenario is supported by previous investigations into peptide derivatives that could potentially inhibit fibrillogenesis of amyloidogenic peptides.[10, 11, 81, 82]

However, SPR-generated data on the effect of the amylin derivatives on amylin-amylin interactions could not be correlated to previously reported outcomes of the potential of these amylin derivatives as inhibitors of amylin-mediated cytotoxicity.[68] In support of this, a similar observation was reported by Lee *et al.* (2005) [83] who found that increased binding of a molecule to A*β* does not necessarily indicate that the molecule has a capacity to reduce cytotoxicity. In addition, even though insulin has been reported to inhibit fibril formation, SPR-based experiments recorded a change of only 15 response units during binding of insulin to sensor chip-bound biotinylated amylin. [53] It is thus suggested that SPR cannot be used as a technique to screen potential inhibitors of amylin-mediated cytotoxicity.

Hence, both DLS and NTA strategies which allows for real-time monitoring of aggregation dynamics in solution were subsequently employed to evaluate the effect of these amylin derivatives on the size of amylin aggregates formed over a 24 hour period and to determine if DLS and NTA-generated data could be correlated to cytotoxicity results.

Dynamic light scattering analysis of various concentrations of disaggregated amylin alone yielded no results since all samples were indicated as poly-disperse and thus not suitable for DLS. The limitation of DLS to accurately size amylin aggregates appear to stem from the inherent principle of the technique which is based on the concept that the intensity of light scattered from particles is proportional to its size. Since larger particles will scatter more light than smaller particles, small particles will be obscured by large ones and thus DLS will not be able to accurately size particles in a poly-dispersed sample.[58] Our observation is also supported by light scattering data on the amyloidogenic proteins Aβ [84] and prion protein [85], both of which have also shown that these samples were poly-disperse.

However, NTA proved to be more successful in sizing amylin aggregates. Nanoparticle tracking analysis of samples containing disaggregated amylin only detected aggregates at the first 10 minute time-point, which seems to be consistent with previous reports using other technologies that have demonstrated almost instantaneous aggregation of amylin.[16, 86, 87] As described above, the highest concentration of amylin aggregates fall into the size ranges 100-150 nm, 150-200 nm and 200-300 nm for the duration of the experiment. Moreover, the concentration of these aggregates decreases by more than 50% within the first hour and then remained constant until 24 hours, suggesting that complete aggregation of amylin occurs within the first hour. Since it has been reported extensively that an incubation period of 20-24 hours is sufficient for amylin to facilitate cytotoxicity [11-13, 16, 18, 64, 68], it can be suggested that either the 100-150 nm, 150-200 nm or 200-300 nm aggregates represent the toxic species of amylin.

Results obtained from NTA of samples containing disaggregated amylin and its derivative n1 imply that this derivative could inhibit fibrillogenesis of amylin or conversely facilitate rapid aggregation of amylin into large aggregates that are out of the detection range (30-1000 nm) of NTA.[58] It was previously shown that the 1-7 region of amylin is in a random coil conformation and could have a modulating effect on amylin aggregation, that is the amyloidogenic nature of amylin is increased if this region is excluded from the amylin sequence.[71] It thus appears that the derivative n1 which is an analog of the 3-6 region of amylin could potentially delay fibril formation.

Based on NTA-generated data, it can be construed that the derivatives n2 and n4 enhances amylin fibril formation to an aggregate size greater than 1000 nm since the concentration of 200-300 nm aggregates are significantly less in samples containing disaggregated amylin and either derivative n2 or n4, than that of samples containing disaggregated amylin only. Analysis of samples containing disaggregated amylin and either the derivative n3 or n5 suggest that these derivatives could also possibly increase or severely impede amylin aggregation since at the start of the experiment there is a small amount of aggregates of all size ranges which increases only marginally over 24 hours.

In 2009, Shim *et al.* proposed a model which demonstrates that residues 8, 13, 17, 25, 27 and 32 act as nucleation points for formation of *β*-sheets.[19] The amylin derivatives n2, n3, n4 and n5 each contain at least one of the proposed nucleation sites thus implying that these derivatives have the inherent potential to facilitate formation of *β*-sheet structures thereby promoting the formation of fully aggregated amylin in a short space of time. In addition, these amylin derivatives also span regions of amylin that have previously been reported to form *β*-sheet structures.[11, 17, 18, 21, 60, 71, 79, 80, 88, 89] It is noteworthy and in keeping with this hypothesis, that a previous report showed that fibril formation of full length amylin was enhanced in the presence of amylin derivatives n3 and n4 which are analogs of the 15-20 and 22-27 regions of amylin respectively.[62, 90] These previous findings would thus account for the potential of derivatives n2, n3, n4 and n5 to increase fibrillogenesis.

However, further NTA-generated data indicate that the amylin derivatives m1, m2, m3 and m4 had no significant effect on amylin aggregation which is supported by a previous observation that the introduction of *N*-methylated amino acids into peptides does not always result in inhibition of fibril formation.[81] In contrast, analysis of samples containing disaggregated amylin and derivative m5 suggest that this derivative either delays or increases amylin aggregation. Since the derivative m5 contains bulky methyl groups, it is most likely that these groups provide steric hindrance when the derivative binds to amylin thereby destabilizing *β*-sheet structures. Thus, derivative m5 could possibly delay amylin aggregation.

Comparison of NTA-generated data to previously published reports implies that the amylin derivatives n1 and m5 inhibits fibrillogenesis whilst the derivatives n2, n3, n4 and n5 have the tendency to increase fibrillogenesis of amylin to an aggregate that is larger than 1000 nm. It is noteworthy that these 1000 nm aggregates are out of the detection range of NTA and could represent the fully aggregated form of amylin which has previously been reported to be non-toxic.[91-96] In the presence of amylin derivatives n1, n2, n3, n4, n5 and m5, the concentration of 200-300 nm amylin aggregates was significantly lower than in samples containing amylin only at 24 hours. These derivatives were also previously reported to reduce amylin-mediated cytotoxicity by more than 40%.[68] Derivatives m1, m2, m3 and m4 were previously shown not to have an inhibitory effect on amylin-mediated cytotoxicity [68] and the concentration of 200-300 nm aggregates in samples containing disaggregated amylin and each of these derivatives were recorded to be similar to or more than the concentration of aggregates in samples containing disaggregated amylin only ($\geq 2.7 \times 10^7$ aggregates/mL). Based on these observations it can thus be tentatively suggested that the 200-300 nm particle is the toxic species of amylin.

This study is the first to report on real time monitoring of the aggregation of unconstrained amylin in solution. Furthermore, amylin was used in its unmodified form, thereby providing an insight into the behavior of amylin under experimental conditions that are closely representative of those employed in mammalian cell line-based cytotoxicity studies. Data obtained also suggest that a critical concentration of 200-300 nm aggregates for amylin-mediated cytotoxicity is more than 2.1×10^7 aggregates/mL. As mentioned previously, cell-based systems for screening potential inhibitors of amylin-mediated cytotoxicity can become cumbersome and time-consuming. Thus, after further optimization and verification studies, NTA could possibly be used as a quick screening technique for inhibitors of amylin-mediated cytotoxicity.

5.6 Conclusion

This study has demonstrated the suitability of SPR for use in pursuit of the association and dissociation rates of amylin aggregation kinetics. In addition, nanoparticle tracking analysis offers an attractive strategy as a rapid evaluative cell-free tool to assess inhibitors of amylin-mediated cytotoxicity. Moreover NTA can also be used as a technique that caters for real time monitoring of the amylin aggregation process whilst it continues unconstrained in solution. Importantly, the data from this study suggests that the size of toxic species of amylin is approximately 200-300 nm.

5.7 Acknowledgements

Karen Pillay is thankful to NRF Thuthuka (grant number 76066) and UKZN for funding this study. Sincere gratitude to Claire Hannel, Agnieszka Siupa and Mark Ware from NanoSight Ltd., Amesbury for their technical advice and assistance.

5.8 References

1. Kruger, D.F., Gatcomb, P. M., and Owen, S. K., *Clinical implications of amylin and amylin deficiency.* Diabetes Educator, 1999. **25**(3): p. 389-397.
2. Martin, C., *The physiology of amylin and insulin: maintaining the balance between glucose secretion and glucose uptake.* The Diabetes Educator, 2006. **32**: p. 101-104.
3. Badman, M.K., Shennan, K.I.J., Jermany, J.L., Docherty, K. and Clark, A., *Processing of pro-islet amyloid polypeptide (proIAPP) by the prohormone convertase PC2.* FEBS Letters, 1996. **378**: p. 227 231.
4. Kodali, R., and Wetzel, R., *Polymorphism in the intermediates and products of amyloid assembly.* Current Opinion in Structural Biology, 2007. **17**: p. 48–57.
5. Kayed, R., Bernhagen, J., Greenfield, N., Sweimeh, K., Brunner, H., Voelter, W. and Kapurniotu, A., *Conformational transitions of islet amyloid polypeptide (IAPP) in amyloid formation in vitro.* Journal of Molecular Biology, 1999. **287**: p. 781-796.
6. Opie, E., *The relation of diabetes mellitus to lesions of the pancreas. Hyaline degeneration of the islands of Langerhans.* The Journal of Experimental Medicine, 1901. **5**: p. 528-540.
7. Cooper, G.J.S., Willis, A.C., Clark, A., Turner, R.C., Sim, R.B. and Reid, K.B.M., *Purification and characterization of a peptide from amyloid-rich pancreases of type 2 diabetic patients.* Proceedings of the National Academy of Science, 1987. **84**: p. 8628-8632.
8. Cooper, G.J.S., Leighton, B., Dimitriadis, G. D., Parry-Billings, M., Kowalchuk, J. M., Howland K., Rothbard, J. B., Willis, A. C., and Reid, K. B. M, *Amylin found in amyloid deposits in human type 2 diabetes mellitus may be a hormone that regulates glycogen metabolism in skeletal muscle.* Proceedings of the National Academy of Science, 1988. **85**: p. 7763-7766.
9. Pawlicki, S., A. Le Bechec, and C. Delamarche, *AMYPdb: A database dedicated to amyloid precursor proteins.* Bmc Bioinformatics, 2008. **9**.
10. Rijkers, D.T.S., Hoppener, J.W.M., Posthuma, G., Lips, C.J.M. and Liskamp, R.M.J, *Inhibition of amyloid fibril formation of human amylin by N-alkylated amino acid and α-hydroxy acid residue containing peptides.* Chemistry: A European Journal, 2002. **8**(18): p. 4285-4291.
11. Kapurniotu, A., Schmauder, A. and Tenidis, K., *Structure-based design and study of non-amyloidogenic, double n-methylated IAPP amyloid core sequences as inhibitors of IAPP amyloid formation and cytotoxicity.* Journal of Molecular Biology, 2002. **315**: p. 339-350.
12. Aitken, J.F., Loomes, K.M., Konarkowska, B. and Cooper, G.J.S, *Suppression by polycyclic compounds of the conversion of human amylin into insoluble amyloid.* Biochemical Journal, 2003. **374**: p. 779–784.
13. Tatarek-Nossol, M., Yan, L., Schmauder, A., Tenidis, K., Westermark, G., and Kapurniotu, A., *Inhibition of hIAPP amyloid-fibril formation and apoptotic cell death by a designed hiapp amyloid-core-containing hexapeptide.* Chemistry & Biology, 2005. **12**: p. 797–809.
14. Yan, L., Tatarek-Nossol, M., Velkova, A., Kazantzis, A. and Kapurniotu, A., *Design of a mimic of nonamyloidogenic and bioactive human islet amyloid polypeptide (IAPP) as nanomolar affinity inhibitor of IAPP cytotoxic fibrillogenesis.* Proceedings of the National Academy of Science, 2006. **103**(7): p. 2046–2051.
15. Abedini, A., Meng, F. and Raleigh, D.P., *A single-point mutation converts the highly amyloidogenic human islet amyloid polypeptide into a potent fibrillization inhibitor.* Journal of the American Chemical Society, 2007. **129**: p. 11300-11301.
16. Kapurniotu, A., Bernhagen, J., Greenfield, N., Al-Abed, Y., Teichberg, S., Frank, R.W., Voelter, W., and Bucala, R., *Contribution of advanced glycosylation to the amyloidogenicity of islet amyloid polypeptide.* European Journal of Biochemistry, 1998. **251**: p. 208-216.
17. Goldsbury, C., Goldie, K., Pellaud, J., Seelig, J., Frey, P., Muller, S. A., Kistler, J., Cooper, G. J. S., and and U. Aebi, *Amyloid fibril formation from full-length and fragments of amylin.* Journal of Structural Biology, 2000. **130**(2-3): p. 352-362.
18. Tenidis, K., Waldner, M., Bernhagen, J., Fischle, W., Bergmann, M., Weber, M., Merkle, M., Voelter, W., Brunner, H., and Kapurniotu, A., *Identification of a penta- and hexapeptide of islet amyloid polypeptide (IAPP) with amyloidogenic and cytotoxic properties.* Journal of Molecular Biology, 2000. **295**: p. 1055-1071.

19. Shim, S.H., Gupta, R., Ling, Y. L., Strasfeld, D. B., Raleigh, D. P., and Zanni, M. T., *Two-dimensional IR spectroscopy and isotope labeling defines the pathway of amyloid formation with residue-specific resolution.* Proceedings of the National Academy of Sciences of the United States of America, 2009. **106**(16): p. 6614-6619.
20. Strasfeld, D.B., Ling, Y. L., Gupta, R., Raleigh, D. P., and Zanni, M. T., *Strategies for extracting structural information from 2D IR spectroscopy of amyloid: application to iIslet amyloid polypeptide.* Journal of Physical Chemistry B, 2009. **113**(47): p. 15679-15691.
21. Luca, S., Yau, W., Leapman, R., and Tycko, R., *Peptide conformation and supramolecular organization in amylin fibrils: constraints from solid-state NMR.* Biochemistry, 2007. **46**(47): p. 13505-13522.
22. Goldsbury, C., Kistler, J., Aebi, U., Arvinte, T. and Cooper, G.J.S., *Watching amyloid fibrils grow by time-lapse atomic force microscopy.* Journal of Molecular Biology, 1999. **285**: p. 33-39.
23. Green, J.D., Goldsbury, C., Kistler, J., Cooper, G.J.S and Aebi, U., *Human amylin oligomer growth and fibril elongation define two distinct phases in amyloid formation.* The Journal of Biological Chemistry, 2004. **279**(13): p. 12206–12212.
24. Goldsbury, C.S., Cooper, G. J. S., Goldie, K. N., Muller, S. A., Saafi, E. L., Gruijters, W. T. M., and Misur, M. P., *Polymorphic fibrillar assembly of human amylin.* Journal of Structural Biology, 1997. **119**(1): p. 17-27.
25. Goldsbury, C., Baxa, U., Simon, M. N., Steven, A. C., Engel, A., Wall, J. S., Aebi, U., and Mueller, S. A., *Amyloid structure and assembly: Insights from scanning transmission electron microscopy.* Journal of Structural Biology, 2011. **173**(1): p. 1-13.
26. Zhou, N., Chen, Z., Zhang, D., and Li, G., *Electrochemical assay of human islet amyloid polypeptide and its aggregation.* Sensors, 2008. **8**(9): p. 5987-5995.
27. Vaiana, S.M., Best, R. B., Yau, W., Eaton, W. A., and Hofrichter, J., *Evidence for a partially structured state of the amylin monomer.* Biophysical Journal, 2009. **97**(11): p. 2948-2957.
28. Patil, S.M., Mehta, A., Jha, S., and Alexandrescu, A. T., *Heterogeneous amylin fibril growth mechanisms imaged by total internal reflection fluorescence microscopy.* Biochemistry, 2011. **50**(14): p. 2808-2819.
29. Multhaup, G., Bush, A. I., Pollwein, P., and Masters, C. L., *Interaction between the zinc (II) and the heparin-binding site of the alzheimers-disease beta-a4 amyloid precursor protein (APP).* FEBS Letters, 1994. **355**(2): p. 151-154.
30. Tjernberg, L.O., Naslund, J., Lindqvist, F., Johansson, J., Karlstrom, A. R., Thyberg, J., Terenius, L., and Nordstedt, C., *Arrest of beta-amyloid fibril formation by a pentapeptide ligand.* Journal of Biological Chemistry, 1996. **271**(15): p. 8545-8548.
31. White, D.A., Buell, A. K., Dobson, C. M., Welland, M. E., and Knowles, T. P. J., *Biosensor-based label-free assays of amyloid growth.* FEBS Letters, 2009. **583**(16): p. 2587-2592.
32. Morton, T.A., D.G. Myszka, and I.M. Chaiken, *Interpreting complex binding-kinetics from optical biosensors - a comparison of analysis by linearization, the integrated rate-equation, and numerical-integration.* Analytical Biochemistry, 1995. **227**(1): p. 176-185.
33. Cannon, M.J., Williams, A. D., Wetzel, R., and Myszka, D. G., *Kinetic analysis of beta-amyloid fibril elongation.* Analytical Biochemistry, 2004. **328**(1): p. 67-75.
34. Wood, S.J., W. Chan, and R. Wetzel, *An ApoE-A beta inhibition complex in A beta fibril extension.* Chemistry & Biology, 1996. **3**(11): p. 949-956.
35. Myszka, D.G., S.J. Wood, and A.L. Biere, *Analysis of fibril elongation using surface plasmon resonance biosensors.* Amyloid, Prions, and Other Protein Aggregates, 1999. **309**: p. 386-402.
36. Cairo, C.W., Strzelec, A., Murphy, R. M., and Kiessling, L. L., *Affinity-based inhibition of beta-amyloid toxicity.* Biochemistry, 2002. **41**(27): p. 8620-8629.
37. Hasegawa, K., Ono, K., Yamada, M., and Naiki, H., *Kinetic modeling and determination of reaction constants of Alzheimer's beta-amyloid fibril extension and dissociation using surface plasmon resonance.* Biochemistry, 2002. **41**(46): p. 13489-13498.
38. Ryu, J., Joung, H. A., Kim, M. G., and Park, C. B., *Surface plasmon resonance analysis of Alzheimer's beta-amyloid aggregation on a solid surface: from monomers to fully-grown fibrils.* Analytical Chemistry, 2008. **80**(7): p. 2400-2407.
39. de Vega, M.J.P., Baeza, J. L., Garcia-Lopez, M. T., Vila-Perello, M., Jimenez-Castells, C., Simon, A. M., Frechilla, D., del Rio, J., Gutierrez-Gallego, R., Andreu, D., and Gonzalez-Muniz, R., *Synthesis and biological properties of beta-turned A-beta (31-35) constrained analogues.* Bioorganic & Medicinal Chemistry Letters, 2008. **18**(6): p. 2078-2082.
40. Lin, M., Chiu, H., Fan, F., Tsai, H., Wang, S. S. S., Chang, Y., and Chen, W., *Kinetics and enthalpy measurements of interaction between P-amyloid and liposomes by surface plasmon resonance and isothermal titration microcalorimetry.* Colloids and Surfaces B-Biointerfaces, 2007. **58**(2): p. 231-236.
41. Ramakrishnan, M., Kandimalla, K. K., Wengenack, T. M., Howell, K. G., and Poduslo, J. F., *Surface plasmon resonance binding kinetics of Alzheimer's disease amyloid beta peptide-capturing and plaque-binding monoclonal antibodies.* Biochemistry, 2009. **48**(43): p. 10405-10415.

42. Robert, R., Dolezal, O., Waddington, L., Hattarki, M. K., Cappai, R., Masters, C. L., Hudson, P. J., and Wark, K. L., *Engineered antibody intervention strategies for Alzheimer's disease and related dementias by targeting amyloid and toxic oligomers.* Protein Engineering Design & Selection, 2009. **22**(3): p. 199-208.
43. Gobbi, M., Re, F., Canovi, M., Beeg, M., Gregori, M., Sesana, S., Sonnino, S., Brogioli, D., Musicanti, C., Gasco, P., Salmona, M., and Masserini, M. E., *Lipid-based nanoparticles with high binding affinity for amyloid-beta (1-42) peptide.* Biomaterials, 2010. **31**(25): p. 6519-6529.
44. Takahashi, T., K. Ohta, and H. Mihara, *Rational design of amyloid beta peptide-binding proteins: Pseudo-A beta beta-sheet surface presented in green fluorescent protein binds tightly and preferentially to structured A beta.* Proteins-Structure Function and Bioinformatics, 2010. **78**(2): p. 336-347.
45. Stravalaci, M., Beeg, M., Salmona, M., and Gobbi, M., *Use of surface plasmon resonance to study the elongation kinetics and the binding properties of the highly amyloidogenic A-beta (1-42) peptide, synthesized by depsi-peptide technique.* Biosensors & Bioelectronics, 2011. **26**(5): p. 2772-2775.
46. Krazinski, B.E., J. Radecki, and H. Radecka, *Surface plasmon resonance based biosensors for exploring the influence of alkaloids on aggregation of amyloid-beta peptide.* Sensors, 2011. **11**(4): p. 4030-4042.
47. Gobbi, M., Colombo, L., Morbin, M., Mazzoleni, G., Accardo, E., Vanoni, M., Del Favero, E., Cantu, L., Kirschner, D. A., Manzoni, C., Beeg, M., Ceci, P., Ubezio, P., Forloni, G., Tagliavini, F., and Salmona, M., *Gerstmann-Strarussler-Scheinker disease amyloid protein polymerizes according to the "dock-and-lock" model.* Journal of Biological Chemistry, 2006. **281**(2): p. 843-849.
48. Kawatake, S., Nishimupa, Y., Sakaguchi, S., Iwaki, T., and Doh-ura, K., *Surface plasmon resonance analysis for the screening of anti-prion compounds.* Biological & Pharmaceutical Bulletin, 2006. **29**(5): p. 927-932.
49. Treiber, C., Thompsett, A. R., Pipkorn, R., Brown, D. R., and Multhaup, G., *Real-time kinetics of discontinuous and highly conformational metal-ion binding sites of prion protein.* Journal of Biological Inorganic Chemistry, 2007. **12**(5): p. 711-720.
50. Thompson, M.J., Louth, J. C., Ferrara, S., Sorrell, F. J., Irving, B. J., Cochrane, E. J., Meijer, A., and Chen, B. N., *Structure-activity relationship refinement and further assessment of indole-3-glyoxylamides as a lead series against prion disease.* Chemmedchem, 2011. **6**(1): p. 115-130.
51. Myszka, D.G., S.J. Wood, and A.L. Biere, *Analysis of fibril elongation using surface plasmon resonance biosensors.* Methods in Enzymology, 1999. **309**: p. 386-402.
52. Aguilar, M.I. and D.H. Small, *Surface plasmon resonance for the analysis of beta-amyloid interactions and fibril formation in Alzheimer's disease research.* Neurotoxicity Research, 2005. **7**(1-2): p. 17-27.
53. Jaikaran, E., Nilsson, M. R., and Clark, A., *Pancreatic beta-cell granule peptides form heteromolecular complexes which inhibit islet amyloid polypeptide fibril formation.* Biochemical Journal, 2004. **377**: p. 709-716.
54. Wei, L., Jiang, P., Yau, Y. H., Summer, H., Shochat, S. G., Mu, Y. G., and Pervushin, K., *Residual structure in islet amyloid polypeptide mediates its interactions with soluble insulin.* Biochemistry, 2009. **48**(11): p. 2368-2376.
55. Cabaleiro-Lago, C., Lynch, I., Dawson, K. A., and Linse, S., *Inhibition of IAPP and IAPP (20-29) fibrillation by polymeric nanoparticles.* Langmuir, 2010. **26**(5): p. 3453-3461.
56. Bootz, A., Vogel, V., Schubert, D., and Kreuter, J., *Comparison of scanning electron microscopy, dynamic light scattering and analytical ultracentrifugation for the sizing of poly (butyl cyanoacrylate) nanoparticles.* European Journal of Pharmaceutics and Biopharmaceutics, 2004. **57**(2): p. 369-375.
57. Malloy, A. and B. Carr, *Nanoparticle tracking analysis - The Halo (TM) system.* Particle & Particle Systems Characterization, 2006. **23**(2): p. 197-204.
58. Filipe, V., Hawe, A., and Jiskoot, W., *Critical evaluation of nanoparticle tracking analysis (NTA) by NanoSight for the measurement of nanoparticles and protein aggregates.* Pharmaceutical Research, 2010. **27**(5): p. 796-810.
59. NanoSight. *Applications of nanoparticle tracking analysis (NTA) in nanoparticle research*. Accessed: 27 February 2012. Available from: http://www.nanosight.com/appnotes/M110B%20Application%20Review%20NTA%20April%202009.pdf.
60. Azriel, R., and Gazit, E., *Analysis of the structural and functional elements of the minimal active fragment of islet amyloid polypeptide (IAPP) - An experimental support for the key role of the phenylalanine residue in amyloid formation.* Journal of Biological Chemistry, 2001. **276**(36): p. 34156-34161.
61. Cao, P. and D.P. Raleigh, *Ester to amide switch peptides provide a simple method for preparing monomeric islet amyloid polypeptide under physiologically relevant conditions and facilitate investigations of amyloid formation.* Journal of the American Chemical Society, 2010. **132**(12): p. 4052.
62. Scrocchi, L.A., Chen, Y., Waschuk, S., Wang, F., Cheung, S., Darabie, A.A., McLaurin, J. and Fraser, P.E., *Design of peptide-based inhibitors of human islet amyloid polypeptide fibrillogenesis.* Journal of Molecular Biology, 2002. **318**: p. 697–706.
63. Porat, Y., Mazor, Y., Efrat, S., and Gazit, E., *Inhibition of islet amyloid polypeptide fibril formation: a potential role for heteroaromatic interactions.* Biochemistry, 2004. **43**(45): p. 14454-14462.

64. Tomiyama, T., Kaneko, H., Kataoka, K., Asano, S. and Endo, N., *Rifampicin inhibits the toxicity of pre-aggregated amyloid peptides by binding to peptide fibrils and preventing amyloid-cell interaction.* Biochemical Journal, 1997. **322**: p. 859-865.
65. Bedrood, S., Jayasinghe, S., Sieburth, D., Chen, M., Erbel, S., Butler, P. C., Langen, R., and Ritzel, R. A., *Annexin A5 directly interacts with amyloidogenic proteins and reduces their toxicity.* Biochemistry, 2009. **48**(44): p. 10568-10576.
66. Meier, J.J., Kayed, R., Lin, C., Gurlo, T., Haataja, L., Jayasinghe, S., Langen, R., Glabe, C.G., and Butler, P.C., *Inhibition of human IAPP fibril formation does not prevent beta-cell death: evidence for distinct actions of oligomers and fibrils of human IAPP.* American Journal of Physiology, Endocrinology and Metabolism, 2006. **291**: p. E1317–E1324.
67. Zhang, S.P., Liu, H., Yu, H., and Cooper, G. J. S., *Fas-associated death receptor signaling evoked by human amylin in islet beta-cells.* Diabetes, 2008. **57**(2): p. 348-356.
68. Muthusamy, K., Arvidsson, P. I., Govender, P., Kruger, H. G., Maguire, G. E. M., and Govender, T., *Design and study of peptide-based inhibitors of amylin cytotoxicity.* Bioorganic & Medicinal Chemistry Letters, 2010. **20**(4): p. 1360-1362.
69. Muthusamy, K., Albericio, F., Arvidsson, P. I., Govender, P., Kruger, H. G., Maguire, G. E. M., and Govender, T., *Microwave assisted SPPS of amylin and its toxicity of the pure product to RIN-5F cells.* Biopolymers, 2010. **94**(3): p. 323-330.
70. Liu, R.T., Yuan, B., Emadi, S., Zameer, A., Schulz, P., McAllister, C., Lyubchenko, Y., Goud, G., and Sierks, M. R., *Single chain variable fragments against beta-amyloid (A beta) can inhibit A beta aggregation and prevent A beta-induced neurotoxicity.* Biochemistry, 2004. **43**(22): p. 6959-6967.
71. Jaikaran, E.T.A.S., Higham, C.E., Serpell, L.C., Zurdo, J., Gross, M., Clark, A. and Fraser, P.E., *Identification of a novel human islet amyloid polypeptide b-sheet domain and factors influencing fibrillogenesis.* Journal of Molecular Biology, 2001. **308**: p. 515-525.
72. Knight, J.D., and Miranker, A. D., *Phospholipid catalysis of diabetic amyloid assembly.* Journal of Molecular Biology, 2004. **341**(5): p. 1175-1187.
73. Karlsson, R. and A. Falt, *Experimental design for kinetic analysis of protein-protein interactions with surface plasmon resonance biosensors.* Journal of Immunological Methods, 1997. **200**(1-2): p. 121-133.
74. Tanious, F.A., B. Nguyen, and W.D. Wilson, *Biosensor-surface plasmon resonance methods for quantitative analysis of biomolecular interactions*, in *Biophysical Tools for Biologists: Vol 1 in Vitro Techniques*, J.J. Correia and H.W. Detrich, 2008. p. 53-77.
75. NanoSight. *How to make Concentration Measurements using NanoSight LM Series Instruments*. Accessed: 27 February 2012.
76. Hu, W.P., Chang, G. L., Chen, S. J., and Kuo, Y. M., *Kinetic analysis of beta-amyloid peptide aggregation induced by metal ions based on surface plasmon resonance biosensing.* Journal of Neuroscience Methods, 2006. **154**(1-2): p. 190-197.
77. Petkova, A.T., W.M. Yau, and R. Tycko, *Experimental constraints on quaternary structure in Alzheimer's beta-amyloid fibrils.* Biochemistry, 2006. **45**(2): p. 498-512.
78. Jarrett, J.T., E.P. Berger, and P.T. Lansbury, *The carboxy terminus of the beta-amyloid protein is critical for the seeding of amyloid formation - implications for the pathogenesis of alzheimers-disease.* Biochemistry, 1993. **32**(18): p. 4693-4697.
79. Westermark, P., Engstrom, U., Johnson, K. H., Westermark, G.T., and Betsholtz, C., *Islet amyloid polypeptide: pinpointing amino acid residues linked to amyloid fibril formation.* Proceedings of the National Academy of Science, 1990. **87**: p. 5036-5040.
80. Kajava, A.V., Aebi, U., and Steven, A. C., *The parallel superpleated beta-structure as a model for amyloid fibrils of human amylin.* Journal of Molecular Biology, 2005. **348**(2): p. 247-252.
81. Gordon, D.J., K.L. Sciarretta, and S.C. Meredith, *Inhibition of beta-amyloid(40) fibrillogenesis and disassembly of beta-amyloid(40) fibrils by short beta-amyloid congeners containing N-methyl amino acids at alternate residues.* Biochemistry, 2001. **40**(28): p. 8237-8245.
82. Doig, A.J., Hughes, E., Burke, R. M., Su, T. J., Heenan, R. K., and Lu, J., *Inhibition of toxicity and protofibril formation in the amyloid-beta peptide beta(25-35) using N-methylated derivatives.* Biochemical Society Transactions, 2002. **30**: p. 537-542.
83. Lee, K.H., Shin, B. H., Shin, K. J., Kim, D. J., and Yu, J., *A hybrid molecule that prohibits amyloid fibrils and alleviates neuronal toxicity induced by beta-amyloid (1-42).* Biochem Biophys Res Commun, 2005. **328**(4): p. 816-823.
84. Corsale, C., Carrotta, R., Mangione, M. R., Vilasi, S., Provenzano, A., Cavallaro, G., Bulone, D., and San Biagio, P. L., *Entrapment of A beta(1-40) peptide in unstructured aggregates.* Journal of Physics-Condensed Matter, 2012. **24**(24).
85. Qi, X., R.A. Moore, and M.A. McGuirl, *Dissociation of recombinant prion protein fibrils into short protofilaments: implications for the endocytic pathway and involvement of the N-terminal domain.* Biochemistry, 2012. **51**(22): p. 4600-4608.

86. Cort, J., Liu, Z. H., Lee, G., Harris, S. M., Prickett, K. S., Gaeta, L. S. L., and Andersen, N. H., *Beta-structure in human amylin and 2 designer beta-peptides - CD and NMR spectroscopic comparisons suggest soluble beta-oligomers and the absence of significant populations of beta-strand dimers.* Biochemical Biophysical Research Communications, 1994. **204**(3): p. 1088-1095.
87. Charge, S.B.P., Dekoning, E. J. P., and Clark, A., *Effect of pH and insulin on fibrillogenesis of islet amyloid polypeptide in-vitro.* Biochemistry, 1995. **34**(44): p. 14588-14593.
88. Nilsson, M.R., and Raleigh, D.P., *Analysis of amylin cleavage products provides new insights into the amyloidogenic region of human amylin.* Journal of Molecular Biology, 1999. **294**: p. 1375-1385.
89. Mazor, Y., Gilead, S., Benhar, I., and Gazit, E., *Identification and characterization of a novel molecular-recognition and self-assembly domain within the islet amyloid polypeptide.* Journal of Molecular Biology, 2002. **322**(5): p. 1013-1024.
90. Scrocchi, L.A., Ha, K., Chen, Y., Wu, L., Wang, F., and Fraser, P. E., *Identification of minimal peptide sequences in the (8-20) domain of human islet amyloid polypeptide involved in fibrillogenesis.* Journal of Structural Biology, 2003. **141**(3): p. 218-227.
91. Janson, J., Ashley, R.H., Harrison, D., McIntyre, S. and Butler, P.C., *The mechanism of islet amyloid polypeptide toxicity is membrane disruption by intermediate-sized toxic amyloid particles.* Diabetes, 1999. **48**: p. 491–498.
92. Anguiano, M., Nowak, R.J. and Lansbury, P.T., *Protofibrillar islet amyloid polypeptide permeabilizes synthetic vesicles by a pore-like mechanism that may be relevant to type II diabetes.* Biochemistry, 2002. **41**: p. 11338-11343.
93. Kayed, R., Sokolov, Y., Edmonds, B., McIntire, T.M., Milton, S.C., Hall, J.E. and Glabe, G.C., *Permeabilization of lipid bilayers is a common conformation-dependent activity of soluble amyloid oligomers in protein misfolding diseases.* The Journal of Biological Chemistry, 2004. **279**(45): p. 46363–46366.
94. Konarkowska, B., Aitken, J. F., Kistler, J., Zhang, S. P., and Cooper, G. J. S., *The aggregation potential of human amylin determines its cytotoxicity towards islet beta-cells.* Febs Journal, 2006. **273**(15): p. 3614-3624.
95. Meier, J.J., Kayed, R., Lin, C. Y., Gurlo, T., Haataja, L., Jayasinghe, S., Langen, R., Glabe, C. G., and Butler, P. C., *Inhibition of human IAPP fibril formation does not prevent beta-cell death: evidence for distinct actions of oligomers and fibrils of human IAPP.* American Journal of Physiology-Endocrinology and Metabolism, 2006. **291**(6): p. E1317-E1324.
96. Aitken, J.F., Loomes, K. M., Scott, D. W., Reddy, S., Phillips, A. R. J., Prijic, G., Fernando, C., Zhang, S. P., Broadhurst, R., L'Huillier, P., and Cooper, G. J. S., *Tetracycline treatment retards the onset and slows the progression of diabetes in human amylin/islet amyloid polypeptide transgenic mice.* Diabetes, 2010. **59**(1): p. 161-171.

Chapter 6

RESEARCH RESULTS IV

A direct fluorescent-based technique for cellular localization of amylin

This manuscript was accepted for publication by
Biotechnology and Applied Biochemistry
on 11 March 2013.

A direct fluorescent-based technique for cellular localization of amylin

Karen Pillay,[a] and Patrick Govender[a]

[a]*School of Life Sciences, University of KwaZulu-Natal, South Africa*

6.1 Abstract

Amylin has been implicated in type II diabetes due to its inherent property to misfold into toxic aggregates. Although it has been shown that amylin interacts with cell membranes, no study to date has monitored the association process using a direct approach. The present study uses confocal microscopy to identify the localization of carboxyfluorescein-labeled amylin in RIN-5F cells. In addition, the size of the aggregates that forms were evaluated using nanoparticle tracking analysis (NTA). In support of previous findings, amylin was observed to interact with and remain associated to the cell membrane. The cell membrane-associated aggregates spanned a size range of 130-800 nm.

6.2 Introduction

Misfolding of peptides or proteins into toxic oligomers and fibrils result in a number of diseases collectively classified as amyloid diseases.[1-5] Of these, type II diabetes and Alzheimer's disease are currently the most prevalent in society.[5] In type II diabetes, the peptide that is implicated in disease progression is amylin which is also referred to as islet amyloid polypeptide.[1-3, 6] Amylin is composed of 37 amino acids with a disulfide bridge between residues 2 and 7 (Figure 6.1), and aggregates into oligomers that are in a β-sheet conformation and which are toxic to pancreatic *beta* cells.[1-3, 7-13] Although there has been extensive research on potential inhibitors of amylin-mediated cytotoxicity, most of these studies have interrogated molecules that bind to amylin, which subsequently inhibits fibrillogenesis.[10, 13-31] However, to the best of our knowledge, there is currently no inhibitor of amylin aggregation that is a potential therapeutic agent for type II diabetes and which is under consideration for clinical development.[32] In an attempt to unravel its cellular pathway, it would be strategically beneficial to map the cellular localization of amylin aggregates so as to effect design of inhibitors of amylin aggregation and toxicity.

Figure 6.1 Primary structure of human amylin with a disulfide bond between amino acid residues 2 and 7.

Initial studies on amylin localization employed immunogold labeling and showed that amylin is present in lipofuscin bodies in pancreatic *beta* cells of diabetic patients.[6] Subsequent studies suggested that amylin is in close proximity to the external cell surfaces, namely the cell membrane and islet capillaries.[33-39] However, none of these studies evaluated amylin localization in an *in vitro* mammalian cell-based system.

The study herein, attempts to describe the real time *in vitro* cellular tracking of carboxyfluorescein-labeled amylin (carboxy-amy) aggregates in the rat pancreatic *beta* (RIN-5F) cell line. This cell line was selected as it represents the *in vivo* cytotoxic target of amylin aggregates and thus observations could provide an insight into what occurs in the biological scenario. The advantages of the proposed strategy are that it employs direct visualization of amylin localization and hence precludes the use of multiple-labeling steps and also limits the possibility of non-specific interactions. Nanoparticle tracking analysis (NTA) was also performed to concisely estimate the size of amylin aggregates that formed.

Most studies up until now have incorporated an indirect labeling approach using Congo red to distinguish amylin aggregates or used other dyes to identify cellular components.[40-43] Congo red has been suggested to identify amyloid aggregates by binding to its β-sheet structure.[44, 45] Congo red was however demonstrated to bind non-specifically to cellular membranes [42], possibly since some membrane proteins are in a β-sheet conformation. In addition, Congo red was found to decrease both the rate of amylin fibrillogenesis and its cytotoxic effect.[18, 28] Hence, it is evident that Congo red interacts with amylin and it can therefore be suggested that studies making use of this dye to localize amylin may have resulted in incorrect data interpretation. In addition, other dyes that were used to identify cellular components could potentially affect amylin-amylin interaction and thus an indirect labeling approach to study amylin localization would not be truly representative of an *in vivo* system.

One of the indirect amylin-labeling studies transfected the Simian fibroblast cell line (Cos-1) with vectors that express human amylin, and performed multiple labeling steps involving rabbit anti-amylin antiserum and sandwich labeling using the Oregon Green fluorochrome (GAR-FITC) to track amylin.[40] This study proposed that amylin is localized in the peri-nuclear region of cells, in particular the endoplasmic reticulum and Golgi apparatus.[40] Another indirect labeling approach used Congo red to pin-point amylin aggregates and the water soluble dye carboxyfluorescein to determine membrane integrity.[41] This study reported that membrane lipids are incorporated into the amylin aggregates during amyloid formation resulting in membrane leakage of giant unilamellar vesicles (GUVs) and the rat insulinoma tumor (RIN) cell line.[41] However, an interesting observation from this study was that membranes remained intact when pre-formed fibrils were added to the GUVs and RIN cells thus suggesting that monomeric or oligomeric amylin binds to membranes.[41]

It is noteworthy that even with the emergence of confocal microscopy-based experiments; fluorescent tags have not been extensively used for *in vitro* studies involving amylin localization. However, their ability to generate highly selective and sensitive results using simple experimental conditions has not gone unnoticed. To date, fluorescent-based investigative techniques have been primarily employed to study amylin aggregation dynamics in cell-free environments.[21, 22, 36, 46-50]

To the best of our knowledge, the only study that made use of fluorescent-labeled amylin to explore amylin localization was initiated by Radovan *et al.* (2009).[42] Their study employed a dual-fluorescent strategy that incorporated both Bodipy-labeled amylin and the membrane specific dye Texas red-DHPE. The results indicated that amylin was inserted into the membranes of rat insulinoma *beta* (INS-1E) cells and artificial model raft GUVs synthesized from DOPC:DPPC:cholesterol 1:2:1.[42] Although data suggested that membrane lipids were incorporated into the growing amyloid fibril, the Texas red-DHPE dye could potentially affect amylin aggregation kinetics thus resulting in incorrect data interpretation.[42]

Interestingly, the study herein is the first to report on a direct fluorescent-based approach for the cellular localization of amylin. Importantly, carboxyfluorescein labeling of human amylin was shown to have no significant effect on the aggregating potential of amylin. It can thus be suggested that this modified form of amylin can be used in fluorescence-based experiments to probe amylin aggregation dynamics and its interaction with mammalian cells grown in culture. The data seems to show that carboxy-amy is predominantly associated with the cell membranes of RIN-5F cells. The size of aggregates that formed in the presence of the pancreatic *beta* cells was shown to span the size range of 130-800 nm.

6.3 Materials and Methods

6.3.1 Reagents

All 9-fluorenylmethoxycarbonyl (Fmoc) protected amino acids and coupling reagents were purchased from GLS Biochem Systems, Inc. (China). The following protecting groups were used for the side chains of the amino acids: trityl (Trt) for asn, cys, gln, and his, *t*-butyl ether (*t*Bu) for ser and thr, 2,2,4,6,7-pentamethyl-dihydrobenzofuran-5-sulfonyl (Pbf) for arg, and *t*-butyloxycarbonyl (Boc) for lys. The PAL-ChemMatrix resin was purchased from Matrix Innovation (Canada). High performance liquid chromatography (HPLC) grade solvents for synthesis and purification, and 5(6)-carboxyfluorescein were purchased from Sigma-Aldrich (U.S.A.).

6.3.2 Peptide synthesis

As proposed by Fulop *et al.* (2001), carboxyfluorescein-labeled amylin was synthesized using standard Fmoc-based solid phase protocol.[51] Full length amylin was synthesized on a 0.1 mmol scale using a CEM microwave peptide synthesizer as previously described.[52] Briefly, deprotection was performed using 20% piperidine in dimethyl formamide (DMF). The activator used in the synthesis was 0.5 M 2-(1H-benzotriazole-1-yl)-1, 1, 3, 3-tetramethyluronium hexafluorophosphate (HBTU) in DMF, with 1 M *N*, *N*-diisopropylethylamine (DIPEA) in DMF serving as the activator base. Oxidation to form the Cys-2 to Cys-7 disulfide bridge was performed as previously described.[52] Briefly, unoxidised resin-bound amylin was allowed to bubble in methanol (3 mL) in a sintered glass bottom reaction vessel and iodine dissolved in methanol (approximately 5 mL) was added drop-wise until a faint yellow color developed. A washing step using DMF was performed, followed by coupling of 5(6)-carboxyfluorescein to the *N*-terminus of the resin-bound amylin. Coupling was performed for 20 hours using a ten times molar excess of 5(6)-carboxyfluorescein with *N*-[(dimethylamino)-1*H*-1,2,3-triazolo[4,5-b]pyridino-1-ylmethylene]-*N*-methylmethanaminium hexafluorophosphate *N*-oxide (HATU) and DIPEA in DMF serving as the activator and activator base respectively. The peptide was subsequently cleaved from the resin using 5% tri-isopropylsilane in trifluoroacetic acid (TFA) for two hours. Chemically synthesized human amylin (amylin) was used as the control for transmission electron microscopy (TEM) and NTA.[52]

6.3.3 Peptide purification

Carboxy-amy was purified on an ACE C18 preparative column (250 × 22 mm, Scotland) as previously described.[52] A dual-buffer system was employed, with TFA serving as the ion-pairing agent. The first buffer consisted of 0.1% TFA/H_2O (v/v) and the second buffer contained 0.1% TFA/acetonitrile (v/v). The peptides were eluted using a gradient of 0-90% buffer B over 90 minutes with a flow rate of 20 mL/min. The solvent from pooled peptide-containing fractions was evaporated to 20 mL and the samples were snap-frozen in liquid nitrogen and lyophilized.

6.3.4 Peptide analysis

The purified peptide was analyzed with an Agilent 1100 HPLC system fitted with a Waters XBridge C18 column, 250 × 3.6 mm as previously described.[52] Chromatography was performed over 90 minutes using a gradient of 0-90% of 0.1% TFA/acetonitrile (v/v) at a flow rate of 0.3 mL/min and the eluent was monitored at a UV wavelength of 215 nm. A Bruker electrospray ionization time-of-flight spectroscope (ESI-QTOF) in positive mode was used to obtain mass spectra (MS) and matrix assisted laser desorption ionization time-of-flight mass spectroscopy (MALDI-TOF MS) was performed with an Autoflex III instrument (Bruker) operated in positive mode with cyano-4-hydroxycinnamic acid being used as the matrix.

6.3.5 Disaggregation method

Disaggregation of carboxy-amy was performed as previously described.[52] Pre-weighed amylin samples were solubilized in 200 µL hexafluoroisopropanol (HFIP):TFA solution (50:50, v/v), sonicated for 10 minutes and left overnight. The solvents were then removed under vacuum using a centrifugal evaporator for approximately 1-2 hours. Approximately 100 µL HFIP was added to the amylin, followed by vortexing and the solvent was removed by rotary evaporation for 1-2 hours. To remove all traces of TFA, the latter process was repeated twice using HFIP (100 µL).

6.3.6 Transmission electron microscopy (TEM)

Carboxy-amy and amylin were disaggregated as described above and dissolved in filter sterilized 10 mM sodium phosphate buffer, pH 7.4 containing 50 mM NaCl (Buffer A) to a final concentration of 30 µM. Samples were incubated at 37°C and at specific time points 2 µL aliquots of each sample were transferred onto formvar coated carbon-stabilized copper grids. After drying for one minute, excess liquid was blot dried and samples were stained with 2% (w/v) uranyl acetate for 30 seconds. Samples were blot dried again before being analyzed with a CM120 Biotwin Philips transmission electron microscope at a voltage of 100 V.

6.3.7 Confocal microscopy

The RIN-5F cell line (European Collection of Cell Cultures, Sigma-Aldrich) was cultured in RPMI 1640 growth medium containing 10% heat-inactivated fetal bovine serum, 2 mM glutamine, 1 mM sodium pyruvate, 25 mM 2-[4-(2-hydroxyethyl)-1-piperazinyl] ethanesulfonic acid (HEPES), and 0.1 mg/mL penicillin/streptomycin, and thereafter plated at a density of 4 x 10^4 cells into 35 mm glass bottom petri dishes containing 14 mm micro wells (kindly donated by Dr Celia Snyman, University of KwaZulu-Natal). After an incubation period of 24 hours, spent media was replaced with fresh media. To establish if carboxyfluorescein was susceptible to photo bleaching effects, carboxyfluorescein only (2.54 μM, equivalent to the amount of carboxyfluorescein present in 30 μM of carboxy-amy) was added to the RIN-5F cells and monitored over time. Images were viewed and captured with a Zeiss 710 laser-scanning confocal microscope and Zeiss LSM 710 software at 10 minute intervals for the first hour and then every 30 minutes up until three hours, using a 63x oil immersion objective. Twelve slices at different focal points were captured at each time interval. A 488 nm argon laser was used for excitation of the fluorophore whilst emission was captured at 520 nm. Images were also simultaneously captured using differential interference contrast microscopy (DIC). To track the cellular localization of carboxy-amy, RIN-5F cells were grown and plated as described above. After an incubation period of 24 hours, spent media was removed and carboxy-amy was dissolved in growth medium and added to the cells to a final concentration of 30 μM. At the end of the experiment, growth medium was recovered from the samples and later analyzed using NTA. All experiments were performed in duplicate with the temperature of the sample chamber set to 37°C. Confocal microscopy images were processed using ImageJ version 1.47d software (U. S. National Institute of Health, U. S. A.).

6.3.8 Nanoparticle tracking analysis (NTA)

NTA measurements were performed with a NanoSight LM20 instrument (NanoSight, Amesbury, United Kingdom) equipped with a 488 nm laser for exciting the carboxyfluorescein tag and a temperature controlled sample chamber set at 37°C. To establish if the carboxyfluorescein tag aggregates on its own, carboxyfluorescein only (2.54 μM, equivalent to the amount of carboxyfluorescein present in 30 μM of carboxy-amy) was prepared in Buffer A and NTA performed by recording 60 second videos with the single shutter and gain modes. Analysis was performed using NanoSight NTA 2.2 software with a viscosity setting of 0.70. Samples recovered from confocal microscopy experiments were

captured and analyzed using NTA as described above. To monitor the aggregation dynamics of carboxy-amy over time, disaggregated peptide was diluted in Buffer A and sonicated for five minutes to yield a concentration of 30 μM before being injected into the sample chamber. Sample temperatures were allowed to equilibrate to 37°C (approximately one minute) before 60 second video recordings were taken at specific time points (every ten minutes for the first hour and then every 30 minutes up until three hours). Videos were captured and analysis performed as described above.

6.4 Results

In developing a suitable fluorescent strategy that will enable real time tracking of the interaction of amylin aggregates with cellular components it was deemed critical that the chemical modification should not interfere with its amyloidogenic potential. In this regard, the *N*-terminal lysine residue was selected as a suitable site of attachment of the fluorophore since there is general agreement that the *N*-terminal region of amylin is not involved in amylin fibril formation.[53, 54] Carboxyfluorescein was chosen as a suitable fluorophore as it was previously reported that a fluorescein label at the *N*-terminal of full length amylin [21] or on Aβ, the amyloidogenic peptide responsible for Alzheimer's disease, had no significant effect on the amyloidogenic properties of these peptides.[53, 54] Moreover, some of the advantages that are associated with the use of carboxyfluorescein (Figure 6.2) are its high molar absorbtivity, excellent fluorescent quantum yield, good solubility in water and an excitation of 494 nm, close to the 488 nm spectral line of the argon laser which makes it suitable for confocal microscopy imaging.[55] As illustrated in Figure 6.3, carboxyfluorescein-labeled amylin was synthesized with high purity and a yield of 8% (34 mg).

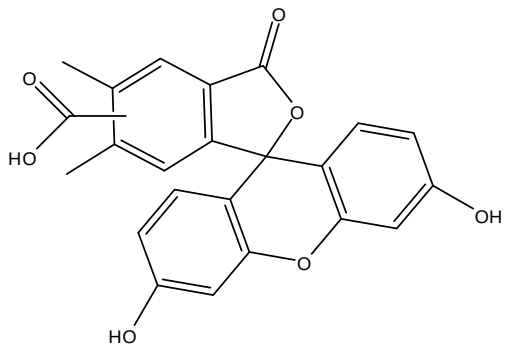

Figure 6.2 Structure of 5(6)-carboxyfluorescein.

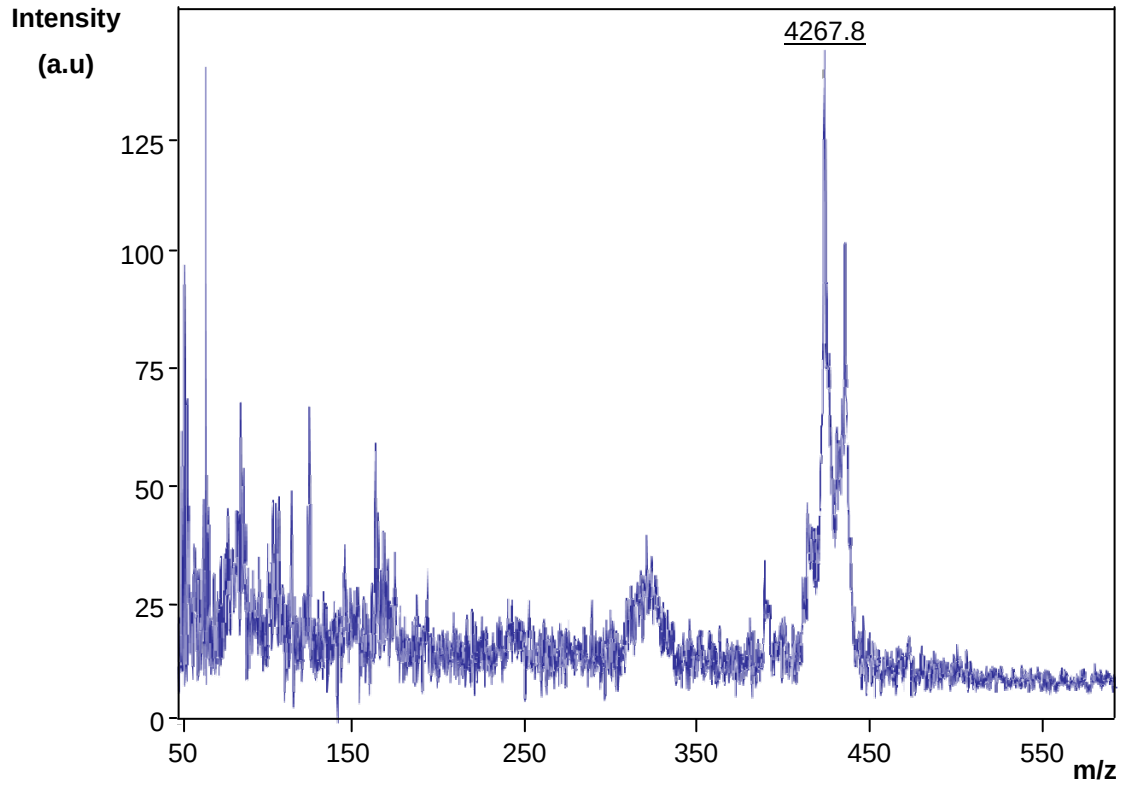

Figure 6.3 MALDI-TOF spectrum of chemically synthesized carboxyfluorescein-labeled amylin.

As ascertained by TEM analysis, amylin fibrils emanating from carboxy-amy exhibited a similar morphology to fibrils formed by unmodified amylin (Figure 6.4).

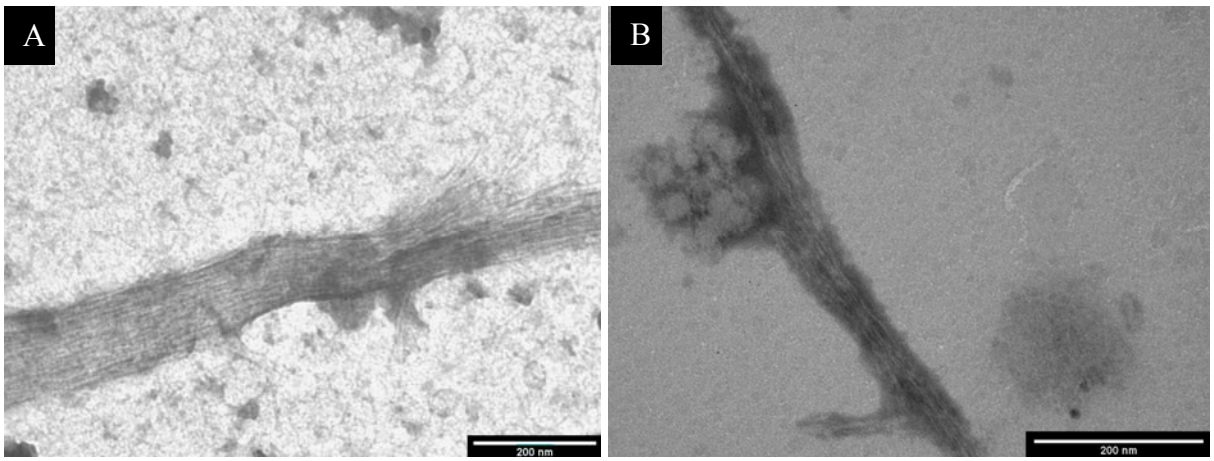

Figure 6.4 Comparison of the amyloidogenic potential of chemically synthesized amylin (A) and carboxy-amy (B) by TEM. Disaggregated peptide samples were prepared in 10 mM sodium phosphate buffer, pH 7.4 containing 50 mM NaCl to a final concentration of 30 µM. Representative electron micrographs of each sample is shown after an incubation time of 60 minutes at 37°C. Scale bars represent 200 nm.

Confocal microscopy imaging analysis confirmed that the carboxyfluorescein fluorophore was stable over the experimental duration, in that no photo-beaching was evident as the intensity of the fluorescent signal was not reduced (Figure 6.5).

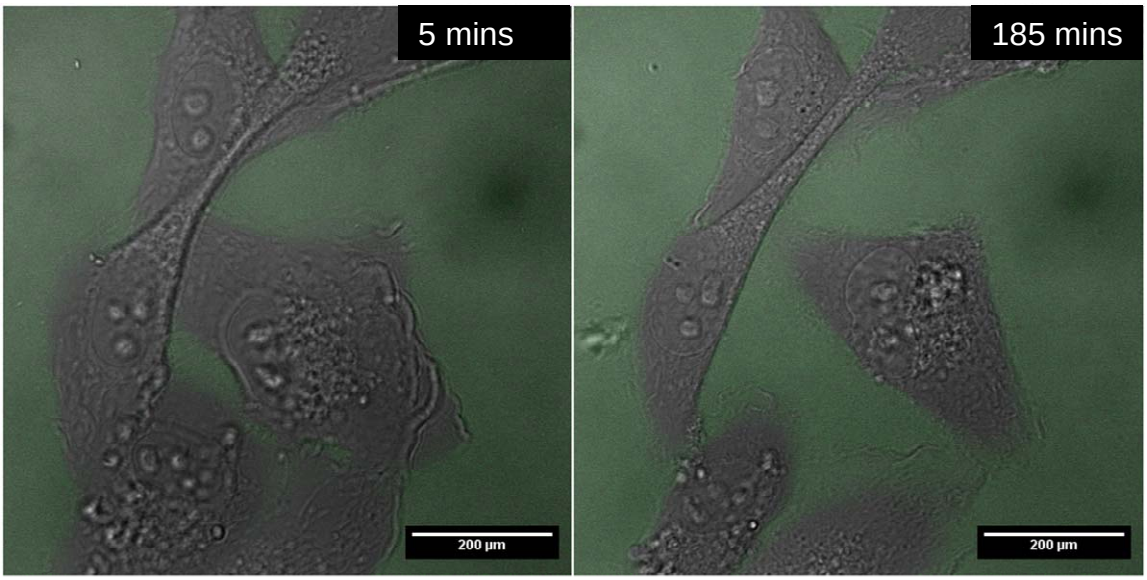

Figure 6.5 Confocal microscopy of RIN-5F cells exposed to carboxyfluorescein only (2.54 µM, equivalent to the amount of carboxyfluorescein present in 30 µM of carboxy-amy) at the start of the experiment and after three hours. The mean fluorescence intensity at 5 mins is 14.5 ± 3.0 and at 185 mins is 14.2 ± 3.0. The fluorescent intensity of carboxyfluorescein at the two time intervals were observed to be statically similar ($p > 0.05$). It is thus evident that the carboxyfluorescein label does not undergo photo-bleaching and neither does it interact with the cells. Each image represents the equatorial region of the cells and are overlays of the green fluorescent channel and the simultaneously obtained DIC image. Scale bars represent 200 µm. Statistical analysis (Welch's unpaired t-test) was performed using GraphPad InStat version 3 (GraphPad Software, U.S.A).

Analysis of confocal microscopy generated images seem to suggest that aggregates of carboxy-amy that are indicated by colored (yellow, white, blue, red and pink) arrows strongly interacts with the extracellular face of the RIN-5F plasma membrane (Figure 6.6). This is evidenced in that aggregates remain associated with the plasma membrane although the cellular morphology in certain instances changes markedly over the three hour duration of the experiment. It is noteworthy that carboxy-amy cannot be observed intracellularly.

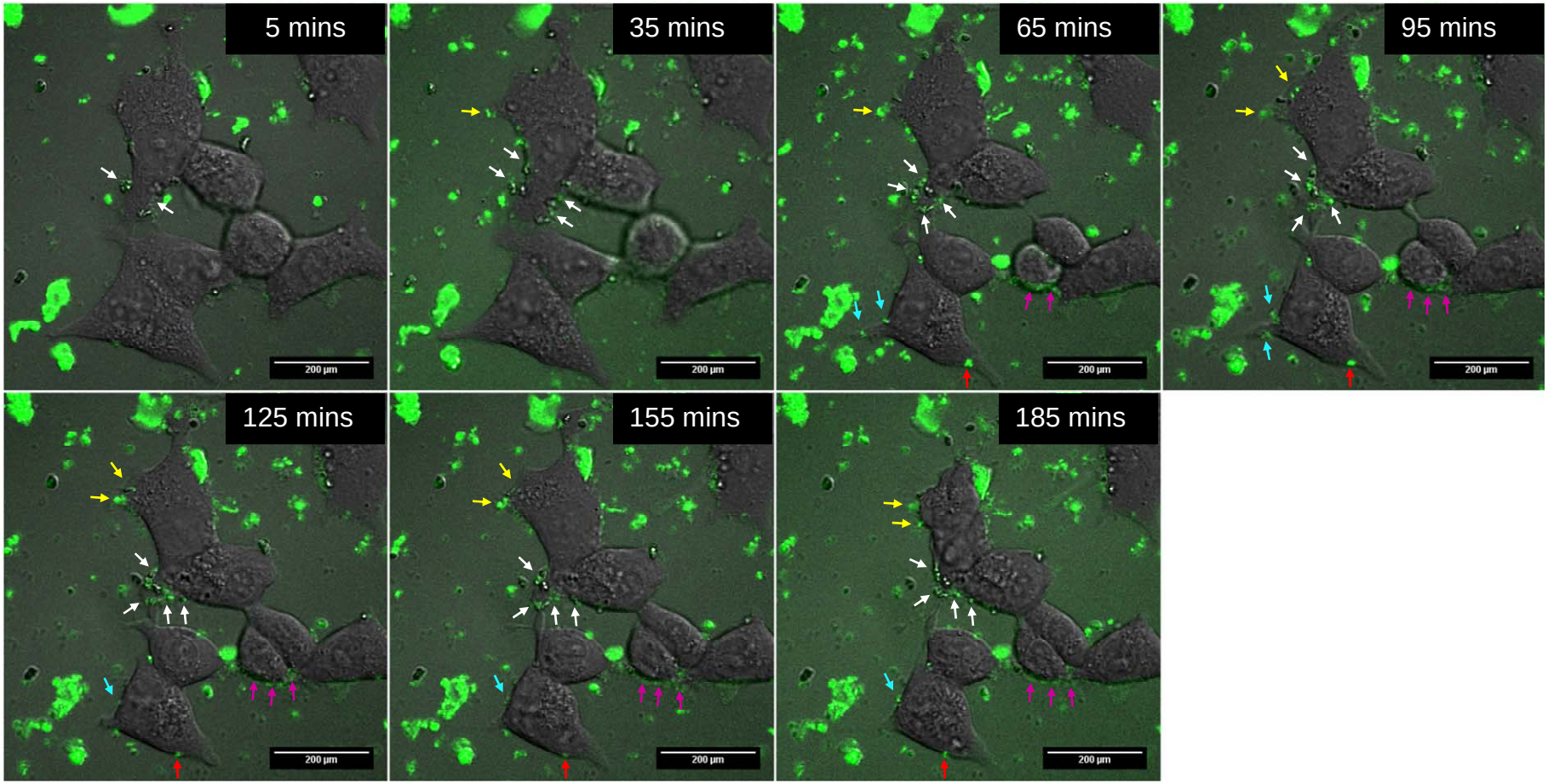

Figure 6.6 Carboxy-amy interaction with the cell membrane of RIN-5F cells at 30 minute intervals as determined by confocal microscopy. Each image represents the equatorial region of the cells and is an overlay of the green fluorescent channel and the simultaneously obtained DIC image. Different colored arrows are used to indicate the cellular localization of amylin over time. Scale bars represent 200 µm.

NTA of samples containing carboxyfluorescein only, illustrated a background fluorescence without any discernible aggregates being observed at all time points. The presence of a faint background indicates that the fluorophore is present but does not form aggregates greater than 30 nm in size and thus cannot be detected since the size range for NTA is 30-1000 nm.[56]

During NTA, resuspension, injection and equilibration times resulted in a time lapse of approximately ten minutes, thereby rendering analysis of a zero time-point impractical. As can be seen in Figure 6.7 (plot A), the predominant size of carboxy-amy at the ten minute time-point is between 40-90 nm, reaching a concentration greater than 2 x 10^7 aggregates/mL. Other peaks represent aggregates that were in the size range 90-260 nm and which occurred at concentrations between 0.5 x 10^7 aggregates/mL and 1 x 10^7 aggregates/mL. In addition another predominant peak represents an aggregate cohort with a size of approximately 510 nm and concentration of approximately 0.7 x 10^7 aggregates/mL. After three hours (Figure 6.7, plot B), the concentration of 100-170 nm aggregates were below 0.5 x 10^7 aggregates/mL whilst the predominant peaks representing aggregates in the 170-250 nm and 250-360 nm ranges were present at concentrations above 1 x 10^7 aggregates/mL, indicating that the smaller sized aggregates (40-90 nm and 90-170 nm) that were present at the ten minute time-point have now grown into larger particles (170-250 nm and 250-360 nm). Interestingly, the observed 510 nm peak at the ten minute interval is not evident after three hours. Rather, the emergence of two new peaks (360-520 nm and 640-850 nm) is observed. Growth medium that was recovered from the confocal microscopy experiment (Figure 6.7, plot C) and which was subjected to NTA revealed a carboxy-amy aggregate size distribution profile that was similar to that of the carboxy-amy sample alone after an incubation period of three hours (Figure 6.7, plot B). However, a higher concentration of particles in all size ranges except the 270-400 nm range was observed in the sample recovered from the confocal microscopy experiment.

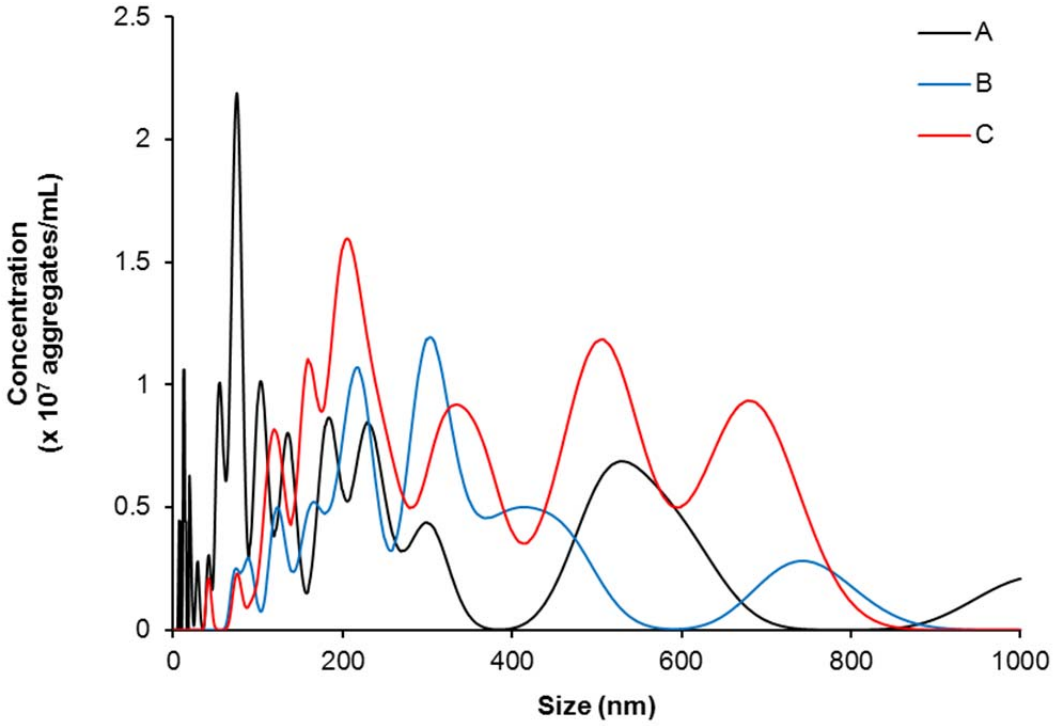

Figure 6.7 NTA size distribution profile of disaggregated carboxy-amy (30 μM) in 10 mM sodium phosphate buffer, pH 7.4 containing 50 mM NaCl after incubation at 37°C for 10 minutes (A) and 180 minutes (B). (C) NTA size distribution profile of the carboxy-amy sample that was recovered from the completed confocal microscopy experiments. Video recordings (duration of 60 seconds) of each sample were taken for NTA using the single shutter and gain mode.

6.5 Discussion

As mentioned previously, it is widely accepted that the aggregated form of amylin is linked to the destruction of pancreatic *beta* cells. It is therefore prudent that technology is developed that provides a closer insight into the interaction of amylin aggregates with cellular structures. This awareness may in part contribute to the successful design of an effective inhibitor of amylin aggregation and cytotoxicity. Up until now the cellular tracking of amylin aggregates has been reliant on indirect labeling strategies that are compromised by non-specific binding interactions and interference of amylin-amylin interactions that precludes reliable data interpretation. The present study was initiated in an attempt to visualize the *in vitro* interaction of amylin aggregates with a cultured mammalian cell line using a confocal microscopy-based fluorescent approach.

To negate any possibility of incorrect data interpretation, it was deemed critical that control experiments using only carboxyfluorescein be performed and the amyloidogenic nature of carboxy-amy be compared to unmodified amylin. In control confocal microscopy experiments using only carboxyfluorescein, it was observed that the fluorophore does not interact with the cells and neither does it aggregate over the duration of the experiment. This was further substantiated by NTA of samples containing carboxyfluorescein only as no particles were detected at all time-points. It is thus noteworthy that all observations on carboxy-amy reported in this study represent the modified peptide and are not due to interactions resulting from the carboxyfluorescein tag alone. In addition, carboxy-amy was shown via TEM analysis to form typical amyloid fibrils that were comparable to those formed by unmodified amylin. It can thus be suggested that attachment of the fluorophore did not impact negatively on the amyloidogenic nature of amylin. Thus it may be suggested that the fluorescent labeling approach as employed in the current study be considered as a viable option to investigate the aggregation dynamics of amylin.

Confocal microscopy imaging resolved that carboxy-amy aggregates specifically interact with the cell membrane of RIN-5F cells. It was also interesting to note that the interactions were limited to certain regions of the membrane as opposed to a more global interactive pattern. As mentioned previously, the carboxy-amy aggregates in certain instances remained strongly associated with the membrane whilst it shifted during cellular morphological changes. The latter observation is suggestive of a physical interaction between the two entities. This is supportive of previous studies which found that amylin associates with synthetic membranes, GUVs, or cell membranes.[33, 36-39, 41-43, 57, 58] Possible reasons for amylin interacting with the cell membrane have previously been proposed with studies suggesting that either hydrophobic or electrostatic interactions are responsible for this association.[36-39, 41-43, 57, 58] Hydrophobic interactions are possible since amylin has more hydrophobic R-groups in its constituent amino acids than hydrophilic R-groups, thus allowing amylin to interact with the non-polar membranes, whilst electrostatic interactions between positively charged amino acids and the negatively charged membrane could also facilitate amylin-membrane association. Reviews by Stefani (2007 and 2010) extensively describe the role of membrane interaction with amyloidogenic peptides and the subsequent cytotoxicity.[59, 60] Amylin has also been shown to bind to heparin sulfate proteoglycans that are present in the basement membrane of pancreatic *beta* cells. The latter binding interaction could also apply to the interaction of carboxy-amy aggregates with RIN-5F cells in this study.[61]

Understanding the fine details of the interaction of amylin aggregates with cellular membranes has the potential to unravel the mechanism of amylin-induced cytotoxicity. One hypothesis supported by experimental findings, is that amylin mediates cytotoxicity by binding to and initiating pore formation in cellular membranes thus compromising its integrity.[7, 8, 62] Another possible amyloidogenic protein-mediated mechanism of cytotoxicity, is that the protein monomer or oligomer would interact with the lipid bilayer of the cell membrane and extract lipids from the membrane during the aggregation process thereby resulting in membrane damage.[41] This is especially significant since it was reported that a high fat intake or change in lipid metabolism was necessary for fibril formation.[63, 64] A subsequent report suggested that these latter events would result in type II diabetes.[36] In addition, examination of islets revealed that membranes in close proximity to the amyloid deposits appeared to be damaged which could disrupt membrane fluidity and affect the uptake of glucose by the pancreatic *beta* cells, thereby leading to cytotoxicity.[35] It was also previously reported that amylin embeds itself in the basement membrane, forming an envelope around the intra-islet capillary endothelium which may have a negative effect on absorption of nutrients and hence could facilitate toxicity.[34] A more recent study has also shown that amylin interacts with and damages synthetic membranes of giant unilamellar vesicles.[43] Based on the confocal microscopy observations described in this study, it will be quite prudent to design an inhibitor of amylin-plasma membrane association since there is only one reported study to date that has used a molecule of this kind (e.g. rifampicin) to decrease amylin-mediated cytotoxicity.[15]

Carboxy-amy aggregation was also followed over time using NTA and it was observed that the concentration and size of aggregates increases over the three hour duration of the experiment. NTA also illustrated that the size distribution profiles of aggregates present in the samples recovered from the confocal microscopy experiment were similar to that of freshly prepared samples. However, it was noted that the concentration of aggregates in the sample recovered from the confocal microscopy experiment was higher than the concentration of aggregates that formed in the carboxy-amy sample that was not exposed to cellular interaction. This finding is similar to that reported by Jaysinghe and Langen (2005) whom also reported that amylin aggregates much more rapidly in the presence of synthetic membranes containing phosphatidylserine.[37] In the presence of RIN-5F cells, the predominant size ranges of amylin aggregates that formed were observed to be 130-270 nm, 270-400 nm, 400-600 nm and 600-800 nm. This data is consistent with a previous study that used total internal reflection fluorescence microscopy and reported that amylin aggregates spanned a size range between 200 nm and 560 nm.[65]

6.6 Conclusion

This study has demonstrated for the first time that labeling of full length human amylin with the fluorescent tag carboxyfluorescein does not alter the aggregating potential of the peptide. Thus, it can be suggested that this fluorescent-labeled peptide could be used to monitor the aggregation dynamics of amylin and hence for screening potential inhibitors of amylin aggregation and possibly even inhibitors of amylin-mediated cytotoxicity. In addition it was demonstrated that amylin interacts with the cell membrane which supports the already proposed hypothesis that amylin-mediated cytotoxicity results from membrane disruption.

6.7 Acknowledgements

Karen Pillay would like to thank NRF Thuthuka (grant number 76066) and UKZN for funding this study. Sincere gratitude to Ms Celia Snyman, UKZN for technical advice on use of the confocal microscope. Heartfelt thanks to Dr James Wesley-Smith, UKZN/CSIR for expert insight during transmission electron microscopy analysis.

6.8 References

1. Opie, E., *The relation of diabetes mellitus to lesions of the pancreas. Hyaline degeneration of the islands of Langerhans.* The Journal of Experimental Medicine, 1901. **5**: p. 528-540.
2. Cooper, G.J.S., Willis, A.C., Clark, A., Turner, R.C., Sim, R.B. and Reid, K.B.M., *Purification and characterization of a peptide from amyloid-rich pancreases of type 2 diabetic patients.* Proceedings of the National Academy of Science, 1987. **84**: p. 8628-8632.
3. Cooper, G.J.S., Leighton, B., Dimitriadis, G. D., Parry-Billings, M., Kowalchuk, J. M., Howland K., Rothbard, J. B., Willis, A. C. and Reid, K. B. M. , *Amylin found in amyloid deposits in human type 2 diabetes mellitus may be a hormone that regulates glycogen metabolism in skeletal muscle.* Proceedings of the National Academy of Science, 1988. **85**: p. 7763-7766.
4. Kayed, R., Bernhagen, J., Greenfield, N., Sweimeh, K., Brunner, H., Voelter, W. and Kapurniotu, A., *Conformational transitions of islet amyloid polypeptide (IAPP) in amyloid formation in vitro.* Journal of Molecular Biology, 1999. **287**: p. 781-796.
5. Pawlicki, S., A. Le Bechec, and C. Delamarche, *AMYPdb: A database dedicated to amyloid precursor proteins.* Bmc Bioinformatics, 2008. **9**.
6. Clark, A., Edwards, C. A., Ostle, L. R., Sutton, R., Rothbard, J. B., Morris, J. F., and Turner, R. C., *Localization of islet amyloid peptide in lipofuscin bodies and secretory granules of human β-cells and in islets of type-2 diabetic subjects.* Cell and Tissue Research, 1989. **257**(1): p. 179-185.
7. Janson, J., Ashley, R.H., Harrison, D., McIntyre, S. and Butler, P.C., *The mechanism of islet amyloid polypeptide toxicity is membrane disruption by intermediate-sized toxic amyloid particles.* Diabetes, 1999. **48**: p. 491–498.
8. Anguiano, M., Nowak, R.J. and Lansbury, P.T., *Protofibrillar islet amyloid polypeptide permeabilizes synthetic vesicles by a pore-like mechanism that may be relevant to type II diabetes.* Biochemistry, 2002. **41**: p. 11338-11343.
9. Kayed, R., Sokolov, Y., Edmonds, B., McIntire, T.M., Milton, S.C., Hall, J.E. and Glabe, G.C., *Permeabilization of lipid bilayers is a common conformation-dependent activity of soluble amyloid oligomers in protein misfolding diseases.* The Journal of Biological Chemistry, 2004. **279**(45): p. 46363–46366.
10. Konarkowska, B., Aitken, J. F., Kistler, J., Zhang, S. P., and Cooper, G. J. S., *The aggregation potential of human amylin determines its cytotoxicity towards islet beta-cells.* Febs Journal, 2006. **273**(15): p. 3614-3624.

11. Meier, J.J., Kayed, R., Lin, C., Gurlo, T., Haataja, L., Jayasinghe, S., Langen, R., Glabe, C.G., and Butler, P.C., *Inhibition of human IAPP fibril formation does not prevent beta-cell death: evidence for distinct actions of oligomers and fibrils of human IAPP.* American Journal of Physiology, Endocrinology and Metabolism, 2006. **291**: p. E1317–E1324.
12. Ritzel, R.A., Meier, J. J., Lin, C., Veldhuis, J. D., and Butler, P. C., *Human islet amyloid polypeptide oligomers disrupt cell coupling, induce apoptosis, and impair insulin secretion in isolated human islets.* Diabetes, 2007. **56**: p. 65-71.
13. Aitken, J.F., Loomes, K. M., Scott, D. W., Reddy, S., Phillips, A. R. J., Prijic, G., Fernando, C., Zhang, S. P., Broadhurst, R., L'Huillier, P., and Cooper, G. J. S., *Tetracycline treatment retards the onset and slows the progression of diabetes in human amylin/islet amyloid polypeptide transgenic mice.* Diabetes, 2010. **59**(1): p. 161-171.
14. Hayashi, T., Asai, T., and Ogoshi, H., *Conformational analysis of beta-turn structure in tetrapeptides containing proline or proline analogs.* Tetrahedron Letters, 1997. **38**(17): p. 3039-3042.
15. Tomiyama, T., Kaneko, H., Kataoka, K., Asano, S. and Endo, N., *Rifampicin inhibits the toxicity of pre-aggregated amyloid peptides by binding to peptide fibrils and preventing amyloid-cell interaction.* Biochemical Journal, 1997. **322**: p. 859-865.
16. Rijkers, D.T.S., Hoppener, J.W.M., Posthuma, G., Lips, C.J.M. and Liskamp, R.M.J, *Inhibition of amyloid fibril formation of human amylin by N-alkylated amino acid and α-hydroxy acid residue containing peptides.* Chemistry: A European Journal, 2002. **8**(18): p. 4285-4291.
17. Scrocchi, L.A., Chen, Y., Waschuk, S., Wang, F., Cheung, S., Darabie, A.A., McLaurin, J. and Fraser, P.E., *Design of peptide-based inhibitors of human islet amyloid polypeptide fibrillogenesis.* Journal of Molecular Biology, 2002. **318**: p. 697–706.
18. Aitken, J.F., Loomes, K.M., Konarkowska, B., and Cooper, G.J.S, *Suppression by polycyclic compounds of the conversion of human amylin into insoluble amyloid.* Biochemical Journal, 2003. **374**: p. 779–784.
19. Scrocchi, L.A., Ha, K., Chen, Y., Wu, L., Wang, F., and Fraser, P. E., *Identification of minimal peptide sequences in the (8-20) domain of human islet amyloid polypeptide involved in fibrillogenesis.* Journal of Structural Biology, 2003. **141**(3): p. 218-227.
20. Porat, Y., Mazor, Y., Efrat, S., and Gazit, E., *Inhibition of islet amyloid polypeptide fibril formation: a potential role for heteroaromatic interactions.* Biochemistry, 2004. **43**(45): p. 14454-14462.
21. Tatarek-Nossol, M., Yan, L., Schmauder, A., Tenidis, K., Westermark, G., and Kapurniotu, A., *Inhibition of hIAPP amyloid-fibril formation and apoptotic cell death by a designed hIAPP amyloid-core-containing hexapeptide.* Chemistry & Biology, 2005. **12**: p. 797–809.
22. Yan, L., Tatarek-Nossol, M., Velkova, A., Kazantzis, A., and Kapurniotu, A., *Design of a mimic of nonamyloidogenic and bioactive human islet amyloid polypeptide (IAPP) as nanomolar affinity inhibitor of IAPP cytotoxic fibrillogenesis.* Proceedings of the National Academy of Science, 2006. **103**(7): p. 2046–2051.
23. Abedini, A., Meng, F. and Raleigh, D.P., *A single-point mutation converts the highly amyloidogenic human islet amyloid polypeptide into a potent fibrillization inhibitor.* Journal of the American Chemical Society, 2007. **129**: p. 11300-11301.
24. Bedrood, S., Jayasinghe, S., Sieburth, D., Chen, M., Erbel, S., Butler, P. C., Langen, R., and Ritzel, R. A., *Annexin A5 directly interacts with amyloidogenic proteins and reduces their toxicity.* Biochemistry, 2009. **48**(44): p. 10568-10576.
25. Cabaleiro-Lago, C., Lynch, I., Dawson, K. A., and Linse, S., *Inhibition of IAPP and IAPP(20-29) fibrillation by polymeric nanoparticles.* Langmuir, 2009. **26**(5): p. 3453-3461.
26. Mishra, R., Sellin, D., Radovan, D., Gohlke, A., and Winter, R., *Inhibiting islet amyloid polypeptide fibril formation by the red wine compound resveratrol.* Chembiochem, 2009. **10**(3): p. 445-449.
27. Potter, K.J., Scrocchi, L. A., Warnock, G. L., Ao, Z., Younker, M. A., Rosenberg, L., Lipsett, M., Verchere, C. B., and Fraser, P. E., *Amyloid inhibitors enhance survival of cultured human islets.* Biochimica Et Biophysica Acta-General Subjects, 2009. **1790**(6): p. 566-574.
28. Zraika, S., Hull, R. L., Udayasankar, J., Aston-Mourney, K., Subramanian, S. L., Kisilevsky, R., Szarek, W. A., and Kahn, S. E., *Oxidative stress is induced by islet amyloid formation and time-dependently mediates amyloid-induced beta cell apoptosis.* Diabetologia, 2009. **52**(4): p. 626-635.
29. Meng, F., Abedini, A., Plesner, A., Middleton, C., Potter, K. J., Zanni, M. T., Verchere, C. B., and Raleigh, D. P., *The sulfated triphenyl methane derivative acid fuchsin is a potent inhibitor of amyloid formation by human islet amyloid polypeptide and protects against the toxic effects of amyloid formation.* Journal of Molecular Biology, 2010. **400**(3): p. 555-566.
30. Muthusamy, K., Arvidsson, P. I., Govender, P., Kruger, H. G., Maguire, G. E. M., and Govender, T., *Design and study of peptide-based inhibitors of amylin cytotoxicity.* Bioorganic & Medicinal Chemistry Letters, 2010. **20**(4): p. 1360-1362.

31. Rigacci, S., Guidotti, V., Bucciantini, M., Parri, M., Nediani, C., Cerbai, E., Stefani, M., and Berti, A., *Oleuropein aglycon prevents cytotoxic amyloid aggregation of human amylin.* Journal of Nutritional Biochemistry, 2010. **21**(8): p. 726-735.
32. Doig, A.J., K. Stott, and J.M. Treherne, *Inhibitors of amyloid aggregation: technologies for the discovery of novel lead compounds.* Biotechnology & genetic engineering reviews, 2004. **21**: p. 197-212.
33. Verchere, C.B., Dalessio, D. A., Palmiter, R. D., Weir, G. C., BonnerWeir, S., Baskin, D. G., and Kahn, S. E., *Islet amyloid formation associated with hyperglycemia in transgenic mice with pancreatic beta cell expression of human islet amyloid polypeptide.* Proceedings of the National Academy of Sciences of the United States of America, 1996. **93**(8): p. 3492-3496.
34. Hayden, M.R. and S.C. Tyagi, *"A" is for amylin and amyloid in type 2 diabetes mellitus.* JOP : Journal of the pancreas, 2001. **2**(4): p. 124-39.
35. Clark, A. and M.R. Nilsson, *Islet amyloid: a complication of islet dysfunction or an aetiological factor in Type 2 diabetes?* Diabetologia, 2004. **47**(2): p. 157-169.
36. Knight, J.D., and Miranker, A. D., *Phospholipid catalysis of diabetic amyloid assembly.* Journal of Molecular Biology, 2004. **341**(5): p. 1175-1187.
37. Jayasinghe, S.A., and Langen, R., *Lipid membranes modulate the structure of islet amyloid polypeptide.* Biochemistry, 2005. **44**: p. 12113-12119.
38. Engel, M.F.M., Yigittop, H., Elgersma, R. C., Rijkers, D. T. S., Liskamp, R. M. J., de Kruijff, B., Hoppener, J. W. M., and Killian, J. A., *Islet amyloid polypeptide inserts into phospholipid monolayers as monomer.* Journal of Molecular Biology, 2006. **356**(3): p. 783-789.
39. Apostolidou, M., S.A. Jayasinghe, and R. Langen, *Structure of alpha-helical membrane-bound human islet amyloid polypeptide and its implications for membrane-mediated misfolding.* Journal of Biological Chemistry, 2008. **283**(25): p. 17205-17210.
40. Hiddinga, H.J., and Eberhardt, N.L., *Intracellular amyloidogenesis by human islet amyloid polypeptide induces apoptosis in COS-1 cells.* American Journal of Pathology, 1999. **154**(4): p. 1077-1088.
41. Sparr, E., Engel, M. F. M., Sakharov, D. V., Sprong, M., Jacobs, J., de Kruijff, B., Hoppener, J. W. M., and Killian, J. A., *Islet amyloid polypeptide-induced membrane leakage involves uptake of lipids by forming amyloid fibers.* Febs Letters, 2004. **577**(1-2): p. 117-120.
42. Radovan, D., Opitz, N., and Winter, R., *Fluorescence microscopy studies on islet amyloid polypeptide fibrillation at heterogeneous and cellular membrane interfaces and its inhibition by resveratrol.* Febs Letters, 2009. **583**(9): p. 1439-1445.
43. Khemtemourian, L., Domenech, E., Doux, J. P. F., Koorengevel, M. C., and Killian, J. A., *Low pH acts as inhibitor of membrane damage induced by human islet amyloid polypeptide.* Journal of the American Chemical Society, 2011. **133**(39): p. 15598-15604.
44. Cooper, J.H., *Selective amyloid staining as a function of amyloid composition and structure - histochemical analysis of alkaline congo red, standardized toluidine blue, and iodine methods.* Laboratory Investigation, 1974. **31**(3): p. 232-238.
45. Lansbury, P.T., *In pursuit of the molecular-structure of amyloid plaque - new technology provides unexpected and critical information.* Biochemistry, 1992. **31**(30): p. 6865-6870.
46. Padrick, S.B., and Miranker, A. D., *Islet amyloid polypeptide: identification of long-range contacts and local order on the fibrillogenesis pathway.* Journal of Molecular Biology, 2001. **308**(4): p. 783-794.
47. Jaikaran, E., Nilsson, M. R., and Clark, A., *Pancreatic beta-cell granule peptides form heteromolecular complexes which inhibit islet amyloid polypeptide fibril formation.* Biochemical Journal, 2004. **377**: p. 709-716.
48. Yan, L., Velkova, A., Tatarek-Nossol, M., Andreetto, E., and Kapurniotu, A., *IAPP mimic blocks Ab cytotoxic self-assembly: cross-suppression of amyloid toxicity of Ab and IAPP suggests a molecular link between Alzheimers disease and type II diabetes.* Angewandte Chemie International Edition, 2007. **46**: p. 1246 –1252.
49. Knight, J.D., Williamson, J. A., and Miranker, A. D., *Interaction of membrane-bound islet amyloid polypeptide with soluble and crystalline insulin.* Protein Science, 2008. **17**(10): p. 1850-1856.
50. Marek, P., Gupta, R., and Raleigh, D. P., *The fluorescent amino acid p-cyanophenylalanine provides an intrinsic probe of amyloid formation.* Chembiochem, 2008. **9**(9): p. 1372-1374.
51. Fulop, L., Penke, B., and Zarandi, M., *Synthesis and fluorescent labeling of beta-amyloid peptides.* Journal of Peptide Science, 2001. **7**(8): p. 397-401.
52. Muthusamy, K., Albericio, F., Arvidsson, P. I., Govender, P., Kruger, H. G., Maguire, G. E. M., and Govender, T., *Microwave assisted SPPS of amylin and its toxicity of the pure product to RIN-5F cells.* Biopolymers, 2010. **94**(3): p. 323-330.
53. Edwin, N.J., Bantchev, G. B., Russo, P. S., Hammer, R. P., and McCarley, R. L., *Elucidating the kinetics of beta-amyloid fibril formation*, in *New Polymeric Materials*, L.S. KorugicKarasz, W.J. MacKnight, and E. Martuscelli, 2005. p. 106-118.

54. Edwin, N.J., Hammer, R. P., McCarley, R. L., and Russo, P. S., *Reversibility of beta-amyloid self-assembly: effects of pH and added salts assessed by fluorescence photobleaching recovery.* Biomacromolecules, 2010. **11**(2): p. 341-347.
55. Goncalves, M.S.T., *Fluorescent labeling of biomolecules with organic probes.* Chemical reviews, 2009. **109**(1): p. 190-212.
56. Filipe, V., Hawe, A., and Jiskoot, W., *Critical evaluation of nanoparticle tracking analysis (NTA) by NanoSight for the measurement of nanoparticles and protein aggregates.* Pharmaceutical Research, 2010. **27**(5): p. 796-810.
57. Lopes, D.H.J., Meister, A., Gohlke, A., Hauser, A., Blume, A., and Winter, R., *Mechanism of islet amyloid polypeptide fibrillation at lipid interfaces studied by infrared reflection absorption spectroscopy.* Biophysical Journal, 2007. **93**(9): p. 3132-3141.
58. Radovan, D., Smirnovas, V., and Winter, R., *Effect of pressure on islet amyloid polypeptide aggregation: revealing the polymorphic nature of the fibrillation process.* Biochemistry, 2008. **47**(24): p. 6352-6360.
59. Stefani, M., *Generic cell dysfunction in neurodegenerative disorders: role of surfaces in early protein misfolding, aggregation, and aggregate cytotoxicity.* Neuroscientist, 2007. **13**(5): p. 519-531.
60. Stefani, M., *Biochemical and biophysical features of both oligomer/fibril and cell membrane in amyloid cytotoxicity.* Febs Journal, 2010. **277**(22): p. 4602-4613.
61. Marzban, L., Park, K., and Verchere, C. B., *Islet amyloid polypeptide and type 2 diabetes.* Experimental Gerontology, 2003. **38**(4): p. 347-351.
62. Mirzabekov, T.A., Lin, M. and Kagan, B.L., *Pore formation by the cytotoxic islet amyloid peptide amylin.* The Journal of Biological Chemistry, 1996. **271**: p. 1988–1992.
63. Hoppener, J.W.M., Oosterwijk, C., Nieuwenhuis, M. G., Posthuma, G., Thijssen, J. H. H., Vroom, T. M., Ahren, B., and Lips, C. J. M., *Extensive islet amyloid formation is induced by development of type II diabetes mellitus and contributes to its progression: pathogenesis of diabetes in a mouse model.* Diabetologia, 1999. **42**(4): p. 427-434.
64. Hull, R.L., Andrikopoulos, S., Verchere, C. B., Vidal, J., Wang, F., Cnop, M., Prigeon, R. L., and Kahn, S. E., *Increased dietary fat promotes islet amyloid formation and beta-cell secretory dysfunction in a transgenic mouse model of islet amyloid.* Diabetes, 2003. **52**(2): p. 372-379.
65. Patil, S.M., Mehta, A., Jha, S., and Alexandrescu, A. T., *Heterogeneous amylin fibril growth mechanisms imaged by total internal reflection fluorescence microscopy.* Biochemistry, 2011. **50**(14): p. 2808-2819.

Chapter 7

GENERAL DISCUSSION AND CONCLUSION

7. GENERAL DISCUSSION AND CONCLUSION

7.1 GENERAL DISCUSSION AND CONCLUSION

To avoid the use of expensive pseudoproline derivatives in the chemical synthesis of full length human amylin [1-6], a microwave-assisted solid phase peptide synthetic strategy that makes use of the ChemMatrix (CM) resin and triple couplings for problematic amino acids was developed. As previously reported for the synthesis of other hydrophobic and highly structured peptides [7-9], the polyethyleneglycol-based resin (CM) resin was observed to be suitable for amylin synthesis. In addition, it was shown that oxidation with iodine is effective in the formation of the disulfide bridge between residues two and seven of full length amylin. Moreover, the use of purified unoxidized amylin in the afore-mentioned oxidation reaction yielded amylin with the requisite secondary disulfide structure without the need for further purification. The chemically synthesized amylin yielded in this study displayed a higher purity than two other commercially available amylin products.

After a comprehensive literature review encompassing all reports on the amyloidogenic properties of amylin, distinct regions of the amino acid sequence of human amylin were identified as potential inhibitors of amylin aggregation. In this regard, non-methylated and *N*-methylated amylin derivatives were synthesized and it was established that the NTAT and ST(N-Me)NV(N-Me)G(N-Me)S(N-Me) amylin derivatives were attractive candidates in their capability to reduce the formation of amylin fibrils. In support of previous findings [10-16], data generated in this study indicates that the fibrillar form of amylin is non-toxic since all the non-methylated amylin derivatives were found to be effective inhibitors of amylin-mediated cytotoxicity, with STNVGS demonstrating superior inhibitory activity. Of significance, the only *N*-methylated amylin derivative that reduced amylin-induced cytotoxicity [ST(N-Me)NV(N-Me)G(N-Me)S(N-Me)] is homologous to the most potent peptide inhibitor of amylin-induced cytotoxicity. Consequently, it can be suggested that this region of amylin plays a key role in fibrillogenesis.

Although cytotoxicity assays provides an invaluable insight into the potential of molecules as inhibitors of amylin-mediated cytotoxicity, the costly and time-consuming nature of this cell-based assay system warrants development of a cell-free approach. To this end, surface plasmon resonance (SPR), dynamic light scattering (DLS) and nanoparticle tracking analysis (NTA) were evaluated. No data was generated from DLS studies due to its limitation in the analysis of poly-disperse samples, and SPR-generated data could not be correlated to previously established cytotoxicity results since the binding of an inhibitor to amylin does not necessarily specify its inhibitory potential.[17] However, it was found that NTA could monitor the change in size of amylin aggregates as it progressed over time and the concentration of certain sized aggregates could be correlated to cytotoxicity data. On further optimization of NTA, this technique seems to be an attractive option as a possible cell-free assay that can be used to reliably screen inhibitors of amylin-induced cytotoxicity.

Furthermore it was also demonstrated that SPR analysis does allow for the quantification of amylin association and dissociation kinetics (association constant (k_a) = 28.7 ± 5.1 $M^{-1}s^{-1}$ and dissociation constant (k_d) = 2.8 ± 0.6 x 10^{-4} s^{-1}). Of note, amylin association kinetics were similar to that reported for Aβ whilst it was evident that Aβ dissociates faster than amylin [18, 19], suggesting that even though amyloidogenic peptides share similarities in their structural properties [20], the intricacies of fibril formation are dissimilar.

A carboxyfluorescein modification of amylin was demonstrated to have no effect on the fibrillogenic nature of the peptide. This modified form of amylin thus provided a direct approach to gain insight into the cellular localization of amylin. As previously reported, amylin was observed to associate with the plasma membrane [21, 22], however the strategy used herein negated any effects of extraneous dyes that have been previously shown to reduce amylin-amylin and amylin-cell interactions. Although it has been previously suggested that amylin exerts its toxic effect by binding to the plasma membrane, possibly resulting in membrane disruption and also activating signaling pathways that are involved in apoptosis [23-28], this is the only study to date that clearly illustrates amylin interaction with the plasma membrane.

Further prospects arising from this study that warrant further investigation can be summarized as follows:

- The biodegradability of ST(N-Me)NV(N-Me)G(N-Me)S(N-Me) should be ascertained and *in vivo* testing performed to establish their potential as effective therapeutic agents for type II diabetes.

- Peptoids homologous to amylin and in particular its 29-34 region can also be synthesized and evaluated as potential inhibitors of amylin-mediated cytotoxicity.

- Since amylin association with the plasma membrane facilitates amylin-induced cytotoxicity, therapeutic molecules that specifically target this interaction can be designed as potential therapeutic agents for type II diabetes.

- It is also recommended that more extensive studies using NTA be implemented to ascertain the suitability of this cell-free approach as an efficient screening technique for potential inhibitors of amylin-mediated cytotoxicity.

7.3 REFERENCES

1. Raleigh, D.P., and Abedini, A., *Incorporation of pseudoproline derivatives allows the facile synthesis of human IAPP, a highly amyloidogenic and aggregation-prone polypeptide.* Orgnic Letters, 2005. **7**(4): p. 693-696.
2. Raleigh, D.P., Abedini, A., and Singh, G., *Recovery and purification of highly aggregation-prone disulfide-containing peptides: application to islet amyloid polypeptide.* Analytical Biochemistry 351 (2006) 181–186, 2006. **351**: p. 181-186.
3. Park, J.H., Page, K., Hood, C.A., Patel, H., Fuentes, G., Menakuru, M., *Fast Fmoc synthesis of hAmylin1–37 with pseudoproline assisted on-resin disulfide formation.* Journal of Peptide Science, 2007. **13**: p. 833-838.
4. Kelly, J.W., Yonemoto, I. T., Kroon, G. J. A., Dyson, H. J., and Balch, W. E., *Amylin proprotein processing generates progressively more amyloidogenic peptides that initially sample the helical state.* Biochemistry, 2008. **47**: p. 9900–9910.
5. Park, J.H., Hood, C.A., Fuentes, G., Patel, H., Page, K., Menakuru, M., *Fast conventional Fmoc solid-phase peptide synthesis with HCTU.* Journal of Peptide Science 2008. **14**: p. 97-101.
6. Marek, P., Woys, A. M., Sutton, K., Zanni, M. T., and Raleigh, D. P., *Efficient microwave-assisted synthesis of human islet amyloid polypeptide designed to facilitate the specific incorporation of labeled amino acids.* Organic Letters, 2010. **12**(21): p. 4848-4851.
7. Garcia-Martin, F., Quintanar-Audelo, M., Garcia-Ramos, Y., Cruz, L.J., Gravel, C., Furic, R., Cote, S., Tulla-Puche, J., and Albericio, F., *ChemMatrix, a poly(ethylene glycol)-based support for the solid-phase synthesis of complex peptides.* Journal of Combinatorial Chemistry 2006. **8**: p. 213-220.
8. Garcia-Martin, F., White, P., Steinauer, R., Cote, S., Tulla-Puche, J., Albericio, F., *The synergy of ChemMatrix resin and pseudoproline building blocks renders RANTES, a complex aggregated chemokine.* Biopolymers, 2006. **84**(6): p. 566-575.
9. de la Torre, B.G., Jakab, A., and Andreu, D., *Polyethyleneglycol-based resins as solid supports for the synthesis of difficult or long peptides.* International Journal of Peptide Research and Therapeutics 2007. **13**(1-2): p. 265–270.

10. Janson, J., Ashley, R.H., Harrison, D., McIntyre, S. and Butler, P.C., *The mechanism of islet amyloid polypeptide toxicity is membrane disruption by intermediate-sized toxic amyloid particles.* Diabetes, 1999. **48**: p. 491–498.
11. Anguiano, M., Nowak, R.J. and Lansbury, P.T., *Protofibrillar islet amyloid polypeptide permeabilizes synthetic vesicles by a pore-like mechanism that may be relevant to type II diabetes.* Biochemistry, 2002. **41**: p. 11338-11343.
12. Kayed, R., Sokolov, Y., Edmonds, B., McIntire, T.M., Milton, S.C., Hall, J.E. and Glabe, G.C., *Permeabilization of lipid bilayers is a common conformation-dependent activity of soluble amyloid oligomers in protein misfolding diseases.* The Journal of Biological Chemistry, 2004. **279**(45): p. 46363–46366.
13. Konarkowska, B., Aitken, J. F., Kistler, J., Zhang, S. P., and Cooper, G. J. S., *The aggregation potential of human amylin determines its cytotoxicity towards islet beta-cells.* Febs Journal, 2006. **273**(15): p. 3614-3624.
14. Meier, J.J., Kayed, R., Lin, C., Gurlo, T., Haataja, L., Jayasinghe, S., Langen, R., Glabe, C.G., and Butler, P.C., *Inhibition of human IAPP fibril formation does not prevent beta-cell death: evidence for distinct actions of oligomers and fibrils of human IAPP.* American Journal of Physiology, Endocrinology and Metabolism, 2006. **291**: p. E1317–E1324.
15. Ritzel, R.A., Meier, J. J., Lin, C., Veldhuis, J. D., and Butler, P. C., *Human islet amyloid polypeptide oligomers disrupt cell coupling, induce apoptosis, and impair insulin secretion in isolated human islets.* Diabetes, 2007. **56**: p. 65-71.
16. Aitken, J.F., Loomes, K. M., Scott, D. W., Reddy, S., Phillips, A. R. J., Prijic, G., Fernando, C., Zhang, S. P., Broadhurst, R., L'Huillier, P., and Cooper, G. J. S., *Tetracycline treatment retards the onset and slows the progression of diabetes in human amylin/islet amyloid polypeptide transgenic mice.* Diabetes, 2010. **59**(1): p. 161-171.
17. Lee, K.H., Shin, B. H., Shin, K. J., Kim, D. J., and Yu, J., *A hybrid molecule that prohibits amyloid fibrils and alleviates neuronal toxicity induced by beta-amyloid (1-42).* Biochem Biophys Res Commun, 2005. **328**(4): p. 816-823.
18. Hasegawa, K., Ono, K., Yamada, M., and Naiki, H., *Kinetic modeling and determination of reaction constants of Alzheimer's beta-amyloid fibril extension and dissociation using surface plasmon resonance.* Biochemistry, 2002. **41**(46): p. 13489-13498.
19. Hu, W.P., Chang, G. L., Chen, S. J., and Kuo, Y. M., *Kinetic analysis of beta-amyloid peptide aggregation induced by metal ions based on surface plasmon resonance biosensing.* Journal of Neuroscience Methods, 2006. **154**(1-2): p. 190-197.
20. Kayed, R., Bernhagen, J., Greenfield, N., Sweimeh, K., Brunner, H., Voelter, W. and Kapurniotu, A., *Conformational transitions of islet amyloid polypeptide (IAPP) in amyloid formation in vitro.* Journal of Molecular Biology, 1999. **287**: p. 781-796.
21. Sparr, E., Engel, M. F. M., Sakharov, D. V., Sprong, M., Jacobs, J., de Kruijff, B., Hoppener, J. W. M., and Killian, J. A., *Islet amyloid polypeptide-induced membrane leakage involves uptake of lipids by forming amyloid fibers.* Febs Letters, 2004. **577**(1-2): p. 117-120.
22. Radovan, D., Opitz, N., and Winter, R., *Fluorescence microscopy studies on islet amyloid polypeptide fibrillation at heterogeneous and cellular membrane interfaces and its inhibition by resveratrol.* Febs Letters, 2009. **583**(9): p. 1439-1445.
23. Westermark, P., Engstrom, U., Johnson, K. H., Westermark, G.T. and Betsholtz, C., *Islet amyloid polypeptide: pinpointing amino acid residues linked to amyloid fibril formation.* Proceedings of the National Academy of Science, 1990. **87**: p. 5036-5040.
24. Lorenzo, A., Razzaboni, B., Weir, G. C., and Yankner, B. A., *Pancreatic-islet cell toxicity of amylin associated with type-2 diabetes-mellitus.* Nature, 1994. **368**(6473): p. 756-760.
25. Ritzel, R.A., J.J. Meier, C.Y. Lin, J.D. Veldhuis, and P.C. Butler, *Human islet amyloid polypeptide oligomers disrupt cell coupling, induce apoptosis, and impair insulin secretion in isolated human islets.* Diabetes, 2007. **56**(1): p. 65-71.
26. Zhang, S., Liu, J., Saafi, E.L. and Cooper, G.J.S, *Induction of apoptosis by human amylin in RINm5F islet L-cells is associated with enhanced expression of p53 and p21$^{(WAF1=CIP1)}$.* FEBS Letters, 1999. **455**: p. 315-320.
27. Zhang, S.P., Liu, H., Yu, H., and Cooper, G. J. S., *Fas-associated death receptor signaling evoked by human amylin in islet beta-cells.* Diabetes, 2008. **57**(2): p. 348-356.
28. Tucker, H.M., Rydel, R. E., Wright, S., and Estus, S., *Human amylin induces "apoptotic" pattern of gene expression concomitant with cortical neuronal apoptosis.* Journal of Neurochemistry, 1998. **71**(2): p. 506-516.